STRENGTH OF Z-PURLIN SUPPORTED STANDING SEAM ROOF SYSTEMS UNDER GRAVITY LOADING

by

Manuel Carballo

Thesis submitted to the Faculty of the
Virginia Polytechnic Institute and State University
in partial fulfillment
of the requirements for the degree of
MASTER OF SCIENCE
in
Civil Engineering

APPROVED:

T. M. Murray, Chairman

S. M. Holzer

W. S. Easterling

January 1989

Blacksburg, Virginia

This thesis is dedicated to my family

for their support and encouragement.

Thanks, you made the difference.

ACKNOWLEDGEMENTS

The author wishes to express his sincere appreciation to his advisors, Dr. Thomas M. Murray and Dr. Siegfried M. Holzer for their counsel and guidance throughout the development of this thesis. Also, the author wishes to thank Dr. W. Samuel Easterling for serving as thesis committee member and to the Metal Building Manufacturers Association for funding the project.

Finally, the author wishes to thank his friends at the Prices Fork Research Laboratory for their help: , , ,
, , , and for her careful typing.

TABLE OF CONTENTS

TABLE OF CONTENTS (cont.)

LIST OF FIGURES

LIST OF FIGURES (cont.)

LIST OF TABLES

CHAPTER I

INTRODUCTION AND LITERATURE REVIEW

1.1 Introduction

Metal roofs have always been popular in metal buildings and on single story nonresidential buildings, but recently they have begun to gain popularity in conventional construction. There are several reasons for this shift in industry and the market, but the two most important are that metal roofs can provide well-functioning and aesthetically-satisfying results. To establish this new market, the roofing industry has to overcome the stereotype of a metal roof being apt to corrode, leak and be aesthetically unpleasant [1]. Today, metal roofs are being specified for their beauty and durability.

These metal roofs can be classified into three categories: through-fastened or conventional roofs; architectural standing seam roofs; and structural standing seam roofs.

The through-fastened or conventional roofs are most commonly used in metal buildings. In these systems, a roof panel is attached to the top flange of each purlin throughout its length. This panel usually provides enough stiffness to prevent the relative movement of the purlins with respect to each other, thus making the system act as a structural diaphragm and providing the joist or purlin full lateral support. This situation will only permit the cross section to behave under constrained bending, therefore allowing the use of simple stress and deflection equations when predicting its behavior (see Figure 1.1). Most design problems have been resolved in ordinary applications of the through-fastened or conventional roof systems. Some of the reasons for selecting a through-fastened roof system include [1]:

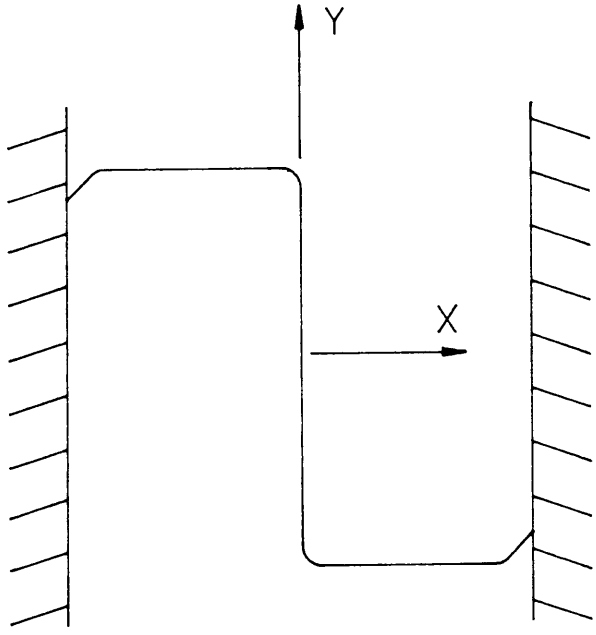

Figure 1.1 Constrained Bending

1. Well-established system
2. Light weight
3. Relatively inexpensive
4. Easy to install
5. Low maintenance
6. Proven performance

The structural standing seam metal roof system, which is the focus of this thesis, is relatively new compared to the through-fastened roof system. In a standing seam system, the panels are attached to clips and the clips attached to the top flange of the joist or purlin. The geometry of the connection is such that relative movement of the purlins with respect to each other is permitted. In this system, the diaphragm capacity is much less because there is no physical connection between the panels unlike the through-fastened system, however the panels will still provide some degree of lateral restraint. For this reason, the cross-section of the purlin or joist will not be under constrained bending, or unconstrained bending, but instead under a more complex situation, partially constrained bending (see Figure 1.2).

The behavior of the system, therefore, lies in between the two extremes of constrained bending (full lateral support, Figure 1.1) and the 1986 AISI Specification for lateral torsional buckling (no lateral support, see Figure 1.3). As a result of this situation, the design considerations and mechanics for a standing seam roof system will be more complex than those of through-fastened roofs. Complexity will also be magnified in the installation of the system due to the newness and number of elements that have to be synchronized in order for the system to act as it was intended to [1]. If the system does not act as it was intended to, the performance and its consequences will be disastrous.

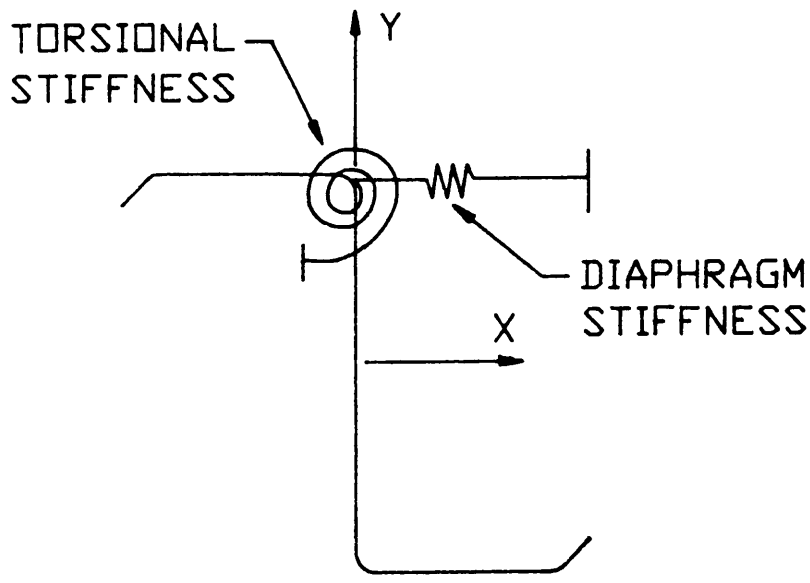

Figure 1.2 Partially Constrained Bending

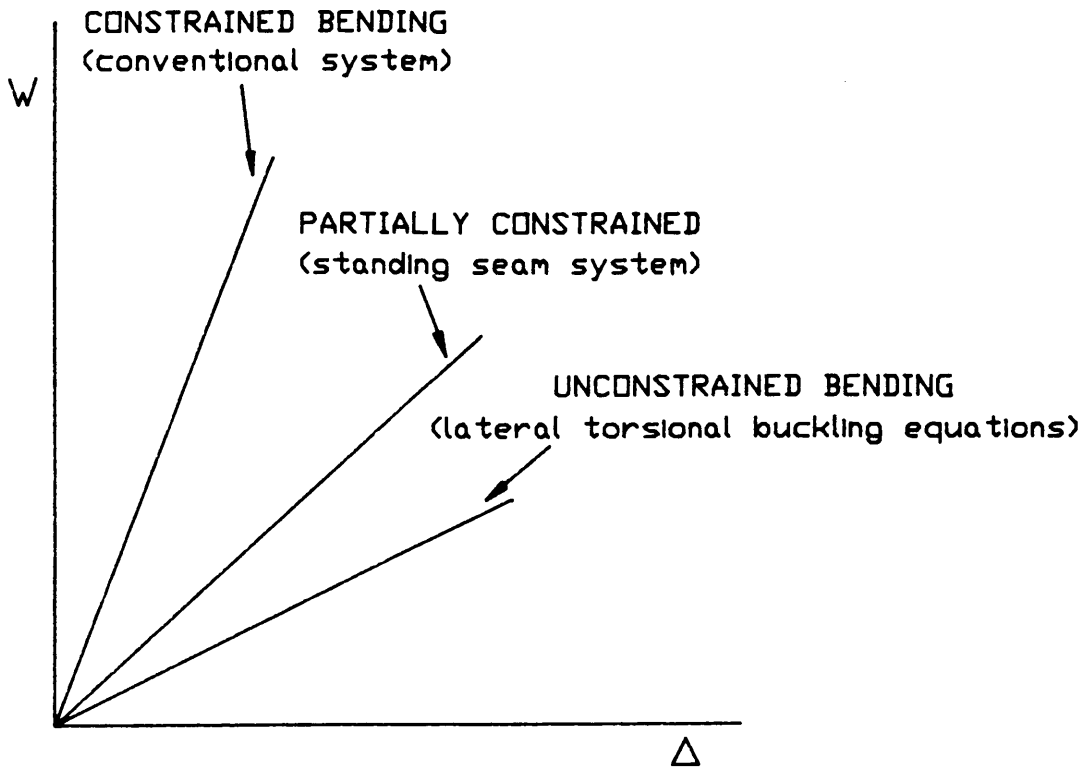

Figure 1.3 Load vs. Deflection for Different Systems

Common reasons for specifying a standing seam system include [1]:

1. Factory-caulked side seams above the drainage plane (less sidelap leak susceptibility)
2. Thermal movement accommodation in expansive roofs
3. Greater adaptability to more sophisticated insulation systems
4. Light weight
5. Reduced maintenance
6. Aesthetically pleasing

Some of the disadvantages include [1]:

1. Costly
2. Expansion and contraction have to be considered because of thermal variation of metal
3. If a leak develops, it can be very difficult to locate it
4. Qualified experience installers are hard to find

1.2 Scope of Research

The Z-shaped purlins used to support standing seam roof systems are cold-formed, relatively thin, light weight sections. Because of their unsymmetrical shape, Z-purlins are loaded obliquely to their principal axes when the line of action of the applied load is in the plane of the web, thus, they tend to deflect perpendicular to, as well as, in the plane of the loading. In addition, if the loads are applied eccentrically or if the purlin is restrained at only one flange, torsional moments are induced causing the purlin to twist around its longitudinal axis. The combination of lateral movement and twisting is known to be detrimental to the load carrying capacity of the member [3].

Results of twelve single and three span continuous tests showed that the flexural failure loads of the tested two purlin line systems were only 40 to 80 percent of the failure loads predicted using the flexural strength provisions of the 1986 AISI Specification, assuming constrained bending.

Apparently, in industry there is a wide range of different approaches in determining the strength of standing seam roof systems. Some designers assume that friction and draping at the clips will provide full lateral support to the system, therefore the condition in Figure 1.1 is used to predict the system's behavior. This approach is unconservative because standing seam roof system strength is significantly less. Other designers brace the purlins but use the total length as the unbraced length. This approach will be conservative and the member will be overdesigned. Due to the lack of consistency among designers and of a method to predict the strength of Z-purlin supported standing seam roof systems, this project was proposed to and approved by MBMA (Metal Building Manufacturers Association). The purpose of this study is to do an analytical analysis of the system, determine which factors have an impact on the system's strength, and verify the design procedure with several full scale tests.

1.3 Review of Previous Research

The only previous research done on standing seam roof systems is reported by Rivard and Murray [2]. The primary purpose of this project was to verify current design equations for predicting anchorage forces in cold-formed Z-purlin supported standing seam roof systems. Even though strength was not the primary focus of the report, the experimental failure loads are available and will be very valuable in the analytical stage of this project.

A total of twelve standing seam tests were conducted: six single span tests and six three-continuous span tests. In addition, one conventional (through-fastened) single span test was conducted for comparison purposes. Span lengths were nominally 20 ft. for the single span tests and 23 ft. for the continuous span tests. In all tests, 8 in. deep Z-purlins with top flanges facing in the same direction were used. Three anchorage brace configurations were used, one with each roof system configuration for each span configuration. Table 1.1 gives the complete test matrix. Test designations are to be interpreted as follows: P1/2-R-1 indicates pan #1 type panel (P1), two purlin lines (/2), anchorage braces at rafters (-R), single span (-1) and R2/2-M-3 indicates Rib #2 type panel (R2), two purlin lines (/2), anchorage braces at midspan (-M), three continuous spans (-3). Results include comparisons of predicted and measured anchorage forces, predicted and experimental failure loads, system restraint forces and diaphragm strengths.

1.4 Overview of Research

In the following chapters of this thesis, four approaches to predict the failure load (strength) of a Z-purlin supported standing seam system under gravity loads were developed and evaluated. The first approach consists in using the Lateral Buckling Strength provisions of the 1986 AISI Specification. This method will be used as a starter in determining the lateral support capacity of the standing seam panels. The basis for the second method, deflection correlation, is that it appears from the tests in Table 1.1 that the deflection of any system at ultimate load is the same. Using this criterion, the predicted failure load for a standing seam system would be the product of the failure load calculated for the system using the local buckling provisions of the 1986 AISI Specification and the ratio of the stiffness of the standing seam system to the stiffness of the system assuming

TABLE 1.1

AVAILABLE DATA FROM PREVIOUS PROJECT

Test No.	Span(s) (ft)	Panel Type	Bracing Configuration			Failure Load (PLF)
			Rafter Brace	Third Point Braces	Mid-Span Braces	
P1/2-R-1	20.0	Pan	X			59.5
P1/2-T-1	20.0	Pan		X		141.0
P1/2-M-1	20.0	Pan			X	138.3
P2/2-R-1	20.0	Rib	X			85.8
R2/2-T-1	20.0	Rib		X		155.1
R2/2-M-1	20.0	Rib			X	160.1
P2/2-R-3	3@23.0	Pan	X			99.5
P2/2-T-3	3@23.0	Pan		X		207.1
P2/2-M-3	3@23.0	Pan			X	154.0
R3/2-R-3	3@23.0	Rib	X			85.1
R3/2-T-3	3@23.0	Rib		X		175.5
R3/2-M-3	3@23.0	Rib			X	137.7
Conv/2-R-1	20.0	Conv.	X			198.0

it behaves as a through-fastened system. A mathematical model was developed to not only predict the stiffness of a standing seam system, but also to study the system's behavior. The third approach, stress correlation, predicts the failure load of a standing seam system by scaling the actual stresses of the cross-section using the stresses calculated from the allowable flexural capacity of the cross section, which are based on the local buckling provisions of the 1986 AISI Specification. The mathematical model developed for the second approach, was used to calculate the maximum stresses on the cross section based on the maximum moments. The last approach is referred to as the base test method. This method predicts the failure load of a multiple span standing seam system by scaling the ultimate load of a corresponding single span test. A more complete discussion and explanation on each method is presented in Chapter II.

Each one of these approaches was evaluated not only to determine their accuracy, but also their feasibility. The data from the previous project (Table 1.1) and a series of full scale tests (Table 3.6) were used in the evaluation. In Chapter III, the results and conclusions from each evaluation are discussed and an approach to predict the strength of standing seam systems is recommended.

Chapter IV explains the recommended approach in more detail and Chapter V summarizes the project and makes some recommendations on the method selected and needed research.

Sample calculations for each approach and member properties of the tests in Tables 1.1 and 3.6 are included in the Appendices.

CHAPTER II

APPROACHES TO CALCULATE STRENGTH OF STANDING SEAM ROOF SYSTEMS

2.1 Lateral Buckling Strength from 1986 AISI Specification

Prior to developing a procedure for predicting the strength of standing seam roof systems, the flexural capacity of the systems on Table 1.1 was calculated using the lateral buckling provisions of the 1986 AISI Specification [5]. Since a fully unbraced system, whose limit state is lateral buckling, will be the lower boundary for these systems (Fig. 1.3), calculating the predicted failure loads on this basis and comparing them to the experimental failure loads will determine to what degree the standing seam systems behave as fully lateral unsupported.

The allowable flexural strength for laterally unbraced segments of doubly- or singly-symmetric sections subject to lateral buckling is determined as follows [5]:

$$M_n = S_c \frac{M_c}{S_f} \tag{2.1}$$

where

S_f = Elastic section modulus of the full unreduced section for the extreme compression fiber

S_c = Elastic section modulus of the effective section calculated at a stress M_c/S_f in the extreme compression fiber

M_c = Critical moment

This procedure can be found on pages I-30 and VI-20 of the 1986 AISI Manual. The results and conclusions reached from this approach are discussed and presented in Chapter III of this thesis. Sample calculations are included in Appendix A.

2.2 Stiffness Model - Deflection Correlation

The data available from Rivard and Murray [2], especially the load vs. deflection graphs, were used in developing this approach. By examining this available data, it appeared that at failure the deflection will be the same for either conventional or standing seam roof systems. The location of the bracing in the standing seam systems will increase or decrease the stiffness of the system but the deflections at failure will remain unchanged (Figure 2.1). This hypothesis, that at failure the deflections will be the same for any system, is the basis for this approach. Using the 1986 AISI Specification [5], the deflection at failure load for a conventional system can be predicted. From this information, a load vs. deflection graph for any conventional system can be developed. So, if there is a model that can accurately predict the load vs. deflection line for a standing seam system using any panel and bracing configuration, all that has to be done is to backtrack the load of the standing seam system corresponding to the deflection at failure load for the conventional roof system. This load obtained from backtracking the deflection will be the predicted failure load for that particular standing seam system (Fig. 2.2). Referring to Fig. 2.2, the predicted failure load for a standing seam roof system is determined as follows:

$$W_{SS} = W_{AISI} \times K_{SS}/K_C \qquad (2.2)$$

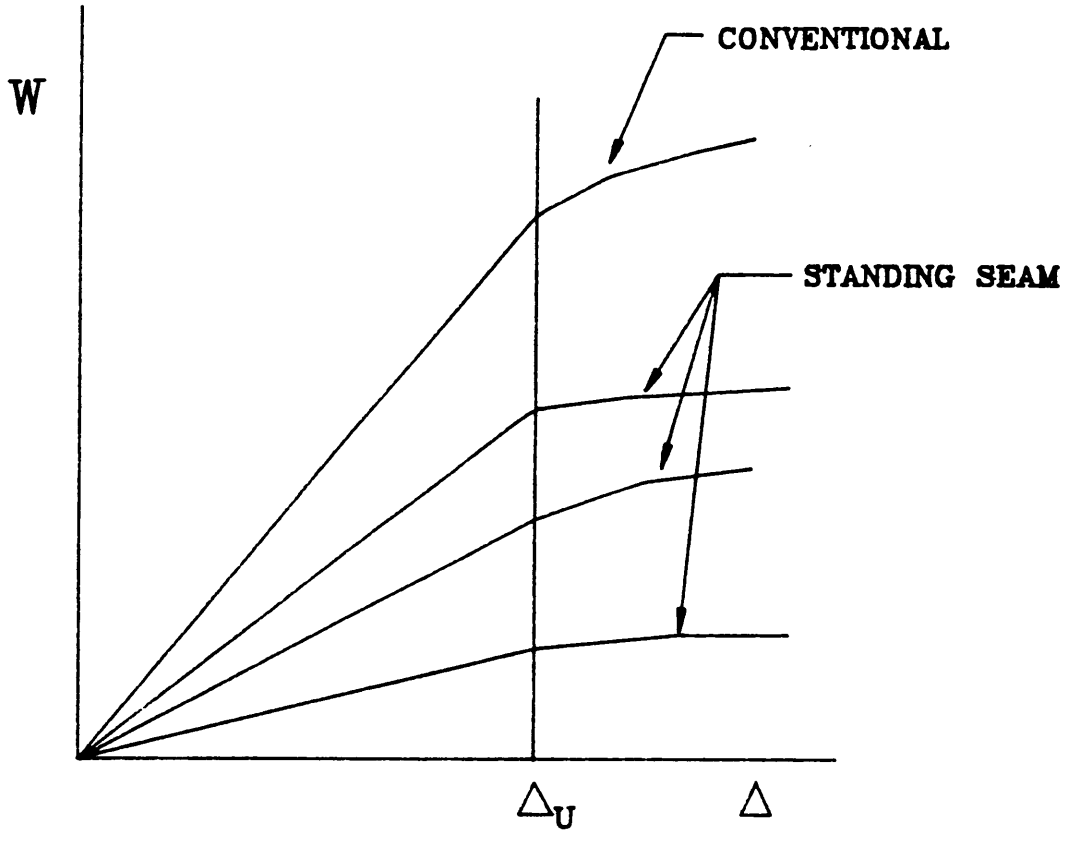

Figure 2.1 Deflection at Failure Load for Different Systems

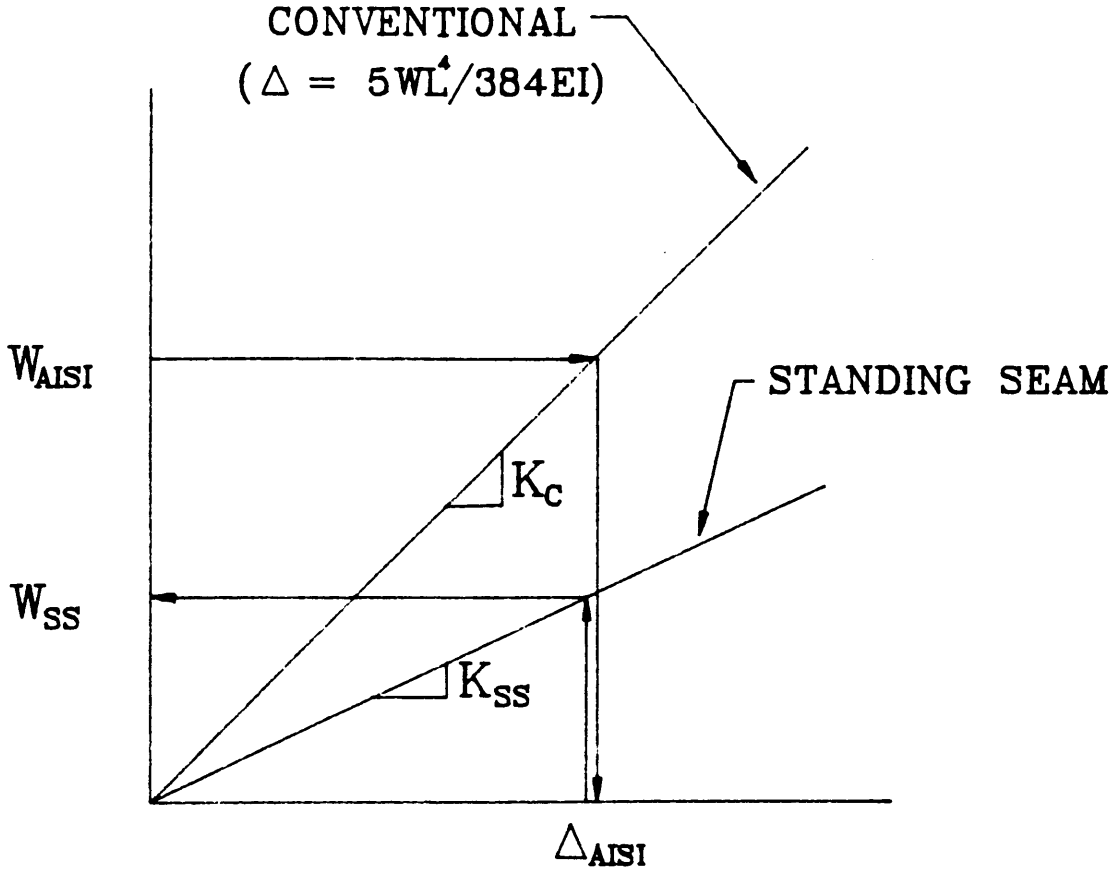

$$W_{SS} = W_{AISI} \times K_{SS} / K_C$$

Figure 2.2 Solution Approach

where

W_{SS} = predicted failure load for the standing seam system.

W_{AISI} = predicted failure load for the system assuming it behaves as a conventional roof system.

K_{SS} = stiffness of standing seam system obtained from analytical model.

K_C = stiffness of system assuming it behaves as a conventional roof system.

The key to this approach is to have an analytical model that can accurately predict the behavior of a standing seam system taking into consideration purlin size, deck and bracing configuration used. If this model is not accurate, the resulting predicted failure loads will not be accurate either. Therefore, the next step in this approach is to develop a model to predict the behavior of one span and three span continuous, two purlin line systems. The reason that one span and three span continuous systems are modeled is because of the availability of experimental data (Table 1.1) to correlate the results. This does not mean that this approach is limited to one span and three span continuous systems.

2.2.1 Prior Mathematical Model

Elhouar and Murray [3] studied the anchorage requirements for through-fastened, corrugated steel panel, multiple purlin line, multiple span roof systems. For this purpose, a stiffness model was developed to predict the magnitude and distribution of the brace forces required to prevent lateral movement. A typical through-fastened roof system is a combination of three types of structural elements: purlins for strength, a panel or deck for serviceability and external restraint braces for stability.

In this study the three bracing configurations that will be modeled are:

1. Torsional Restraint (Figure 2.3a): Braces are located at the rafters and provide a torsional simple support condition at the ends of the braced purlin.

2. Third Point Restraint (Figure 2.3b): Braces are at the purlin span third points and restrain lateral movement at these locations.

3. Mid-span Restraint (Figure 2.3c): Braces are at the purlin mid-span and restrain lateral movement at this location.

The finite element method was considered to be appropriate for roof system modeling and a hybrid space frame/space truss model was developed. Figure 2.4 illustrates the actual system and the proposed mathematical model by Elhouar [3]. The three main components of the system: purlin, panel, and brace are first considered separately and then combined to develop the entire model.

This mathematical model for conventional or through-fastened roof systems will be the basis for a model to predict the behavior of a standing seam roof system.

First, the model has to be reproduced using a finite element program discussed later in this section. Once the model is reproduced, it will be used to model all six one span and six three span continuous tests from Table 1.1. A nominal load will be applied to all twelve models and the corresponding deflections will be recorded. The accuracy of this model will depend on how close these deflections are to the deflections calculated using the same nominal load in Equation 2.3.

$$\Delta = \frac{5wl^4}{384EI} \tag{2.3}$$

Equation 2.3 is used because in conventional roof systems, it is assumed that the system is fully braced. Once the model accurately predicts the behavior

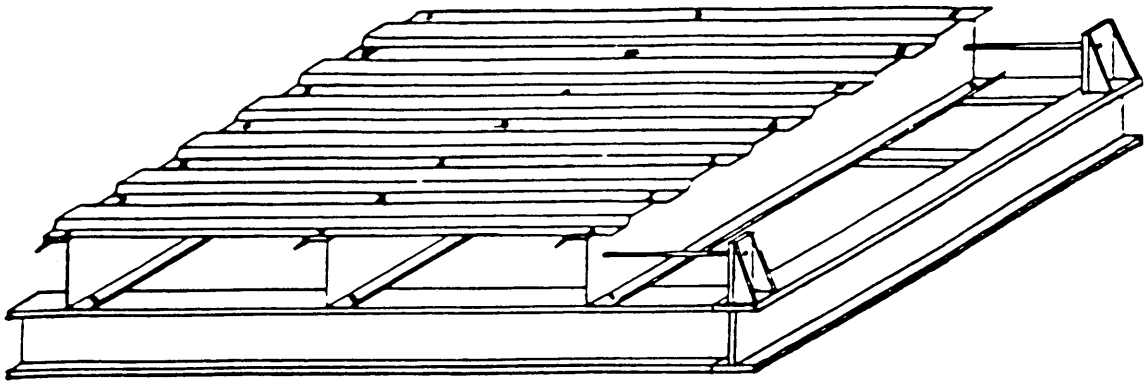

Figure 2.3a Torsional Restraint

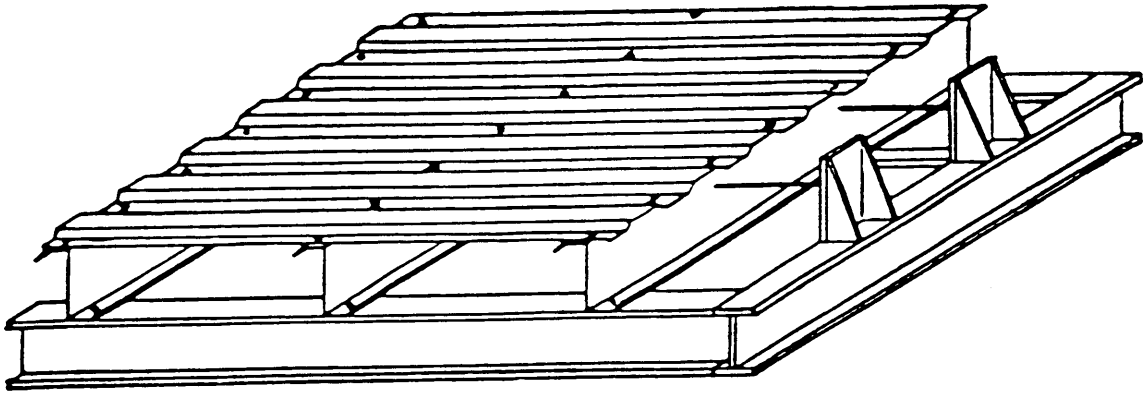

Figure 2.3b Third Point Restraint

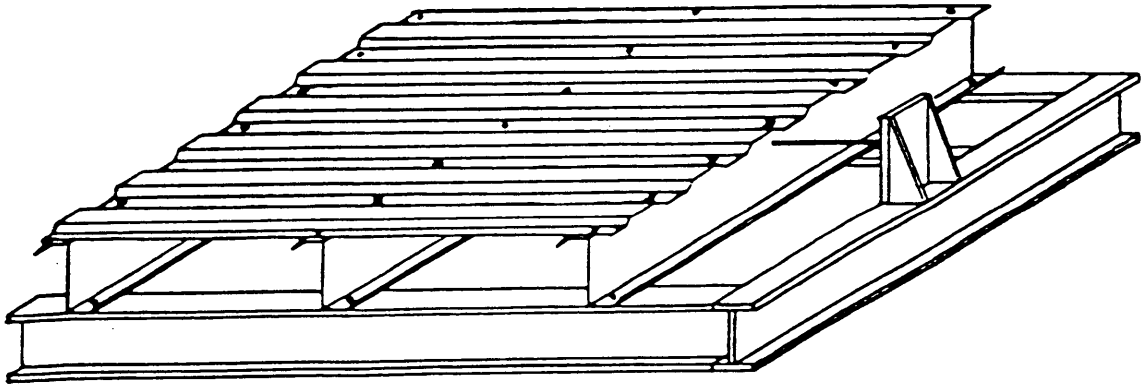

Figure 2.3c Mid-Span Restraint

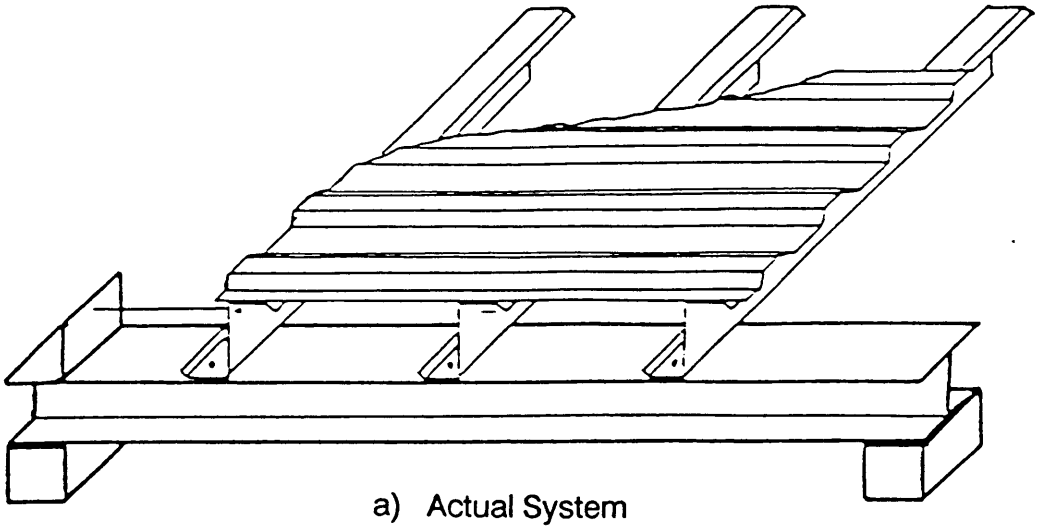

a) Actual System

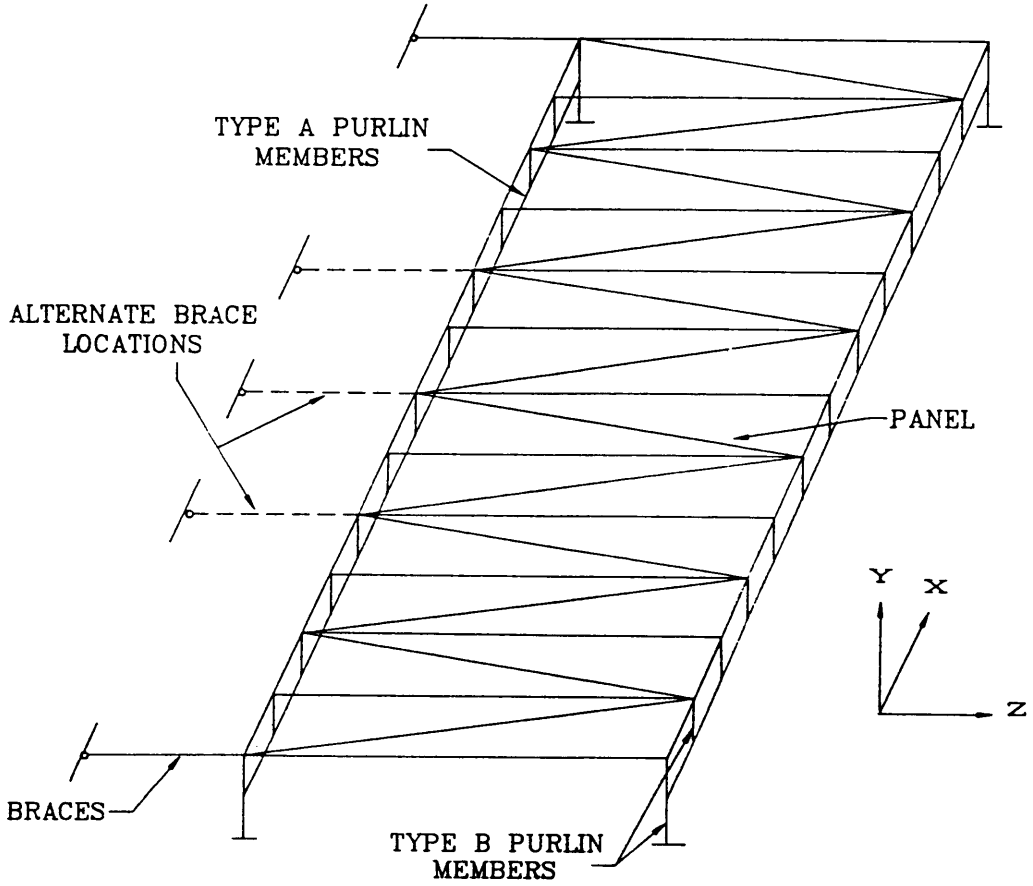

b) Mathematical Model

Figure 2.4 Proposed Mathematical Model

of a conventional roof system, it will be modified to predict the behavior of a standing seam roof system.

Modeling of Purlin. The purlin is divided into twelve sub-members using a space frame line element. These elements will be referred to as Type A elements (Figure 2.5). The area and moment of inertia properties of these elements are the same as the purlin's cross-sectional properties except for the torsional constant (I_x). Values for this constant will be discussed later in this chapter. Type B elements are also space frame line elements and will provide compatibility of displacements between the purlin and the panel and rafter (Figure 2.7). The cross-sectional properties of these elements was obtained by trial and error until there was good correlation with prototype and model test results.

Modeling of the Panel. The panel can be represented as a plane truss (Figure 2.6) assuming that the purlin-to-panel connection does not provide rotational restraint to the purlin. This condition makes it possible to disregard the panel bending stiffness and only its shear stiffness need be considered. For a known shear stiffness G', the deflection of a shear panel in the direction of the load P (Figure 2.6a) can be determined from

$$\Delta = (PL)/(4G'a) \tag{2.4}$$

where L and a are the dimensions of the panel. By applying the same load P to the truss in Figure 2.6B, the area, A, of the truss members can be determined, and consequently, the truss will have the same stiffness G' when loaded at its midspan.

Ghazanfari and Murray [4] studied the variation of lateral forces with an increasing panel shear stiffness and found that the forces will increase from zero to a maximum as G' is increased from zero to approximately 1500 lbs/in and then remains nearly constant as G' is increased to infinity. It is assumed that the

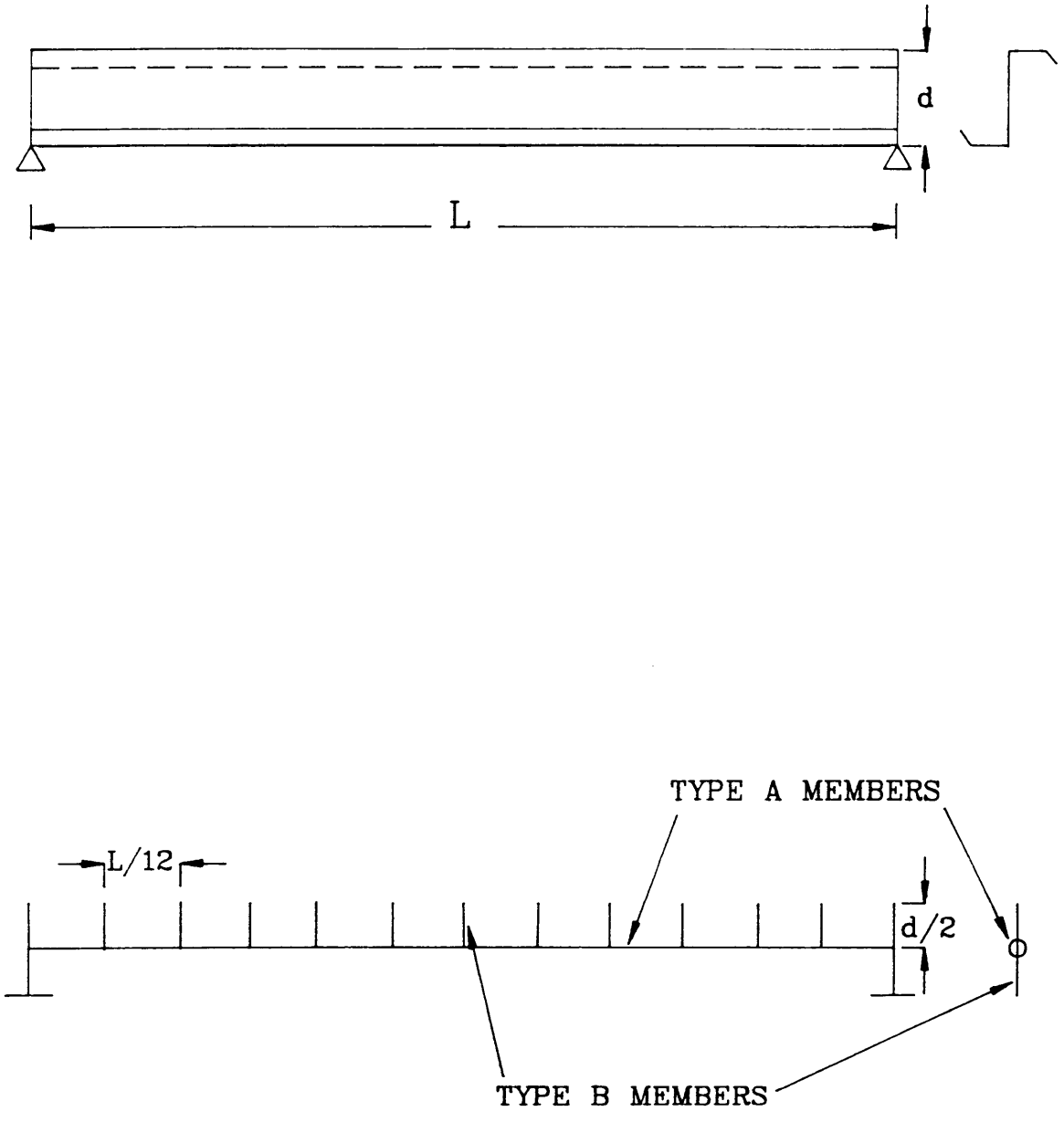

Figure 2.5 Purlin Stiffness Model

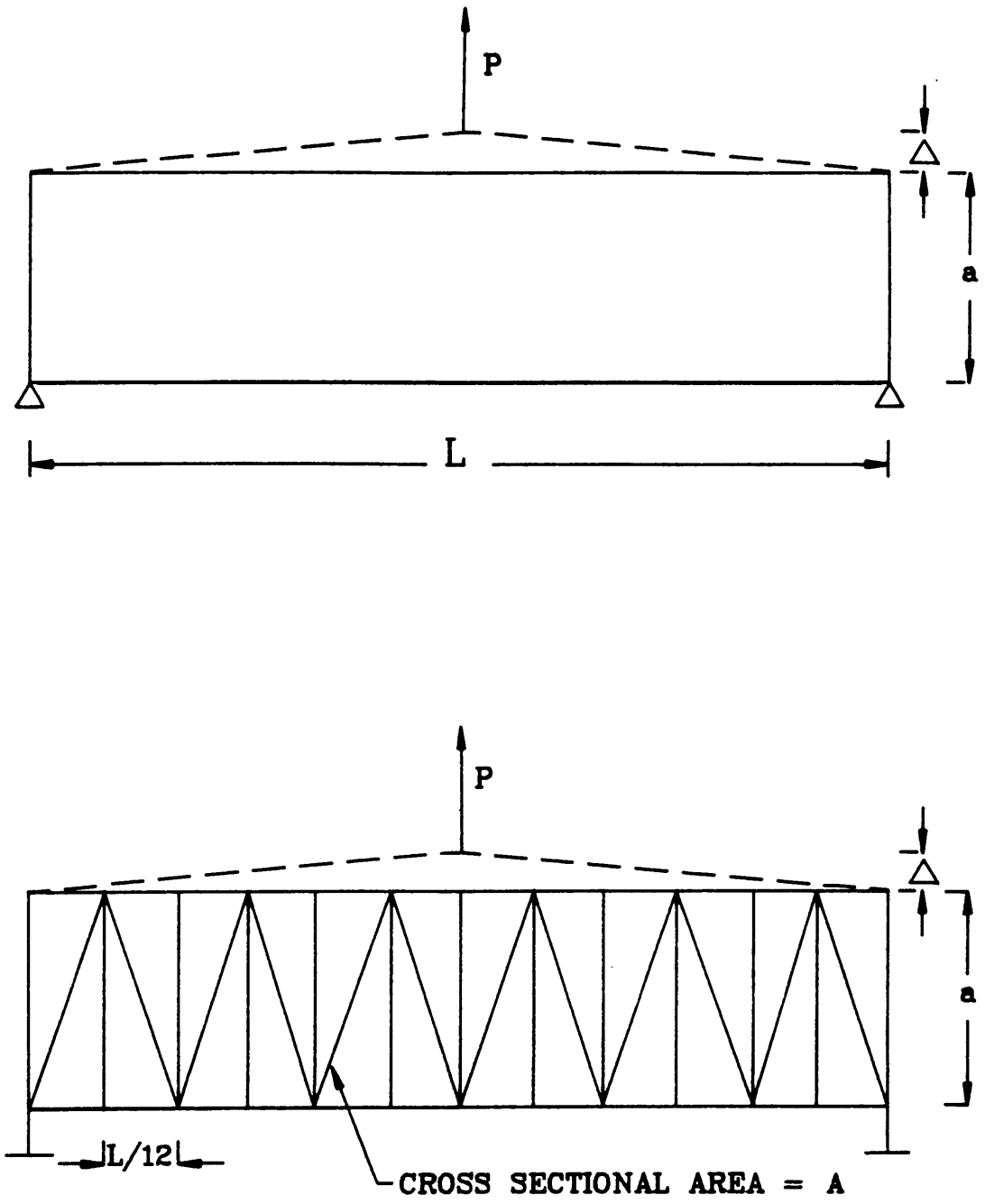

Figure 2.6 Panel Stiffness Model

variation of truss stiffness can be disregarded if the actual panel shear stiffness is greater than 1500 lbs/in.

According to Curtis and Murray [7], the shear stiffness of a decking system is between 1000 lbs/in and 3300 lbs/in when typical metal building steel roof panels are used with self-drilling fasteners as panel-to-panel connectors. A value of 2500 lbs/in is used for calculations.

Modeling of the Braces. These members are subjected to an axial tensile force only. Therefore, they will be modeled as truss type line elements having the cross-sectional area of the brace itself.

Cross-Sectional Properties of the Purlin Members. The final cross-sectional properties of the Type B members are given in Figure 2.7. They are specified according to the location of the member within the purlin, i.e., at the rafter or midspan. The cross-sectional properties of the Type A members will be those of the purlin itself, except for the torsional constant I_x which is 10.0 in^4 for full scale systems.

Applied Load. In an actual roof system, gravity loads are transmitted to the purlins eccentrically with respect to the shear center because the load distribution on the flange varies from zero at the lip location to a maximum at the web (Figure 2.8a). To simplify the problem, Elhouar and Murray [3] approximated this distribution of the load across the flange by using a triangular distribution. The resultant load is then applied to the purlin at a distance $e = b_f/3$ from the plane of the web (Figure 2.8b). The system is then analyzed for a uniformly distributed vertical load, w, and a uniformly distributed torque (Figure 2.8c), which is given by:

$$M_x = w(b_f/3) \tag{2.5}$$

where b_f is the purlin flange width.

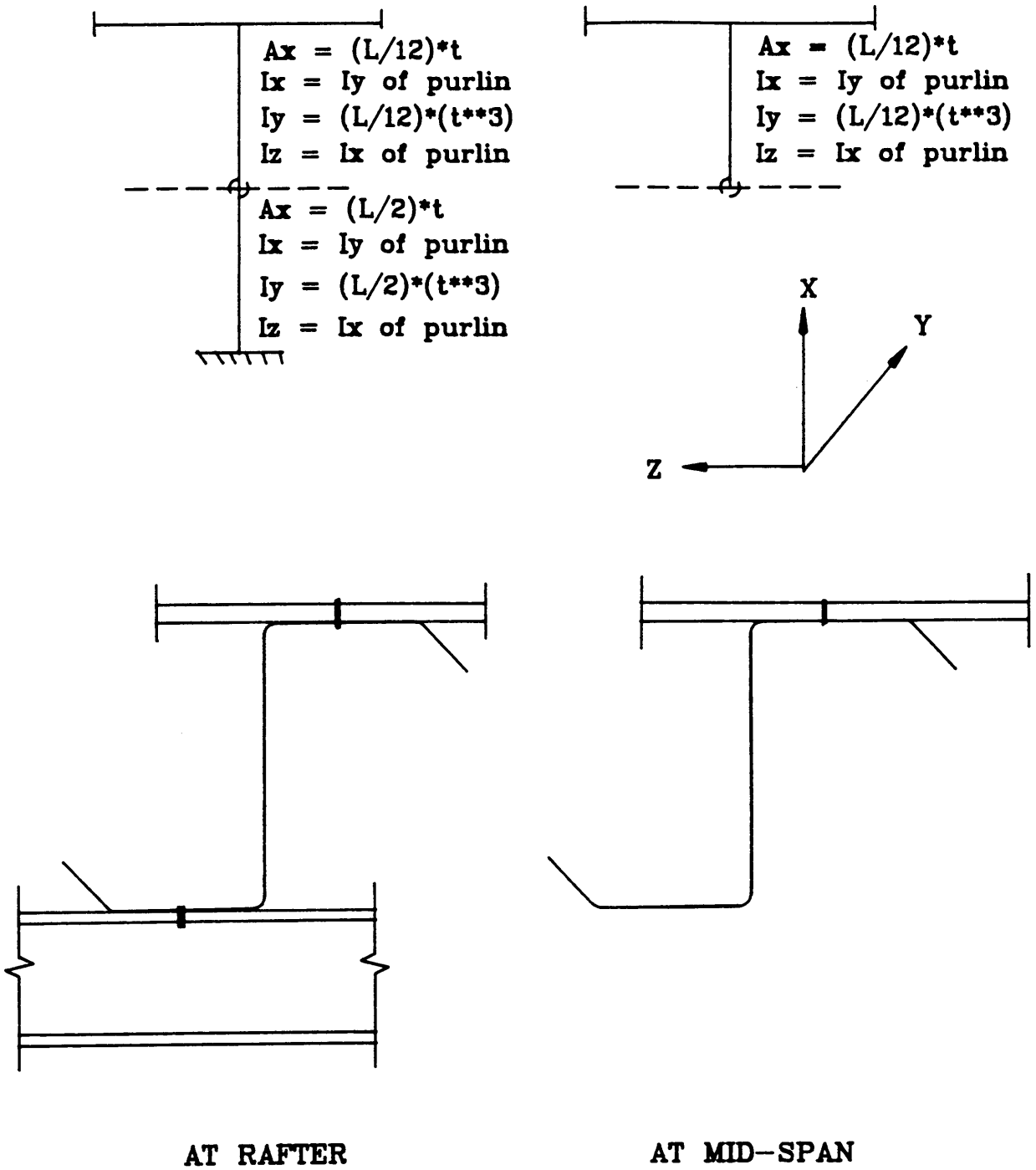

Figure 2.7 Purlin Cross Section

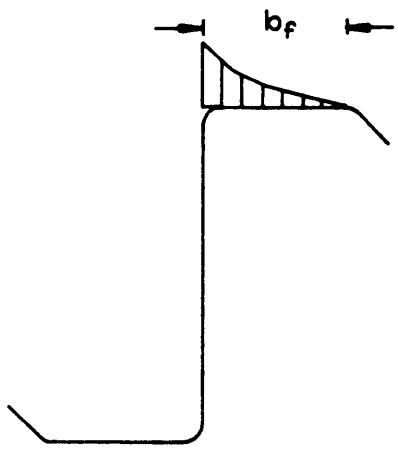

a) Probable Load Distribution

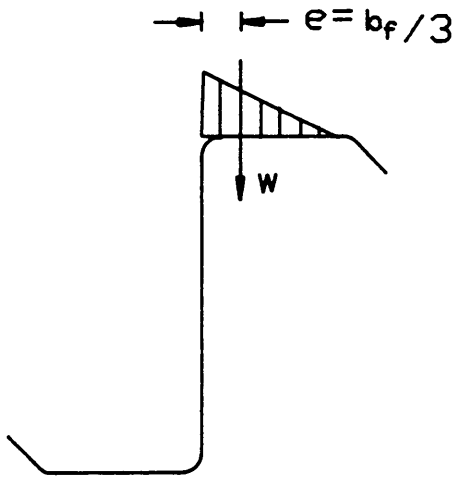

b) Linear Approximation of Load Distribution

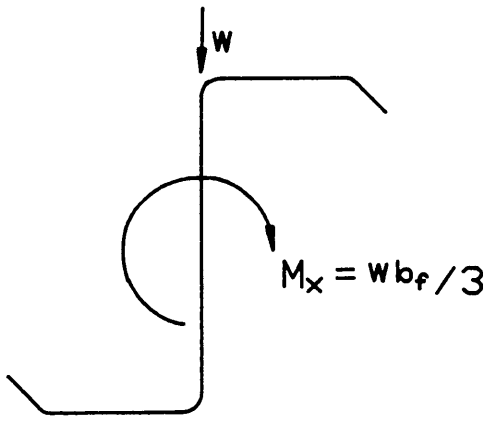

c) Analysis Load Configuration

Figure 2.8 Applied Purlin Load

Method of Solution. The computer software package called ABAQUS available on the IBM 3480 at Virginia Polytechnic Institute and State University was used to perform the analyses. The program itself did not impose any restrictions on the size of the models, but the CPU time did. For this reason, symmetry had to be exploited when modeling the three span continuous systems. One span and three span continuous systems models will be discussed later in this chapter and sample input data and results for both systems are given in Appendix B.

Evaluation of Model. Before any modifications can be made to this model to predict the behavior of a standing seam system, it has to be evaluated and verified as to how accurately it predicts the behavior of a conventional roof system. This is where the data from the tests in Table 1.1. becomes very important. From the load vs. deflection plots, the theoretical load-deflection line, assuming constrained bending, is known for all tests. From this data, the deflection corresponding to a given load can be found. Before continuing, it is important to remember that conventional roof systems behave under constrained bending (full lateral support) and their behavior can be predicted using linear-elastic behavior, Equation 2.3.

All six one span tests were modeled and a load of 40 plf was applied. The deflection at midspan was recorded and compared to the theoretical deflection for the same load. Referring to Table 2.1, it is clear that the model is predicting the behavior of a conventional roof system very accurately, within 10% of the theoretical deflection.

Now that the accuracy of the model has been verified, modifications will be made to predict the behavior of one span and three span continuous standing seam roof systems.

TABLE 2.1

PRIOR MODEL EVALUATION

(40 plf)

Test No.	Deflections at Mid-Span (in.) Model	Constrained Bending	% Deviation from Actual
R2/2-R-1	0.4976	0.5179	+4
R2/2-T-1	0.4476	0.4821	+7
R2/2-M-1	0.4507	0.4857	+7
P1/2-R-1	0.4697	0.4786	+2
P1/2-T-1	0.4315	0.4643	+7
P1/2-M-1	0.4406	0.4714	+6

-: unconservative

+: conservative

2.2.2 Modifications to Prior Model

Before modifying the model, the behavior of a standing seam roof system and its differences with a conventional roof system has to be studied and understood to determine which parameters affect the behavior of these particular systems.

From the load vs. deflection plots of available data, it is clear that standing seam systems have considerably less stiffness than conventional roof systems, this is not surprising since standing seam systems allow relative movement of the purlins or joists. This panel-clip-purlin interaction is the major difference between both systems and modifications to the model have to be targeted at creating a less stiff model. The equations to calculate the cross-sectional properties of some members in the conventional roof systems model are not good approximations for standing seam systems and will have to be modified.

The following sections will discuss more detail the modifications and evaluation of the modified model.

Modeling of the Purlin. The same criterion in Section 2.2.2 will be used when modeling the one span and three span continuous systems. The only difference will be the value used for the torsional constant, I_x, which will be discussed later in this section. Refer to Figure 2.5 which identifies the components of the models. The values of these components will be discussed in the following sections of this chapter.

Modeling of the Panel. To determine the area of the truss members for a conventional roof system, an average diaphragm shear stiffness of 2500 lb/in was used in Equation 2.4.

This approach cannot be used in standing seam systems for the following reasons. It is clear that the diaphragm shear stiffness of a standing seam system is less than that of a conventional roof system. Unlike the conventional roof

system, the behavior of a standing seam system will be affected to a higher degree by the panel used (pan, rib, etc.) and clip used (one piece, two piece, etc.). This broad range of products in the market makes it impossible and impractical to calculate a constant for the diaphragm shear stiffness that can be used in the model and still get accurate results. For this reason, it will be recommended that each manufacturer conduct an accurate test of its panels to determine the actual diaphragm shear stiffness. To calculate the actual diaphragm shear stiffness and therefore use the correct area for the truss members is the key to the model and this approach. As explained in Section 2.2, this approach of determining the strength for standing seam systems is based on deflections and if the model does not accurately predict the behavior of a given system, the corresponding failure load is incorrect (Figure 2.2).

When modeling the twelve tests in Table 1.1, a different approach to calculate the area of the truss members was taken. Since the value of G′ for the panels used was not known, a series of iterations were performed. It is important to note that there are four different panels used, two in the one span (R2, P1) and two in the three span continuous systems (R3, P2), therefore, four different areas for the truss members are expected. First, one test from each of the four different panel types was selected. Then, each one of these four tests was modeled and a load of 40 plf was applied. Since the load vs. deflection plots are available for these four tests, the experimental deflection corresponding to 40 plf is known. An iterative process was carried out changing the areas of the models until the experimental and predicted deflections matched. At this point, the area of the truss members is known for one of the three tests using the same panels. So, to evaluate this area, the other two tests will be modeled using this area and the same load. The asterisk next to the test number on Table 2.2 indicates the test

TABLE 2.2

DEFLECTIONS: MODIFIED MODEL VS. EXPERIMENTAL
(40 plf)

Test No.	Area of Truss Members ($in.^2$)	Maximum Deflection (in.) Model	Experimental	% Deviation from Actual
*R2/2-R-1	0.000062	0.895	0.895	0
R2/2-T-1	0.000062	0.5588	0.5107	-9
R2/2-M-1	0.000062	0.5921	0.5071	-16
*P1/2-R-1	0.00037	0.7143	0.7143	0
P1/2-T-1	0.00037	0.5136	0.5179	+1
P1/2-M-1	0.00037	0.5453	0.5107	-6
*R3/2-R-3	0.000068	0.7587	0.7619	+1
R3/2-T-3	0.000068	0.5028	0.4821	-4
R3/2-M-3	0.000068	0.5332	0.4930	-8
*P2/2-R-3	0.0017	0.4960	0.4964	0
P2/2-T-3	0.0017	0.4264	0.4071	-5
P2/2-M-3	0.0017	0.4679	0.4643	-1

-: unconservative

+: conservative

selected in determining the area of the truss members for the tests using that particular panel type (R2, P1, R3, P2).

It is clear from the results on Table 2.2 that the model is predicting the deflections for a standing seam system accurately.

Modeling of the Braces. These members will be modeled as truss elements having the cross sectional area of the brace itself.

Modified Cross-Sectional Properties. For conventional roof systems, a value of 10 in^4 was recommended for I_x for the Type A purlin members. After various trials using different values, good correlation was obtained when the actual value for the torsional constant of the cross section was used. However, the brace forces from the model did not match the experimental brace forces as shown in Table 2.3. After studying various parameters, it was determined that the value of I_x for the Type B vertical members at the rafter (see Figure 2.7) is not a good approximation for standing seam systems.

For conventional systems, I_x for Type B members at the rafters is approximated by the following equation:

$$I_x = (L/2) \times t^3 \qquad (2.6)$$

where

L = span length

t = thickness of the purlin

After various attempts, a value of 0.00001 in^4 gave good agreement between predicted and experimental brace forces. This modification will have an almost insignificant effect on deflections but the areas of the truss members were adjusted accordingly using the same procedure described previously. Table 2.4 summarizes the results obtained after the following modifications were made to the model:

TABLE 2.3

BRACE FORCES: MODIFIED MODEL VS. EXPERIMENTAL (40 plf)

Test No.	Brace Force (lbs.) Model	Experimental
R2/2-R-1	125.0	45.4
R2/2-T-1	147.5	129.6
R2/2-M-1	240.0	192.3
P1/2-R-1	175.0	100.8
P1/2-T-1	134.4	137.4
P1/2-M-1	232.0	207.2

TABLE 2.4

DEFLECTIONS AND BRACE FORCES:

MODIFIED MODEL VS. EXPERIMENTAL

(40 PLF)

Test No.	Area of Truss Members ($in.^2$)	Experimental		Model	
		Brace Force (lbs.)	Deflection (in.)	Brace Force (lbs.)	Deflection (in.)
R2/2-R-1	0.000067	125.0	0.895	125.8	0.9068
R2/2-T-1	0.000067	147.5	0.5107	126.5	0.5630
R2/2-M-1	0.000067	240.0	0.5071	240.3	0.5224
P1/2-R-1	0.000037	175.0	0.7143	112.5	0.7144
P1/2-T-1	0.000037	134.4	0.5179	127.9	0.5239
P1/2-M-1	0.000037	232.0	0.5107	248.3	0.5128

1. Torsional constant - actual value for the cross section.
2. Moment of inertia for lower vertical members = 0.00001 in^4.
3. New area of truss members.

All other values for the cross-sectional properties of one span systems as defined in Figure 2.7 do not change.

For the three span continuous systems, the value of the torsional constant for Type A members is the same as for one span systems, the actual value for the cross section is used. The values for the Type B elements will be slightly different. It is important to note that when modeling the three span continuous systems symmetry had to be exploited (Figure 2.9) due to CPU constraints. In these systems, there will be four different types of Type B elements:

1. Lower Type B member at supports A and B (Member #1, #2)
2. Upper Type B member along support span including exterior support (Member #3-#14)
3. Upper Type B at interior support B (Member #15)
4. Upper Type B at point of symmetry (Member #21)

Refer to Figure 2.9 for sketch of model. The properties for these members are in Figures 2.10, 2.11, 2.12, 2.13.

Summary of Modifications. Two major modifications were imposed on the model that predicts the behavior of conventional roof systems. The first one consists of using the actual value of the torsional constant of the purlin cross section and not 10 in^4 as recommended by Elhouar and Murray [3]. The second modification to the model was in determining the area of the truss members when modeling the panels. Elhouar and Murray [3] used a value for the diaphragm shear stiffness, G', of 2500 lb/in in Equation 2.4 to calculate the area of the truss members. This area will be a constant and does not change with the

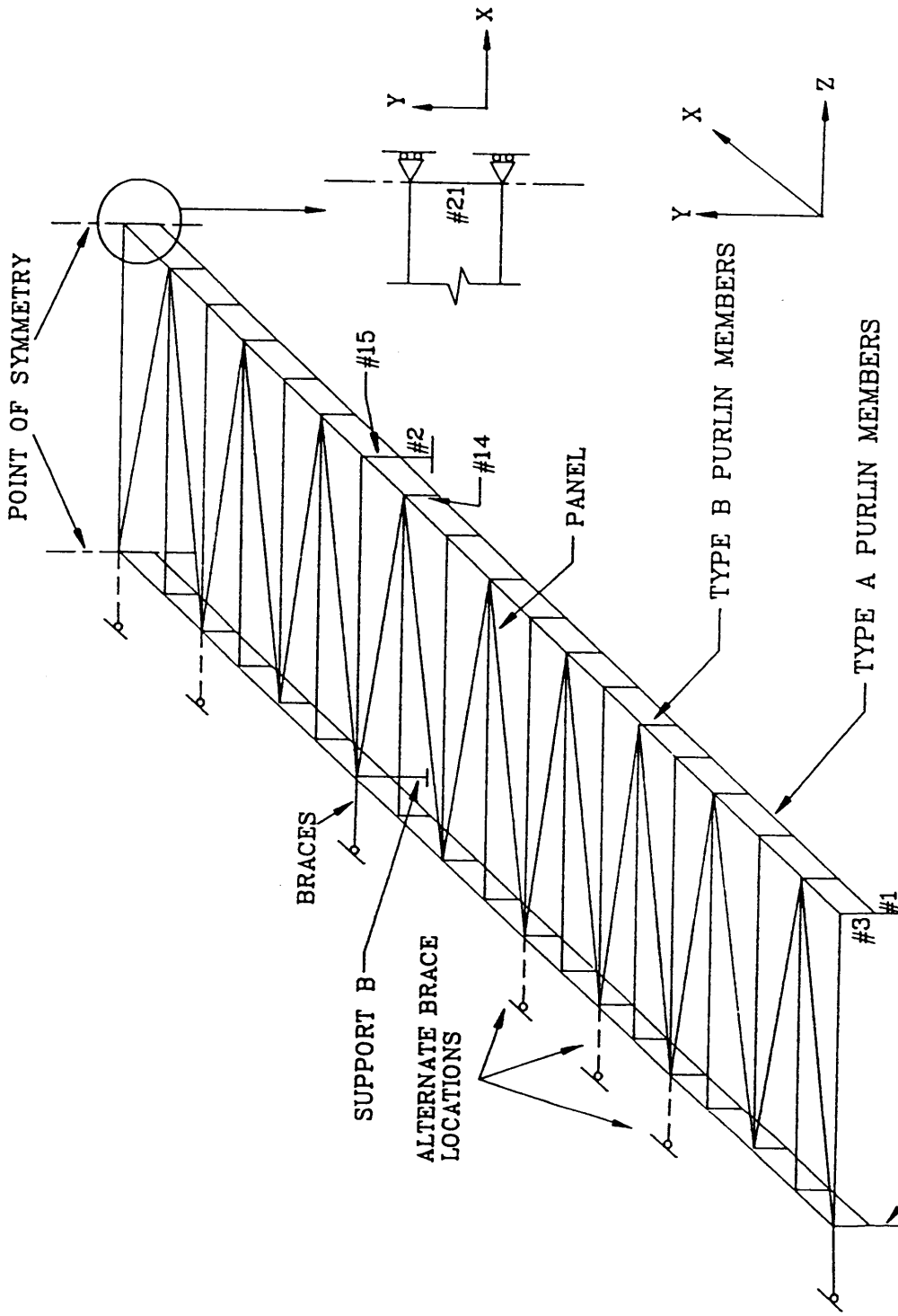

Figure 2.9 Proposed Mathematical Model for Three Span Continuous Systems

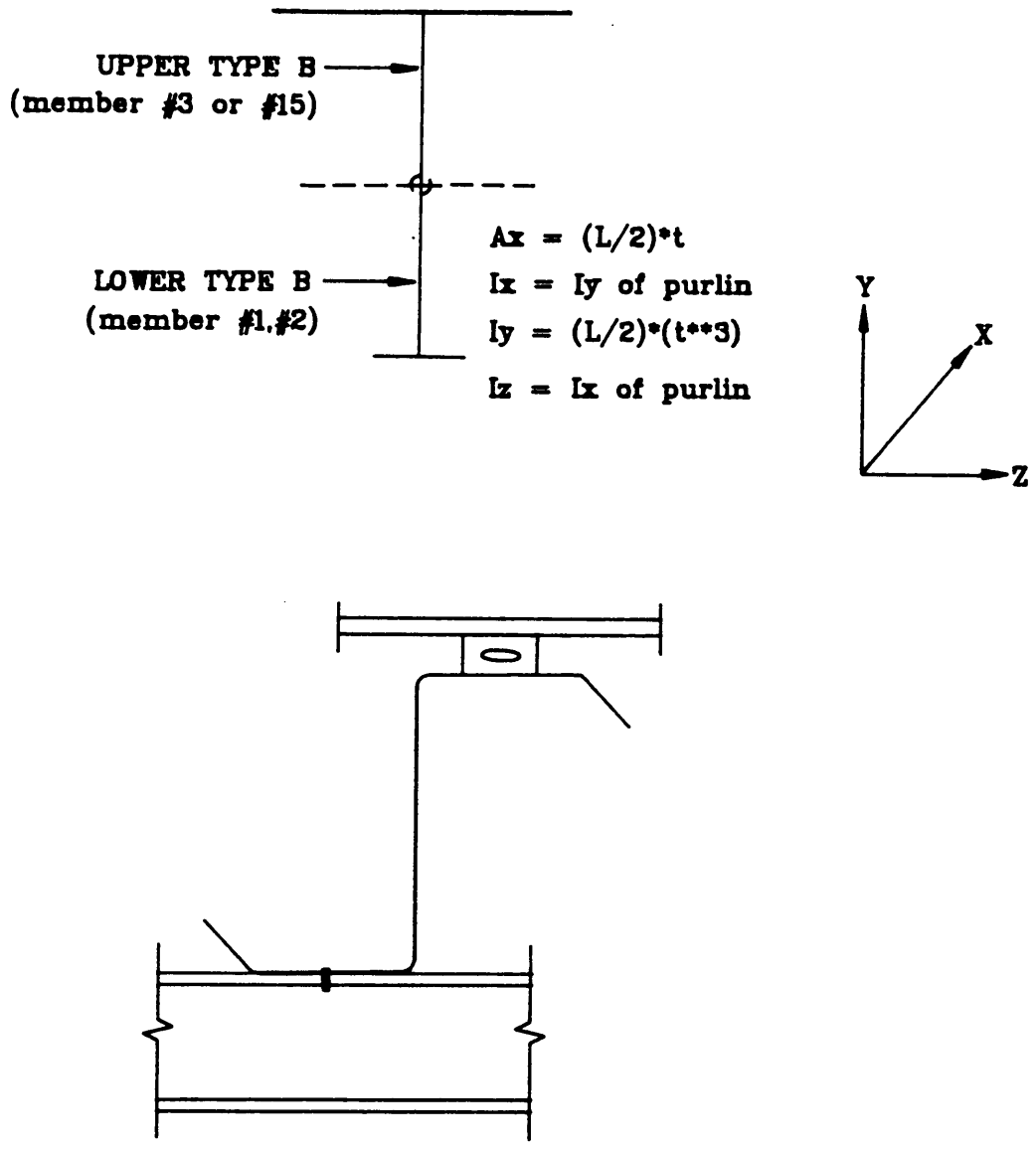

Figure 2.10 Properties for Lower Type B Members at Supports A and B

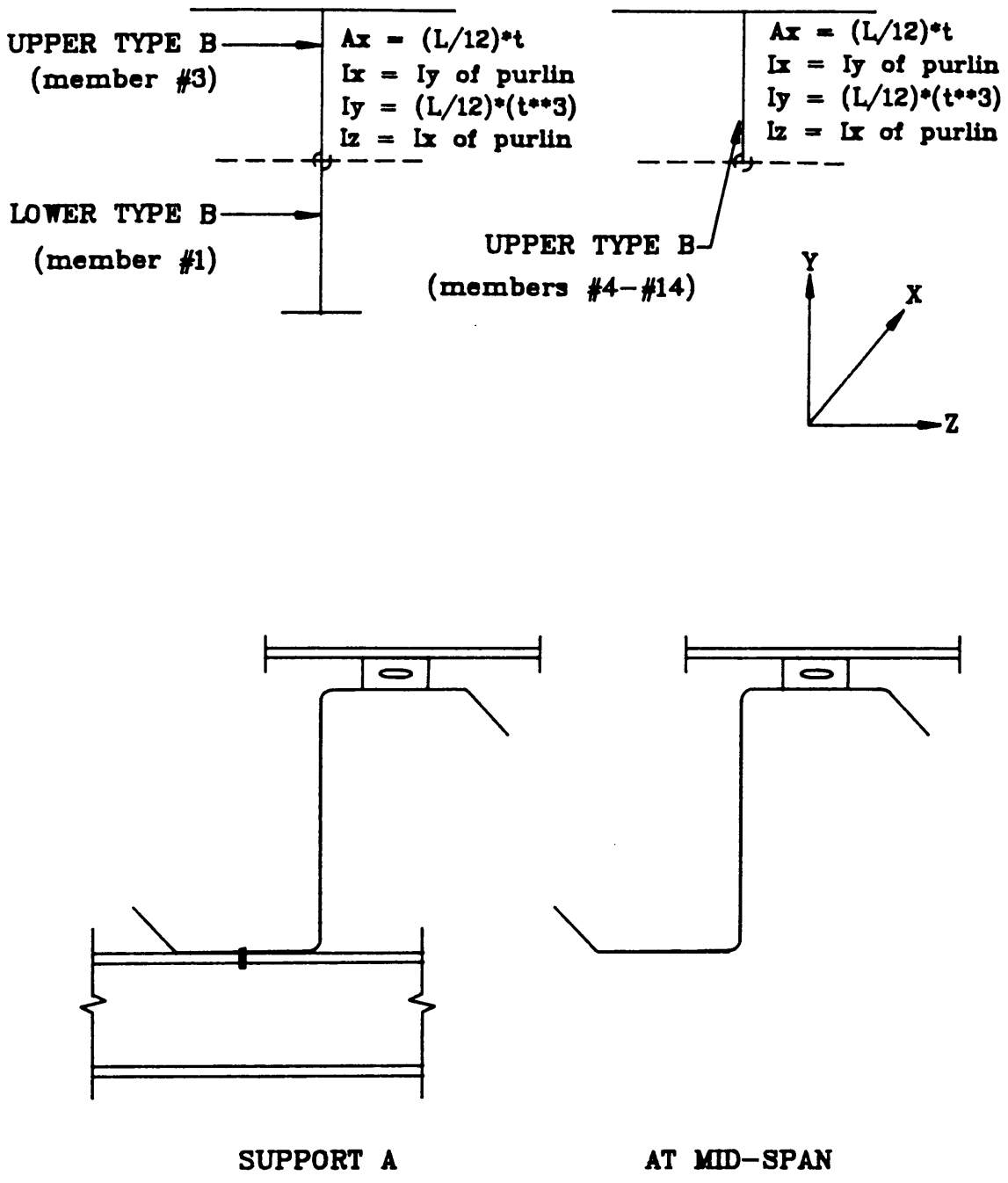

Figure 2.11 Properties for Upper Type B Members Along Span

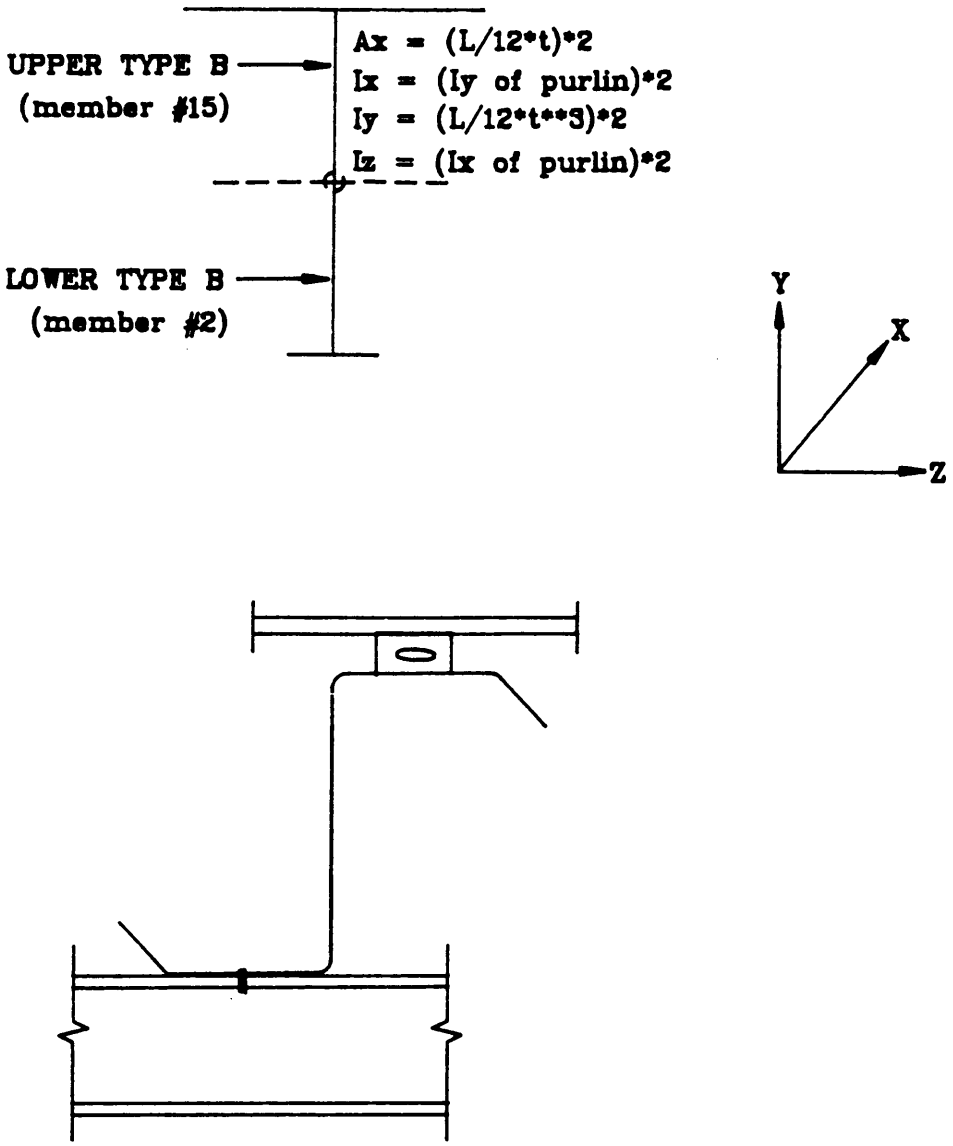

Figure 2.12 Properties for Upper Type B Member at Support B

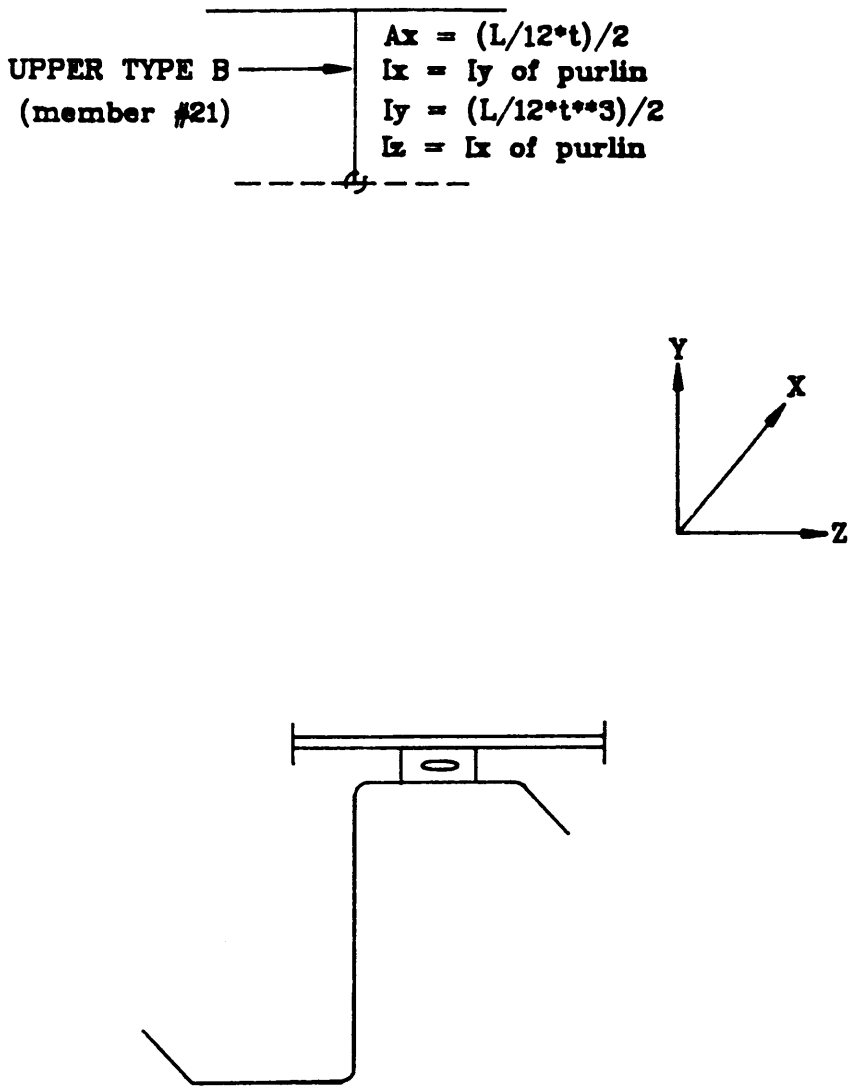

Figure 2.13 Properties for Upper Type B Members at point of Symmetry

configuration of the system. In the modified model the area is not a constant, a panel diaphragm shear stiffness test has to be performed to determine G′. This method will require a test for every different panel that is going to be modeled to determine G′ and then calculate the area of the truss members using Equation 2.4.

A third modification was made to make the model more complete and not necessarily to increase its accuracy in predicting deflections. The moment of inertia (I_x) for the lower type B members at the supports was changed to a constant, 0.00001 in^4. This modification increased the capacity of the model to predict brace forces without disturbing its capacity to predict deflections as well. Table 2.5 summarizes the three modifications.

By successfully completing the modification of the model, this deflection correlation approach can be evaluated. The results of this approach and the comparison with experimental results are discussed in Chapter III. Sample calculations are included in Appendix B.

2.3 Stiffness Model - Stress Correlation

For a given cross section with known dimensions, an allowable flexural capacity can be calculated using the 1986 AISI specification. From this capacity, the stress distribution along the cross section can also be determined (Figure 2.14) by using the general flexure formula [6]:

$$\sigma_{zz} = \frac{M_y I_x - M_x I_{xy}}{I_x I_y - I_{xy}^2} x + \frac{M_x I_y - M_y I_{xy}}{I_x I_y - I_{xy}^2} y \qquad (2.7)$$

Table 2.5

SUMMARY OF MODIFICATIONS

Properties	Conventional Roof System Model	Standing Seam System Model
Torsional Constant (I_x)	10 in.^{4}	Actual
Area of Truss Members	Constant	Depends on panel type
Moment of inertia of lower vertical Members	(L/2) x t^3	0.00001 in^4

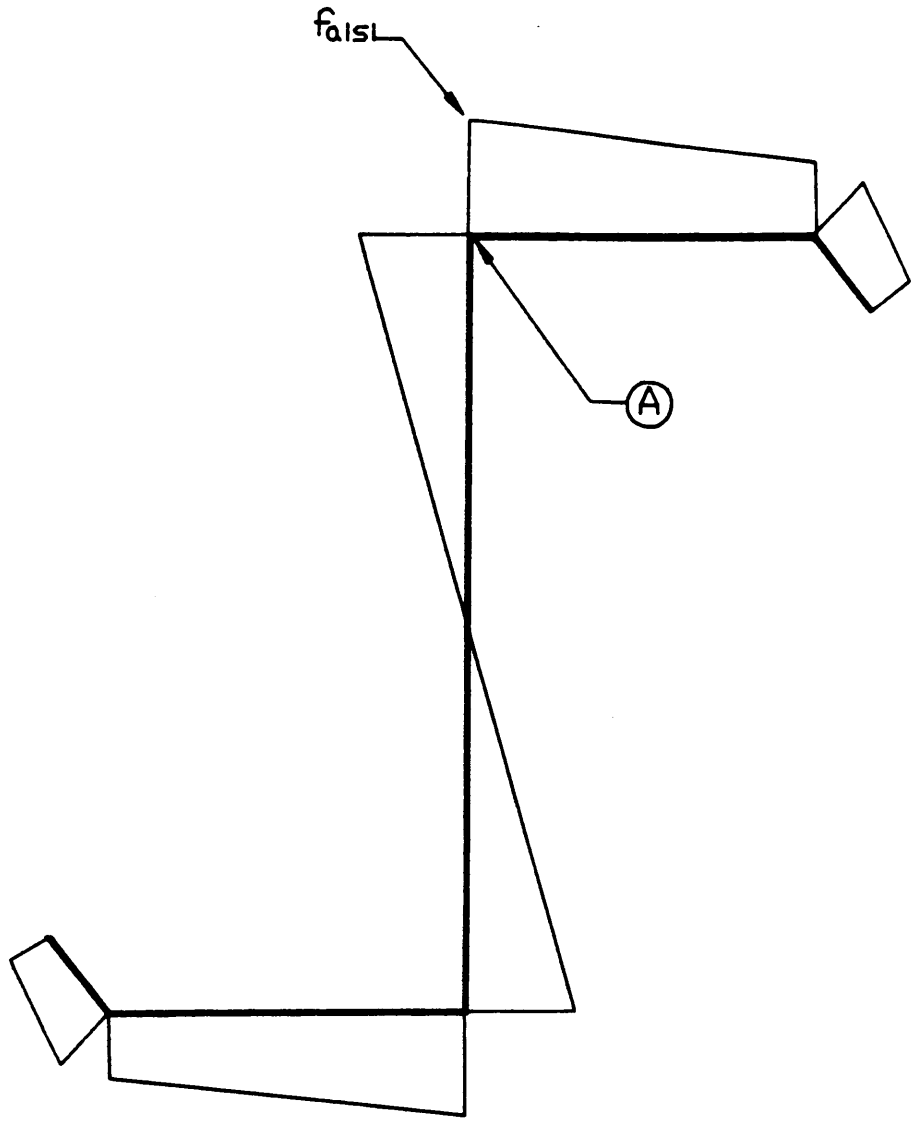

Figure 2.14 Stress Distribution from AISI Allowable Flexural Capacity

From the model developed in Section 2.2, the maximum positive moments on the principal axes of the cross section (Type A elements, Figure 2.4) corresponding to the nominal load W used in the analysis are known. Again, from this maximum moments, the stress distribution along the cross section can be calculated using Equation 2.7 (Figure 2.15).

The predicted failure load for a standing seam system can then be calculated by the following equation:

$$W_{ss_u} = \frac{f_{aisi}}{f_{max}} \times W \times 1.67 \qquad (2.8)$$

where

W_{ss_u} = predicted failure load

f_{aisi} = stress at point A in Figure 2.14 calculated from the allowable flexural capacity of the cross section

f_{max} = stress at point A in Figure 2.15 calculated from the maximum positive moments (M_x and M_y) in the model for a load W.

W = Nominal load in plf used in the mathematical model analysis

1.67 = Load factor

Since all dimensions are known, and analyses done using the mathematical model in Section 2.2 for the twelve tests of Table 1.1, verification of this approach was almost immediate. The discussion of the results and comparison with experimental results is presented in Chapter III of this thesis. Sample calculations and sample input and output data files are included in Appendix C.

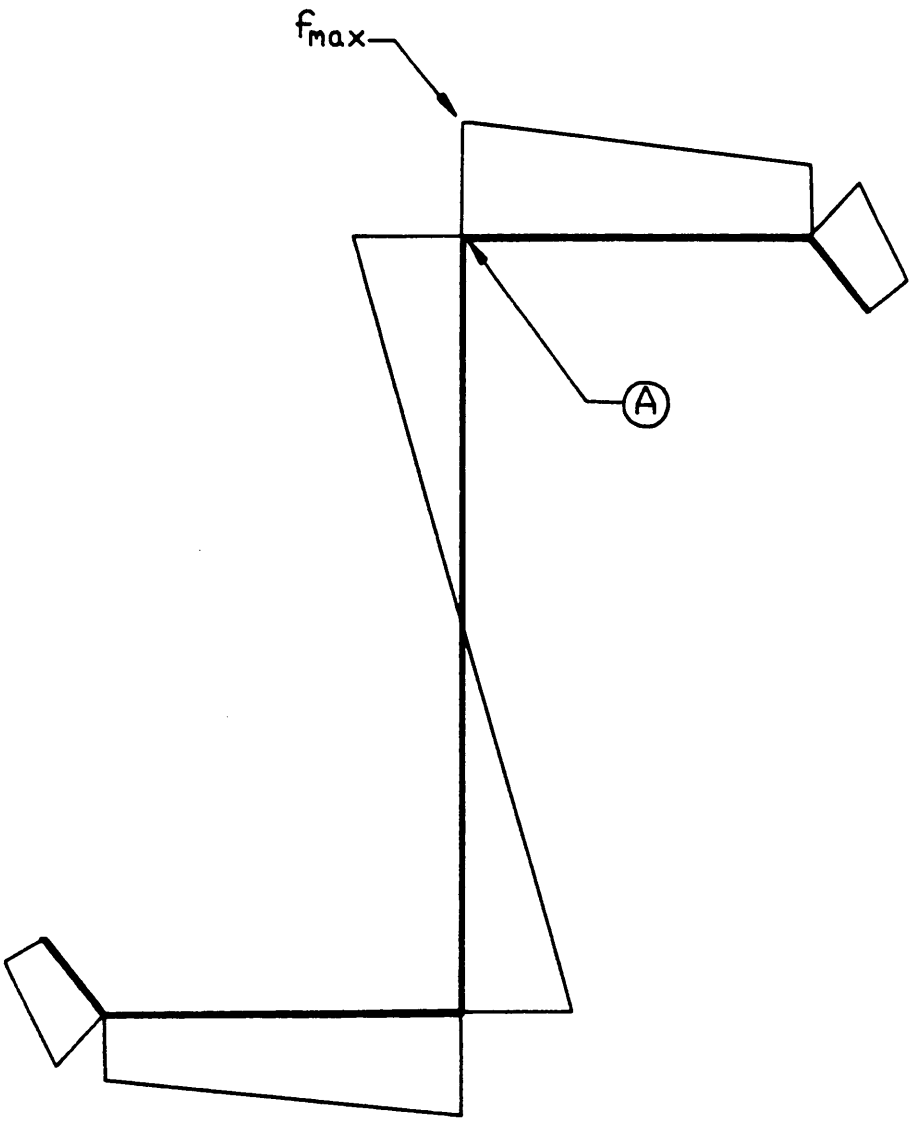

Figure 2.15 Stress Distribution from Mmax using Mathematical Model

2.4 Base Test

The base test approach calculates the predicted failure load for a multiple span standing seam system based on the experimental failure load of a one span system by simply scaling the maximum moment due to a nominal uniform load calculated from a stiffness analysis of the multiple span system. This approach is divided into two parts:

a. Experimental (Base Test) - This approach requires that a full scale test to failure be done on a one span system using the same panel type, bracing configuration and purlin size that will be used in the multiple span system. This means that for every panel type, bracing and purlin size combinations that a manufacturer has, a one span test (Base Test) is required. The results from a one span test using a specific panel type, bracing and purlin size cannot be used in predicting the failure load of a multiple span system that will use a different panel type and/or purlin size. When the one span test is complete, the failure load of the system is known (Figure 2.16) and a corresponding failure moment can be easily calculated using the following equation:

$$M_{US} = \frac{W_{US}L^2}{8} \tag{2.9}$$

where

M_{US} = Ultimate moment for single span system of span L.

W_{US} = Failure load of the single span system of span L.

b. Analytical (Stiffness Analysis) - A stiffness analysis with a nominal uniform load W has to be done for the multiple span system under consideration. From this analysis the maximum positive moment and the negative moments at the beginning of the lap are determined (Figure 2.17).

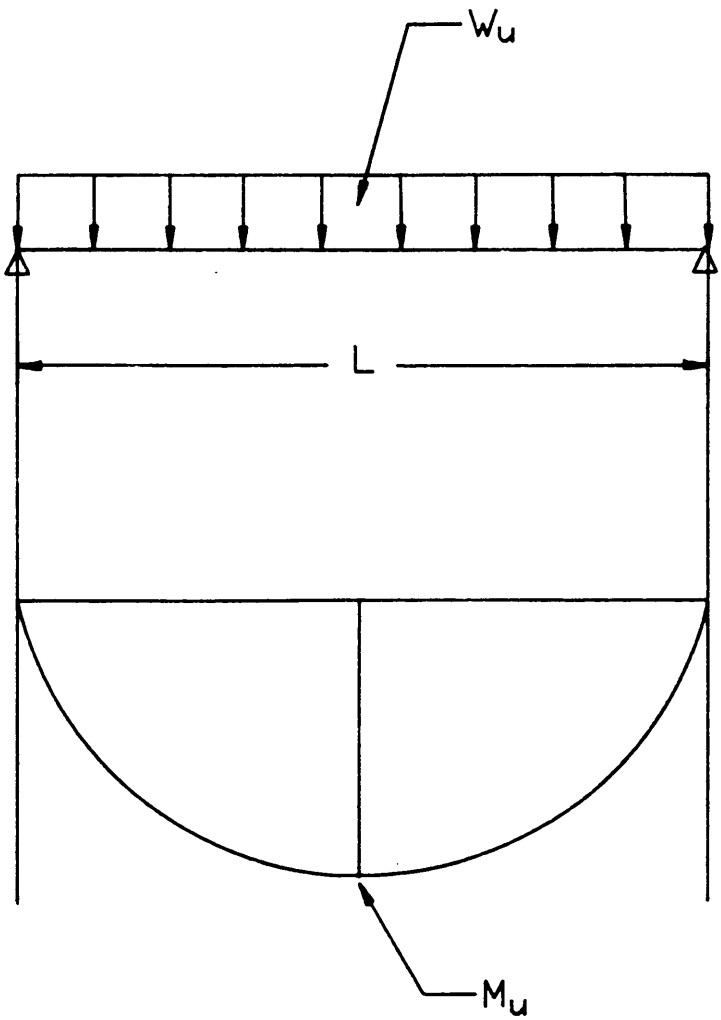

Figure 2.16 Base Test

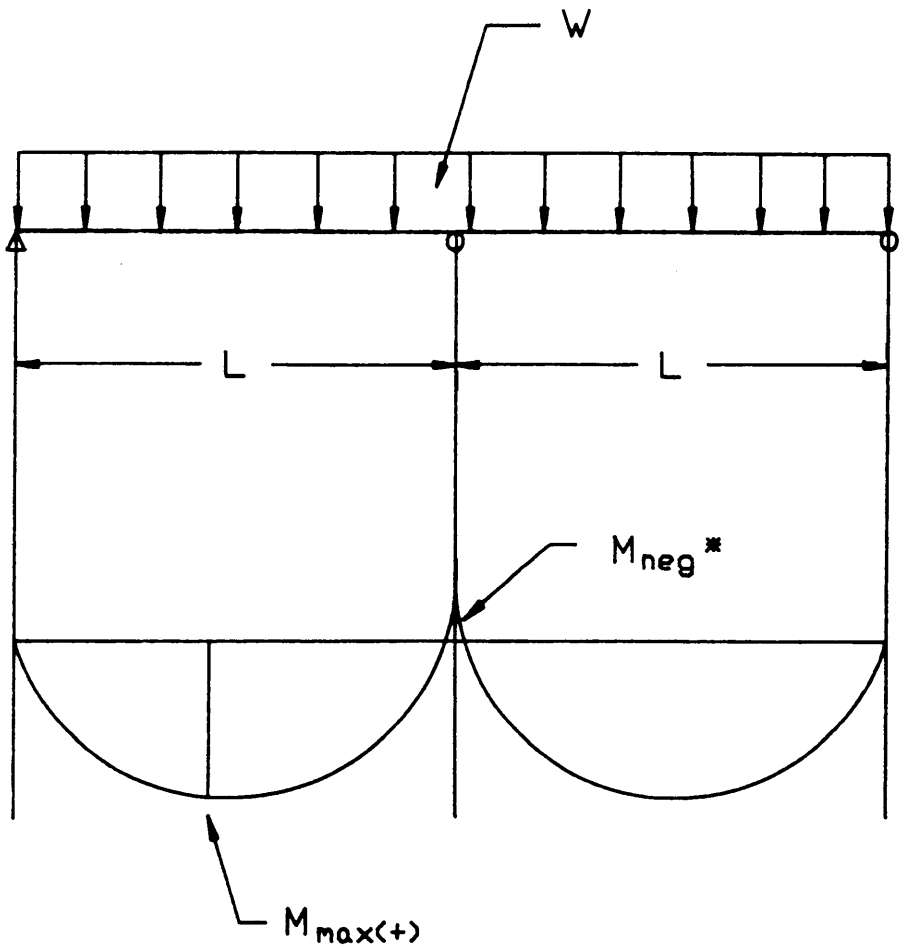

* = negative moment at beginning of lap

Figure 2.17 Stiffness Analysis

The predicted failure load for the multiple span system can be calculated as follows:

$$W_{um} = \text{min.} \begin{matrix} \dfrac{M_{us}}{M_{max(+)}} \times W \\ \dfrac{M_{aisi}}{M_{neg}} \times W \end{matrix} \qquad (2.10)$$

where

W_{um} = predicted failure load for a multiple span system

M_{us} = ultimate moment for single span system

$M_{max(+)}$ = maximum positive moment for the multiple span system from stiffness analysis

M_{aisi} = allowable flexural capacity of the cross section using the 1986 AISI Specification

M_{neg} = negative moment at the beginning of lap for the multiple span system from stiffness analysis

W = nominal load used in the stiffness analysis

To evaluate this approach, identical single span and two span continuous systems were tested using the procedure in Section 1.4. The results and comparison of predicted vs. experimental loads are discussed in Chapter III. Sample calculations are included in Appendix D.

CHAPTER III

COMPARISON OF ANALYTICAL AND EXPERIMENTAL RESULTS

3.1 Lateral Torsional Buckling vs. Experimental Results

The predicted failure loads for the six one-span tests in Table 1.1 were calculated using Equation 2.1. These predicted failure loads were compared with the experimental failure loads of the corresponding test (Table 3.1). From this comparison, it is clear that using the lateral torsional buckling equations in the 1986 AISI Specification could predict a failure load up to 86% conservative. These results are not only an indication of how conservative this approach is but also to what degree the systems are behaving as fully laterally braced. In Table 3.2, the predicted failure loads using Equation 2.1 (fully laterally unbraced) which is the lower limit and the 1986 AISI Specification for a conventional roof (fully laterally braced) which is the upper limit for a standing seam system, are tabulated. The degree of lateral restraint that standing seam panels provide will be directly related to the percent difference between the actual failure load and these predicted failure loads. When the bracing is at the rafters, only the panel shear stiffness will prevent the system from failing by lateral torsional buckling because there is no other lateral restraint on the purlins. From Table 3.2, it is clear that the panels are providing some lateral support to the purlins, but not enough to make the system behave as a conventional roof system (fully braced). When the bracing is located at the third points or midspan, the system behaves more like fully braced. The predicted failure loads for the systems with bracing at the third point or midspan using the fully constrained assumption are only 22-35% unconservative. The reason for this is that the bracing reduces the relative movement of the purlins therefore increasing the stiffness of the system.

TABLE 3.1

LATERAL TORSIONAL BUCKLING VS. EXPERIMENTAL RESULTS

Test No.	Predicted Failure Load (plf)	Actual Failure Load (plf)	% Deviation from Actual
R2/2-R-1	11.7	85.8	+86
R2/2-T-1	110.7	155.1	+29
R2/2-M-1	85.8	160.1	+46
P1/2-R-1	12.5	59.5	+79
P1/2-T-1	115.0	141.0	+18
P1/2-M-1	86.8	138.3	+37

-: unconservative

+: conservative

TABLE 3.2

UPPER AND LOWER FAILURE LOADS FOR STANDING SEAM SYSTEMS

Test No.	Predicted Fully Unbraced Failure Load (plf)	Actual Failure Load (plf)	Predicted Fully Braced Failure Load (plf)
R2/2-R-1	11.7	85.8	198.9
R2/2-T-1	110.7	155.1	204.9
R2/2-M-1	85.8	160.1	205.6
P1/2-R-1	12.5	59.5	207.2
P1/2-T-1	115.0	141.6	216.4
P1/2-M-1	86.8	138.3	210.8

This approach for calculating the predicted failure load for a standing seam system using the lateral torsional buckling equation was abandoned because the results were too conservative. Even though it was abandoned, it gave very valuable insight on the behavior of standing seam systems. When calculating the strength of a conventional system, it is assumed that the panels provide full lateral bracing. For this reason, the location of the external bracing is not a variable and only the cross-sectional properties of the purlin are used to calculate the system's strength. When considering a standing seam roof system, it is clear form Table 3.2 that the panel shear stiffness will provide some lateral restraint but not enough to make the system behave as a conventional system. Unlike a conventional system, the location of the bracing will have a significant effect on the strength of the system by increasing its stiffness. These characteristics of a standing seam system were very useful when developing other approaches and a mathematical model.

3.2 Stiffness Model-Deflection Correlation

After modeling and analyzing the six one-span tests of Table 1.1 with the mathematical model developed in Chapter II, the stiffness of the standing seam system (K_{SS}) can be calculated. It is important to recall that the only reason a mathematical model was developed is to predict the load vs. deflection curve (stiffness) for a given standing seam test in order to use it in Equation 2.2. Now that the stiffnesses for the standing seam systems are known, Equation 2.2 can be evaluated. Table 3.3 compares the predicted failure loads calculated using this approach vs. the actual failure loads, the test number with an asterisk indicates that it is not useful data because its failure mode was not the predicted failure mode. Excluding the two tests not considered useful data, the results show that this method predicts a failure load from 3.0 to 28% unconservative.

TABLE 3.3

DEFLECTION CORRELATION VS. EXPERIMENTAL RESULTS

Test No.	Predicted Failure Load (plf)	Actual Failure Load (plf)	% Deviation from Actual
R2/2-R-1	109.0	85.8	-27.0
R2/2-T-1	160.1	155.1	-3.0
R2/2-M-1	171.8	160.1	-7.3
*P1/2-R-1	129.8	59.5	-118.1
*P1/2-T-1	188.6	141.0	-33.7
P1/2-M-1	176.7	138.3	-27.8

*Not useful data.

-: unconservative

+: conservative

Even though these results look promising, the method was abandoned. The fact that the predicted failure load calculated with this method could be 25% unconservative was considered, but the main reason is that this approach requires that for every type of panel a manufacturer uses, an expensive and very accurate diaphragm shear stiffness test has to be done. This test is necessary in order to calculate the area of the truss members in the model using Equation 2.4. The mathematical model is very sensitive to the area of these members, therefore, the accuracy of the predicted failure load will be directly related to the accuracy of the truss members (panel shear stiffness). For this reason, it was concluded that this approach was not practical.

3.3 Stiffness Model - Stress Correlation

From the computer analysis done on the six one-span and twelve three span continuous tests, the maximum moments on the principal axes of the cross-section are known. Using Equation 2.7, the stress at point A in Figure 2.14 was calculated. The allowable flexural capacity based on the cross-sectional properties was also calculated using the 1986 AISI Specification. Again, the stress at point A in Figure 2.14 corresponding to the allowable flexural capacity is known. After calculating these stresses, the method can be evaluated using Equation 2.8. The results from the evaluation in Table 3.4, show that this method is from 0 to 22% conservative predicting the failure load of a system, except test R3/2-R-3 which is 9% unconservative. Again, this range excludes two tests whose failure mode was not the predicted failure mode. These results are encouraging but this method would again require the same diaphragm shear stiffness test discussed in the previous section. For this reason, this method was abandoned and a different approach that would not require such an expensive and complex test was developed.

TABLE 3.4

STRESS CORRELATION VS. EXPERIMENTAL RESULTS

Test No.	Predicted Failure Load (plf)	Actual Failure Load (plf)	%Deviation from Actual
R2/2-R-1	86.1	86.1	-0.3
R2/2-T-1	155.1	141.0	+9.3
R2/2-M-1	160.1	125.1	+22.0
*P1/2-R-1	59.5	94.8	-59.3
P1/2-T-1	141.0	128.9	+8.6
P1/2-M-1	138.3	127.1	+8.1
R3/2-R-3	85.1	92.7	-8.9
R3/2-T-3	175.5	138.8	+20.9
R3/2-M-3	137.7	131.0	+4.9
*P2/2-R-3	99.5	140.9	-41.6
P2/2-T-3	207.1	168.1	+18.8
P2/2-M-3	154.0	149.5	+2.9

*Not useful data.

-: unconservative

+: conservative

3.4 Base Test

When evaluating this approach, two sets of data were available. The first set is the data in Table 1.1 obtained from a previous project, the second set of data was obtained by conducting a series of full scale tests. Before explaining the evaluation of this data, it is important to recall the steps necessary and the limitations of this method. The objective of this approach is to calculate a predicted failure load for a multiple span standing seam system based on the experimental failure load of a one span system. This requires:

1. Full scale test to failure of a one span system using same panel type and purlin size as multiple span system.
2. Stiffness analysis of multiple span system.
3. Allowable flexural capacity of multiple span system determined from 1986 AISI Specification.

When all these quantities are known, Equation 2.10 can be evaluated to calculate the predicted failure load for a multiple span system. Following is the explanation and evaluation of this method using both sets of data.

a. Data from Table 1.1: The evaluation of the base test method using this data will consist in predicting the failure load of the three-span continuous systems and comparing it to the actual failure load. Referring to Equation 2.10, the only unknowns in the equation are the maximum positive moment and the negative moment from a stiffness analysis of the multiple span system. The allowable flexural capacity for the multiple span system and the failure load for the one-span systems are known. One of the characteristics and limitations of this approach, as previously discussed, is the fact that the same panel type and purlin size used in the one span system has to be used in the multiple span system. From Table 1.1, none of the three span systems have the same panel type as the one span systems. The one span systems use rib type number 2 and pan type

number 1 panels; the three-span systems use rib type number 3 and pan type number 2 panels. Even though the panels are not the same, the one span systems using rib type number 2 panels will be used in predicting the failure loads of the three-span systems using rib type number 3 panels, the same approach for the pan type panels. When discussing the results, this inconsistency will be considered. All the parameters necessary to evaluate Equation 2.10 and the corresponding load for all six three span systems, are tabulated in Table 3.5.

b. Data from Full Scale Testing: Full scale testing was done to gather more data to verify this approach. Two single span base tests with a span length of 25 ft and using rib type and pan type panels with the bracing at the rafters were conducted (Figure 3.1). The multiple span systems consisted of two, two-span system with spans of 25 ft. Both multiple span tests were done using the same rib and pan type panels and purlin size as the base test. The bracing configuration was the same, at the rafters, and the compression flange in the negative moment region was fully braced. In all tests, 10 in. deep Z-purlins, with the top flanges facing in the same direction were used. Table 3.6 gives a complete test matrix. Test designations are to be interpreted as follows: P/2-R-1 indicates pan type panel (P), two purlin lines (2), anchorage braces at rafters (-R), Single span (-1). R/2-R-2 indicates rib type panel (R), two purlin lines (2), anchorage braces at rafters (-R), two span (-2). After collecting the data from the full scale testing, the method was again evaluated using Equation 2.10. All the parameters necessary to evaluate Equation 2.10 and the corresponding failure load for both two span systems are tabulated in Table 3.7.

From the evaluation done with the data in Table 1.1, the base test method predicts a failure load for the multiple span systems within 3-22% of the actual failure load. These results are very encouraging because the range is not only good but also, the panels used were mixed. If the panels matched, the percent

TABLE 3.5

BASE TEST VS. EXPERIMENTAL RESULTS FROM TABLE 1.1

Test No.	M_{us} (ft-lb)	$M_{max}^{(+)}$ (ft-lb)	M_{aisi} (ft-lb)	M_{neg} (ft-lb)	W_{um}^{+} (plf)	W_{um}^{-} (plf)	Actual Failure Load (plf)	% Deviation from Actual
R3/2-R-3	4290	4125	7207	4,426	104.0	162.8	85.1	-22.2
R3/2-T-3	7755	4125	7138	4,426	188.0	161.3	175.5	+8.1
*R3/2-M-3	8005	4125	7207	4,426	194.1	162.8	137.7	-18.2
*P2/2-R-3	2975	4125	6563	4,426	72.1	148.3	99.5	+27.5
P2/2-T-3	7050	4125	7238	4,426	170.9	163.5	207.1	+21.0
P2/2-M-3	6915	4125	7041	4,426	167.6	159.1	154.0	-3.3

*Not useful data

-: unconservative

+: conservative

$M_{max}^{(+)}$ and $M_{max}^{(-)}$ from nominal load of 100 plf

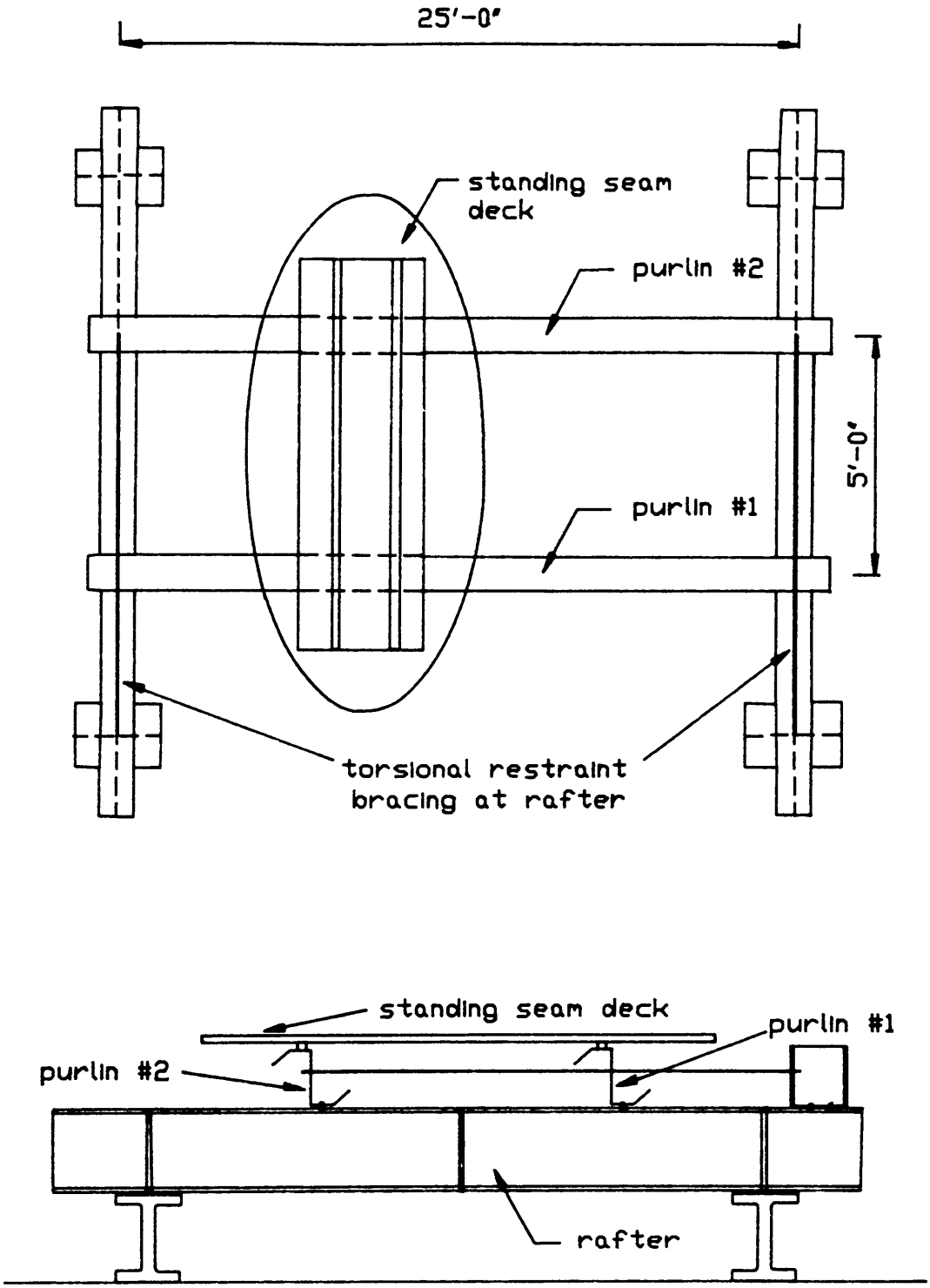

Figure 3.1 Simple Span Test Setup at Prices Fork Laboratory

TABLE 3.6

TEST MATRIX

Test No.	Span(s) (ft)	Panel Type	Clip Type	Bracing Configuration
R/2-R-1	25	Rib	Two Piece	Rafters
P/2-R-1	25	Pan	One Piece	Rafters
R/2-R-2	2@25	Rib	Two Piece	Rafters
P/2-R-2	2@25	Pan	One Piece	Rafters

TABLE 3.7

BASE TEST VS. EXPERIMENTAL RESULTS FROM FULL SCALE TESTING

Test No.	M_{us} (ft-lb)	$M_{max}^{(+)}$ (ft-lb)	M_{aisi}^{*} (ft-lb)	M_{neg} (ft-lb)	W_{um}^{+} (lb)	W_{um}^{-} (plf)	Actual Failure Load (plf)	% Deviation from Actual
R2-R-2	6688	4308	10,133	6,608	155.2	153.3	155.0	+1.1
P2-R-Z	7734	4208	9,975	6,542	183.8	152.5	143.5	-6.3

*Based on assumed yield stress of 55 ksi

- : unconservative

+ : conservative

$M_{max}^{(+)}$ and $M_{max}^{(-)}$ from nominal load of 100 plf

difference between the predicted and actual failure loads is expected to decrease. That is exactly what happened when the method was evaluated using the data from the full scale testing. Referring to Table 3.7, the percent difference between the predicted and actual failure loads is only 1.0-6.0%. Another parameter which is very important to consider when studying these results is if $M_{max(+)}$ or M_{neg} control the predicted failure load of the multiple span system. When $M_{max(+)}$ controls, it means that the shear stiffness of the panels is very weak, therefore it does not provide the system with significant lateral support. Under this condition, the system's stiffness and strength are decreased significantly. When the M_{neg} controls, it is more a design situation. The standing seam panels will provide enough lateral support so that $M_{max(+)}$ doesn't govern because it is a small value. This situation will make the allowable flexural capaicty (local buckling provisions) of the cross-section the controlling parameter in the system's strength.

From Table 3.5, only in Tests R3/2-R-3 and P2/2-R-3 the $M_{max(+)}$ was the controlling parameter, in the other tests M_{neg} controlled the predicted failure load. In Table 3.7, both tests were controlled by M_{neg}.

Even though the amount of data is insufficient to prove that this is an infallible approach, the data available makes it one of the most accurate, inexpensive and simple procedures. It is true that this method will require some experimental testing, but so do the approaches using the mathematical model. The advantage is that a full scale test of a single span system is much less complicated and expensive than a very accurate diaphragm shear stiffness test required by the mathematical model. Reducing the complexity of the approach without compromising its accuracy seems the most practical and reasonable alternative for the solution. Taking this into consideration, the approach to determine the strength of Z-purlin supported standing seam systems that will be recommended is the base test method.

CHAPTER IV

DESIGN PROCEDURE

4.1 Methodology

The development of Equation 2.10 did not require an extensive manipulation of data or mathematical analysis. It was first used as an approximation of the behavior of multiple span conventional roof systems and for that reason, it was decided to determine its accuracy and its feasibility as a method for determining the strength of multiple span standing seam systems. Since evaluation of the approach using previous data was encouraging, the method was refined and a series of tests done to verify its validity.

From the results obtained after the experimental testing was completed, it was concluded that this method is the most convenient (Section 3.4). Equation 2.10 and its variables will be defined and discussed in more detail in Section 4.3. Refer to Appendix D for sample calculations.

4.2 Limits of Parameters and Configurations

The base test method predicts the failure load for a multiple span standing seam system based on the failure load of a single span system. The approach requires that full scale testing be done for single span systems. The number of tests will depend on the number of bracing configurations (unbraced length), panel types, purlin sizes and their combinations that a manufacturer has. The reason for this is that the bracing configuration, the panel type (shear stiffness) and purlin cross-section (flexural capacity) control the strength of the system.

From the mathematical model of a system using a given span, it was determined that no other member properties have such an impact on the system's strength as the bracing, panel type and purlin size. The span of the base test (single span system) does not have to be the same as the spans of the multiple span systems but it is recommended when possible to use the same span length for both systems. The bracing configuration, panel type, and purlin size must be the same in both systems. If the multiple span system uses pan type panels, the base test must use pan type panels. These limitations on the parameters and configurations are to control the variables that were determined to control the system's strength (unbraced length, diaphragm shear stiffness, and flexural capacity of the cross section).

4.3 Design Equations

The failure load for a multiple span standing seam system can be predicted using equation 2.10. When evaluating this equation, two values will be calculated of which the minimum will be the predicted failure load.

The first predicted load is calculated using the following equation:

$$W_{um} = \frac{M_{us}}{M_{max(+)}} \times W \qquad (4.1)$$

where

W_{um} = predicted failure load for a multiple span system

M_{us} = ultimate moment for base test

$M_{max(+)}$ = maximum positive moment for the multiple span system from stiffness analysis

W = nominal load used in stiffness analysis of multiple span system

Equation 4.1 predicts the failure load for a multiple span standing seam system by scaling the failure load of the corresponding base test.

The second predicted failure load is given by the equation:

$$W_{um} = \frac{M_{AISI}}{M_{neg}} \times W \qquad (4.2)$$

where

W_{um} = predicted failure load for a multiple span system

M_{AISI} = allowable flexural capacity of the purlin's cross section using the 1986 AISI Specification

M_{neg} = negative moment at beginning of lap for the multiple span system from stiffness analysis

W = nominal load used in stiffness analysis of multiple span system

Equation 4.2 is based on the assumption that the system's laps (supports) are fully braced (Figure 2.17). This assumption is made because at that location there is usually another structural member or bracing system framed perpendicular to the purlin's cross section providing lateral support. Under this situation, the local buckling provisions of the 1986 AISI Specification have to be considered. The allowable flexural capacity assuming constrained bending (M_{AISI}) will be used instead of the failure load for the base test. The value calculated by Equation 4.2 will insure that the predicted failure load calculated for the system does not exceed the maximum possible load for a cross section based on the allowable flexural capacity assuming constrained bending. The reason this is the upper limit is because when the cross section is fully braced (conventional roof systems), the capacity of the cross section will be at its maximum. This maximum capacity or allowable flexural capacity can be

calculated using the 1986 AISI Specification. A predicted failure load that exceeds Equation 4.2 is physically impossible to reach because it would imply the fact that the flexural capacity of the cross section is greater than the maximum allowable flexural capacity permitted by the 1986 AISI Specification. For this reason, the predicted failure load for a multiple span system is the minimum of Equations 4.1 and 4.2.

4.4 Conclusion

Even though Equation 2.10 was not derived analytically, the parameters that control it (diaphragm shear stiffness, flexural capacity, and unbraced length) are the same ones that the mathematical model proved to have a significant effect on the system's strength. These parameters are not explicitly used in equation 2.10 but they are included in the ultimate moment of the base test (M_{us}). The ultimate moment of the base test is directly affected by these parameters, therefore, the predicted failure load for a multiple span system will also be a function of these parameters. This is why it is so important to be consistent and use the same panel type, bracing, and purlin size in the base test and the multiple span system.

CHAPTER V

SUMMARY AND RECOMMENDATIONS

5.1 Summary

Four approaches were developed and evaluated for their accuracy in predicting the strength of Z-purlin supported standing seam roof systems under gravity loading.

a. Lateral Buckling Strength from the 1986 AISI Specification

This approach was evaluated to determine how much lateral support the standing seam panels provide to the purlins. This is an important parameter in the behavior of standing seam systems because the failure load is directly related to the system's stiffness. The results showed that this approach is too conservative, implying that the panels provide a considerable amount of lateral support but not enough for the system to behave as a conventional roof system (continuous lateral support). The approach was abandoned due to its lack of accuracy in predicting the failure load.

b. Stiffness Model - Deflection Correlation

The basis for this approach is the fact that at failure it appeared that the deflections at failure were the same for any system. A mathematical model was developed to predict the deflections (stiffness) of any standing seam system in order to back track a corresponding predicted failure load. From the model

developed, it was found that only three parameters will have a significant effect on the system's strength: panel type (diaphragm shear stiffness), bracing configuration (unbraced length) and purlin size (allowable flexural capacity). Sliding friction in the clips and "drape" restraint effects of the standing seam deck on the system's strength are negligible.

Even though the results were encouraging, the approach was abandoned because it requires that a very accurate and expensive diaphragm shear stiffness test be done on every panel type that the manufacturer has. This was considered to be impractical and complex.

c. Stiffness Model - Stress Correlation

The mathematical model developed was used to calculate the maximum stresses on the cross section of the system's purlins. These stresses were then used to predict a failure load simply by scaling them using the stresses calculated from the allowable flexural capacity of the cross sections from the 1986 AISI Specification.

Again, the results were encouraging but the approach was abandoned on the basis of cost and complexity since the model would require the same diaphragm shear stiffness test.

d. Base Test

This method predicts the failure load of a multiple span standing seam system by scaling the ultimate load of a corresponding single span test that uses the same panel type, purlin size and bracing configuration. A full scale test of a single span system and a stiffness analysis of the multiple span system under consideration are required to calculate a predicted failure load. Even though

some experimental testing is necessary, the complexity and cost are minimum compared to a diaphragm shear stiffness test required by the previous approaches. The same parameters that control the system's strength as determined from the mathematical model are considered in this approach, therefore, accuracy is not sacrificed for simplicity. It is important to remember that the panel type, bracing configuration, and purlin size must be the same for the base test and multiple span system in order to obtain acceptable predicted failure loads.

Based on the encouraging evaluation results and the method's characteristics, it was concluded that this is the most practical and reasonable approach to determine the strength of multiple span Z-purlin supported standing seam roof systems under gravity loading.

5.2 Recommendations

As discussed in the previous section, the base test method is recommended to predict the strength of Z-purlin supported standing seam systems under gravity loads. Even though accuracy might not be significantly higher as compared to the deflection and stress correlation approaches, feasibility and practicality are. On either approach experimental testing is required. For this reason, if accuracy is consistent among them, the approach with the simpler and more cost effective testing is the best alternative. This is the criterion used in selecting the base test method. Unlike the other two approaches mentioned above, the base test method does not require a diaphragm shear stiffness test. This test is very complex and its accuracy has to be very high in order to obtain good results. On the other hand, a full scale test of a single span system, required by the base test, does not require a high degree of accuracy to obtain accurate results and complexity is also decreased.

When using the Base Test Method, these recommendations should be followed:

1. Base Test and multiple span system must be identical (bracing, panel type and purlin size).
2. Use same span length in Base Test and multiple span system.
3. Due to the limited amount of data available for the method's evaluation, no definite conclusion can be made on its capacity to predict the strength of a system. It is obvious that the results are very encouraging and for this reason it is also recommended that more testing be done in order to have a more complete and dependable approach.

REFERENCES

1. "Metal Roofs Gaining Popularity", Building, The College of Engineering, University of Wisconsin-Madison, Volume 4, Number 1, Winter 1988, pp. 1-5.

2. Rivard, P., and Murray, T. M., "Anchorage Forces in Two Purlin Line Standing Seam z-Purlin Supported Roof Systems", Fears Structural Engineering laboratory, Report No. FSEL/MBMA 86-01, University of Oklahoma, Norman, Oklahoma, December 1986.

3. Elhouar, S., and Murray, T. M., "Prediction of Lateral Restraint Forces for Z-Purlin Supported Roof Systems", Fears Structural Engineering Laboratory, Report No. FSEL/MBMA 85-03, University of Oklahoma, Norman, Oklahoma, May 1985.

4. Ghazanfari, A., and Murray, T. M., "Prediction of Lateral Restraint Forces of Single Span Z-Purlins with Experimental Verification", Fears Structural Engineering Laboratory, Report No. FSEL/MBMA 83-04, University of Oklahoma, Norman, Oklahoma, October 1983.

5. Cold-Formed Steel Design Manual, American Iron and Steel Institute, Washington, D.C., 1986.

6. Boresi, Arthur P., and Sidebottom, Omar M., Advanced Mechanics of Materials, John Wiley & Sons, Fourth Edition, New York, 1985.

7. Curtis, L. E., and Murray, T. M., "Simple Span Z-Purlin Tests to Determine Brace Force Accumulation", Fears Structural Engineering Laboratory, Report No. FSEL/MBMA 83-02, University of Oklahoma, Norman, Oklahoma, July 1983.

APPENDIX A

LATERAL BUCKLING STRENGTH SAMPLE CALCULATIONS

Calculate the predicted failure load in plf for test No. R2/2-T-1 (see Table 1.1) using the lateral buckling strength provisions of the 1986 AISI Specification.

Span: 20 ft

Restraint Configuration: Third points

Purlin Data: See Figure A.1 for cross section dimensions and properties

Yield Stress: 56.6 ksi

For the lateral unbraced segments of doubly-or singly-symmetric sections subject to lateral buckling, M_n shall be determined as follows (Section 2.1):

$$M_n = S_c \frac{M_c}{S_f} \qquad (A.1)$$

Since there are two different laterally unbraced segments in the system, two predicted failure loads will be calculated with the minimum controlling.

a. Laterally unbraced segment from support to first lateral restraint.

1. Calculate the elastic critical moment for point symmetric cross-section (Z)

$$M_e = \frac{\pi^2 E C_b d I_{yc}}{2L^2} \qquad (A.2)$$

where

L = unbraced length of member

I_{yc} = Moment of inertia of the compression portion of a section about the gravity axis of the entire section parallel to the web, using the full unreduced section.

$C_b = 1.75 + 1.05[(M_1/M_2) + 0.3[(M_1/M_2)]^2 \leq 2.3$

d = Depth of section

For this problem:

L = 80.0 in

$I_{yc} = I_y/2 = 0.8079/2 = 0.404$ in^4

C_b = 1

d = 8.03 in

$$M_e = \frac{\pi^2(29{,}500)(1.75)(8.03)(0.404)}{2(80.0)^2} = 129 \text{ k-in}$$

2. Calculate the moment causing initial yield at the extreme compression fiber of the full section.

$$M_y = S_f F_y \qquad \text{(A.3)}$$

where

S_f = Elastic section modulus of the full unreduced section for the extreme compression fiber.

F_y = yield stress of the material

$$S_f = \frac{Ig}{d/2} = \frac{10.36}{4.01} = 2.58 \text{ in}^3$$

F_y = 56.6 ksi

$M_y = 2.58(56.6) = 146$ k-in

3. For $2.78\ M_y > M_e > 0.56\ M_y$ the critical moment (M_c) is calculated:

$$M_c = \frac{10}{9} M_y \left(1 - \frac{10M_y}{36\ M_e}\right) \qquad (A.4)$$

$$M_c = \frac{10}{9}(146)\left[1 - \frac{10(146)}{36(129)}\right] = 111.2 \text{ k-in}$$

4. Evaluate Equation A.1

$$S_c = \frac{I_{eff}}{d/2} = \frac{9.38}{4.03} = 2.3 \text{ in}^3$$

$$M_c = 111.2 \text{ k-in}$$

$$S_f = 2.58 \text{ in}^3$$

$$M_n = 2.3 \left(\frac{111.2}{2.58}\right) = 99 \text{ k-in}$$

$$W_n = \frac{M_n(8)}{L^2} = \left[\frac{(99 \div 12)8}{20^2}\right] 1000 = 165 \text{ plf}$$

b. Laterally unbraced segment from lateral restraint to lateral restraint.

1. Calculate the elastic critical moment for point symmetric cross-section using Equation A.2

$$M_e = \frac{\pi^2(29{,}500)(1)(8.03)0.404}{2(80)^2} = 73.7 \text{ k-in}$$

2. The moment causing initial yield at the extreme compression fiber of the full section (M_y) is known from part a.

$$M_y = 146 \text{ k-in}$$

3. For $M_e \leq 0.56\ M_y$. The critical moment (M_c) is calculated

$$M_c = M_e \qquad (A.5)$$

4. Evaluate Equation A.1

$$M_n = 2.3(\frac{73.7}{2.58}) = 66 \text{ k-in}$$

$$W_n = [\frac{(66 \div 12)8}{20^2}]\ 1000 = 110 \text{ plf (controls)}$$

The predicted failure load for test No. R2/2-T-1 is

$W_n = 110$ plf

(The actual failure load was 155.1 plf.)

Purlin #1

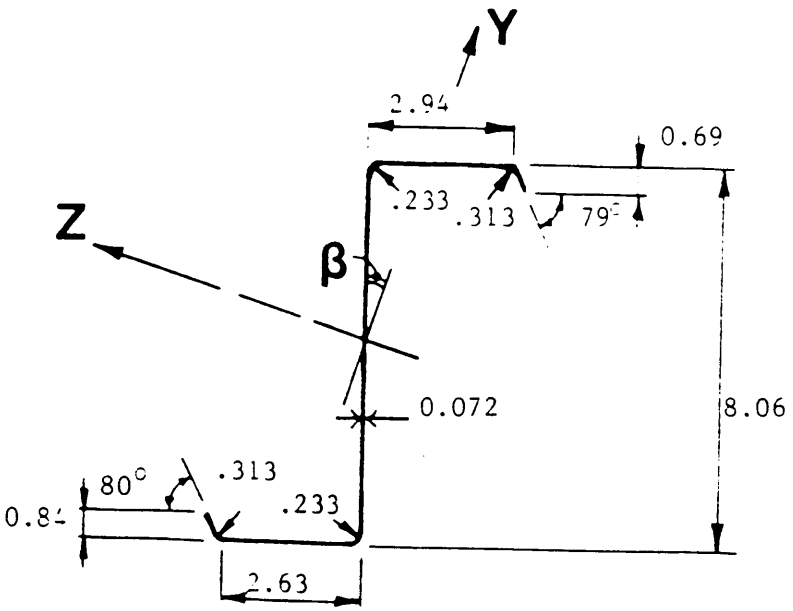

Properties: Span (ft) = 20.0 I_x (in^4) = 0.0019
Area (in^2) = 1.0657 I_y (in^4) = 0.7863
β(deg) = 18.2899 I_z (in^4) = 11.8114

Purlin #2

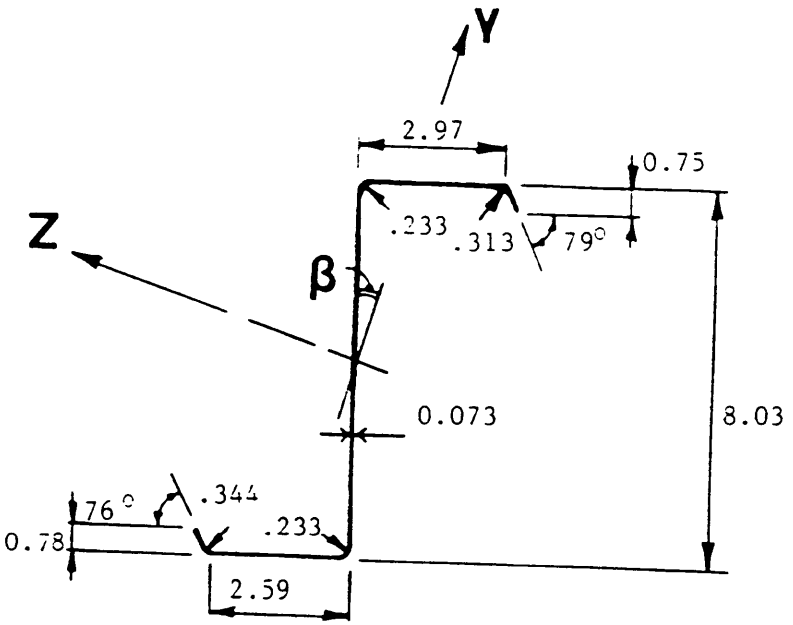

Properties: Span (ft) = 20.0 I_x (in^4) = 0.0019
Area (in^2) = 1.0789 I_y (in^4) = 0.8079
β(deg) = 18.5396 I_z (in^4) = 11.9048

Figure A.1 Measured Purlin Dimensions and Calculated Properties, Test R2/2-T-1

APPENDIX B

DEFLECTION CORRELATION SAMPLE CALCULATIONS

Calculate the predicted failure load in plf for test No. R2/2-R-1 (see Table 1.1) using the deflection correlation approach.

Span: 20 ft

Restraint Configuration: Supports

Purlin Data: See Figure B.1 for cross section dimensions and properties

Yield Stress: 56.6 ksi

The predicted failure load for a standing seam system using this approach can be calculated using the following equation (see Section 2.2):

$$M_{SS} = W_{AISI} \times K_{SS}/K_C \qquad (B.1)$$

Two steps are necessary in determining the values for the unknowns in Equation B.1. The first step is to calculate the allowable flexural capacity of a cross-section using the 1986 AISI provisions for local buckling. From this analysis, the values for W_{AISI} (allowable flexural capacity) and K_C (stiffness of system assuming it behaves as a conventional system) are known. The second step requires the use of the mathematical model to calculate K_{SS} (stiffness of standing seam system).

a. Calculate W_{AISI} and K_C

1. Using the dimensions in Figure B.1, an allowable flexural capacity for both cross-sections was calculated (see Figure B.2 and B.3). The minimum of both capacities will be used in the calculations.

Therefore, the ultimate capacity of the system according to the 1986 AISI Specification is:

$$M_u = 71.46 \times 1.67 = 119.3 \text{ k-in}$$

The corresponding ultimate failure load is:

$$M_u = \left[\frac{(119.3 \div 12)8}{(20)^2}\right] 1{,}000 = 199 \text{ plf}$$

The deflection at ultimate load is:

$$\Delta = \frac{5(199 \div 12)(20 \times 12)^4}{384(29{,}500)(9.91)} = 2.45 \text{ in.}$$

2. The stiffness of the system assuming it behaves as a conventional or through-fastened system can be calculated:

$$K_c = \frac{199(20)}{2.45} = 1{,}624 \text{ lb/in}$$

b. Calculate K_{ss}

1. Calculate the cross-section properties for the elements on the model. Refer to Figures 2.4 and 2.7 for the location and equations corresponding to these members.

For purlin #1:

Member/Type	Area (in^2)	I_x (in^4)	I_y (in^4)	I_z (in^4)	β (deg.)
Purlin A/ Type A	1.0225	0.0016	0.7645	11.3487	18.396
Upper A/Type B	1.38	0.7645	0.00055	0.0016	--
Lower A/Type B	8.28	0.7645	0.03942	0.0016	--

For purlin #2:

Member/Type	Area (in^2)	I_x (in^4)	I_y (in^4)	I_z (in^4)	β (deg.)
Purlin B/ Type A	1.073	0.0019	0.7964	11.9071	18.341
Upper B/Type B	1.45	0.7964	0.00064	0.0019	--
Lower B/Type B	8.7	0.7964	0.04573	0.0019	--

2. A load of 40 plf will be used in the analysis. As discussed in Section 2.2.1, this load has to be divided into a uniform applied torque and a uniform distributed load applied to the Type A members.

The uniform applied torque on both purlins is calculated:

$$M_x = W(b_f/3) \qquad \text{(B.2)}$$

where

$W = 40$ plf

$b_f = 2.97$ in

therefore

$$M_x = \frac{40(2.97.3)}{12} = 3.3 \text{ lb-ft/ft}$$

The uniform distributed load will have two components applied in the direction of the principal axes for the cross section (y and z). Refer to Figure B.1 for geometry. These components can be calculated using the following equations:

$$W_y = W \cos\beta \tag{B.3}$$

$$W_z = W \sin\beta \tag{B.4}$$

where

W = 40 plf

β = Angle to principal axis

therefore

W_y = 40 (cos 18.396) = 37.96 plf

W_z = 40 (sin 18.396) = 12.62 plf

Now that the member properties and the applied loads are known, the model was analyzed using ABAQUS (see Section 2.2.1). Figure B.4 contains the input data file used to do the analysis of the system.

From the analysis, the maximum deflection (node 7) of the system is known and the corresponding stiffness can be calculated:

$$K_{ss} = \frac{W}{\Delta_{ss}}$$

where

W = 40 plf

Δ_{SS} = Maximum deflection of the standing seam system from model.

therefore

$$K_{SS} = \frac{(40)20}{90} = 888 \text{ lb/in}$$

c. Calculate W_{SS}

Equation B.1 can now be evaluated to calculate the predicted failure load of the system:

$$W_{SS} = 199 \times 888/1{,}624 = 109 \text{ plf}$$

(The actual failure load was 85.8 plf.)

Purlin #1

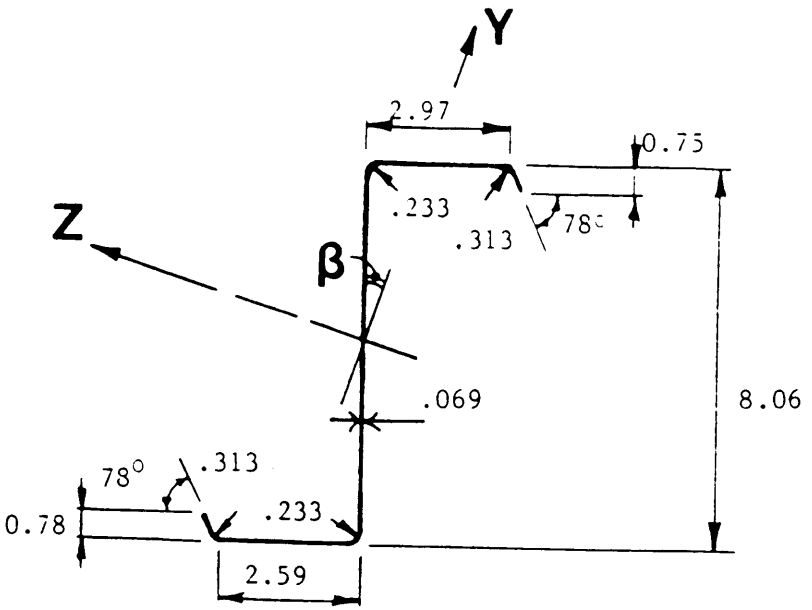

Properties: Span (ft) = 20.0
Area (in^2) = 1.0225
β(deg) = 18.3960
I_x (in^4) = 0.0016
I_y (in^4) = 0.7645
I_z (in^4) = 11.3487

Purlin #2

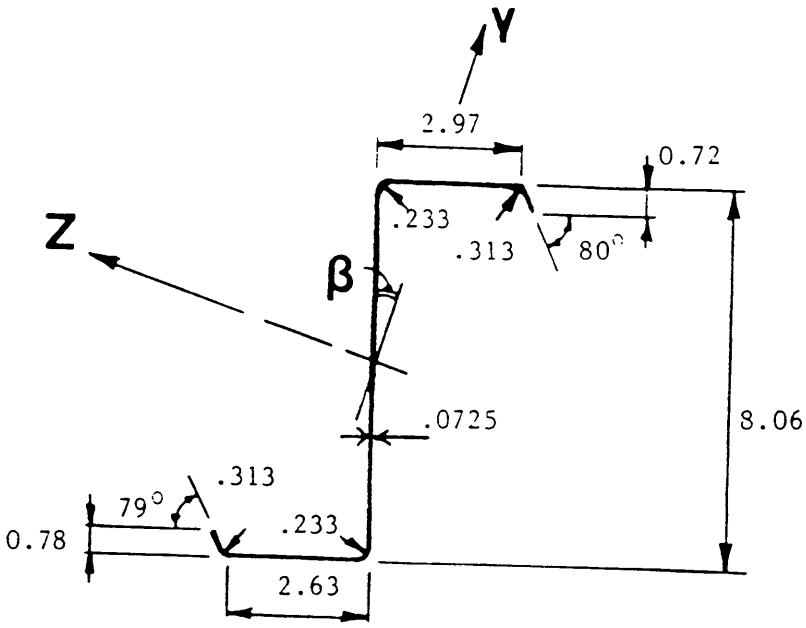

Properties: Span (ft) = 20.0
Area (in^2) = 1.0730
β(deg) = 18.3410
I_x (in^4) = .0019
I_y (in^4) = 0.7964
I_z (in^4) = 11.9071

Figure B.1 Measured Purlin Dimensions and Calculated Properties, Test R2/2-R-1

(a) Purlin #1

GEOMETRY OF CROSS-SECTION

		Top	Bottom
Vertical lip dimensions		0.7500 in.	0.7813 in.
Lip angles		78.0000 deg.	78.0000 deg.
Flange widths		2.9688 in.	2.5938 in.
Radii			
Lip to flange		0.3125 in.	0.3125 in.
Flange to web		0.2330 in.	0.2330 in.
Total purlin depth	8.0625 in.		
Purlin thickness	0.0690 in.		

Material Properties

Material yield stress	56.6	ksi
Modulus of elasticity	29500.0	ksi

General

Flat width of compression flange	2.3579	in.
Gross moment of inertia	9.91	$in.^4$

1986 AISI Procedure

Flange is not fully effective		
Effective flange width	1.7528	in.
Effective moment of inertia	8.87	$in.^4$
Allowable flexural capacity	71.46	kip-in

Figure B.2 Strength Calculations, Test R2/2-R-1, Continued

(b) Purlin #2

GEOMETRY OF CROSS-SECTION

		Top	Bottom
Vertical lip dimensions		0.7188 in.	0.7813 in.
Lip angles		80.0000 deg.	79.0000 deg.
Flange widths		2.9688 in.	2.6250 in.
Radii			
Lip to flange		0.3125 in.	0.3125 in.
Flange to web		0.2330 in.	0.2330 in.
Total purlin depth	8.0625 in.		
Purlin thickness	0.0725 in.		

Material Properties

Material yield stress	56.6 ksi
Modulus of elasticity	29500.0 ksi

General

Flat width of compression flange	2.3402 in.
Gross moment of inertia	10.37 $in.^4$

1986 AISI Procedure

Flange is not fully effective	
Effective flange width	1.7499 in.
Effective moment of inertia	9.31 $in.^4$
Allowable flexural capacity	74.78 kip-in

Figure B.3 Strength Calculations, Test R2/2-R-1

A B A Q U S I N P U T E C H O

```
*HEADING
 ROOF SYSTEM MODEL (R2/2-R-1) J=IX, BOTH PURLINS MODELED USING THE
 B31 ELEMENT. THE AREA OF THE TRUSS MEMBERS IS 0.00027.
 THE FILE NAME IS: MBMAX2
*NODE
1,0.,0.,0.
13,240,0,0
*NGEN
1,13
*NODE
14,0,-4,0
26,240,-4,0
*NGEN
14,26
*NODE
27,0,-8,0
28,240,-8,0
*NODE
29,0,0,60
41,240,0,60
*NGEN
29,41
*NODE
42,0,-4,60
54,240,-4,60
*NGEN
42,54
*NODE
55,0,-8,60
56,240,-8,60
85,0,0,60
86,240,0,-60
*ELEMENT , TYPE=B31, ELSET=PURLINA
13,14,15
14,15,16
15,16,17
16,17,18
17,18,19
18,19,20
19,20,21
20,21,22
```

Figure B.4 Input Data File for Test R2/2-R-1, Continued

```
21,22,23
22,23,24
23,24,25
24,25,26
*ELEMENT, TYPE=B31, ELSET=PURLINB
37,42,43
38,43,44
39,44,45
40,45,46
41,46,47
42,47,48
43,48,49
44,49,50
45,50,51
46,51,52
47,52,53
48,53,54
*ELEMENT , TYPE=B31, ELSET= UPPERA
73,1,14
74,2,15
75,3,16
76,4,17
77,5,18
78,6,19
79,7,20
80,8,21
81,9,22
82,10,23
83,11,24
84,12,25
85,13,26
*ELEMENT, TYPE=B31, ELSET=UPPERB
86,29,42
87,30,43
88,31,44
89,32,45
90,33,46
91,34,47
92,35,48
93,36,49
94,37,50
95,38,51
96,39,52
97,40,53
98,41,54
```

Figure B.4 Input Data File for Test R2/2-R-1, Continued

```
*ELEMENT , TYPE=B31, ELSET=LOWERA
112,14,27
113,26,28
*ELEMENT, TYPE=B31, ELSET=LOWERB
114,42,55
115,54,56
*ELEMENT , TYPE=C1D2, ELSET=TRUSS
1,1,2
2,2,3
3,3,4
4,4,5
5,5,6
6,6,7
7,7,8
8,8,9
9,9,10
10,10,11
11,11,12
12,12,13
25,29,30
26,30,31
27,31,32
28,32,33
29,33,34
30,34,35
31,35,36
32,36,37
33,37,38
34,38,39
35,39,40
36,40,41
118,1,29
119,1,30
120,2,30
121,3,30
122,3,31
123,3,32
124,4,32
125,5,32
126,5,33
127,5,34
128,6,34
129,7,34
130,7,35
131,7,36
```

Figure B.4 Input Data File for Test R2/2-R-1, Continued

```
132,8,36
133,9,36
134,9,37
135,9,38
136,10,38
137,11,38
138,11,39
139,11,40
140,12,40
141,13,40
142,13,41
*ELEMENT, TYPE=C1D2, ELSET=BRACING
168,1,85
169,13,86
*BEAM GENERAL SECTION, SECTION=GENERAL,ELSET=PURLINA
1.0225, , , 11.349, , 0.7645, 0.0016
0,0.31558,-0.9489
29.5E6,1.12E7,6.5E-6
*BEAM GENERAL SECTION, SECTION=GENERAL,ELSET=PURLINB
1.0730, , , 11.9071, , 0.7964, 0.0019
0,0.31467,-0.9492
29.5E6,1.12E7,6.5E-6
*BEAM GENERAL SECTION,SECTION=GENERAL,ELSET=UPPERA
1.38, , , 0.0016, ,0.00055,0.7645
0,0,-1
29.5E6,1.12E7,6.5E-6
*BEAM GENERAL SECTION, SECTION=GENERAL,ELSET=UPPERB
1.45, , , 0.0019, , 0.00064,0.7964
0,0,-1
29.5E6,1.12E7,6.5E-6
*BEAM GENERAL SECTION,SECTION=GENERAL,ELSET=LOWERA
8.28, , , 0.0016, , 0.03942,0.7645
0,0,-1
29.5E6,1.12E7,6.5E-6
*BEAM GENERAL SECTION,SECTION=GENERAL,ELSET=LOWERB
8.7, , , 0.0019, , 0.04573, 0.7964
0,0,-1
29.5E6,1.12E7,6.5E-6
*ATTRIBUTE, ELSET=TRUSS
0.00027
*ATTRIBUTE, ELSET=BRACING
0.19635
*MATERIAL
*ELASTIC
29.5E6,0.3
```

Figure B.4 Input Data File for Test R2/2-R-1, Continued

```
*BOUNDARY
27,1
27,2
27,3
27,4
27,6
28,1
28,2
28,3
28,4
28,6
55,1
55,2
55,3
55,4
55,6
56,1
56,2
56,3
56,4
56,6
85,1
85,2
85,3
86,1
86,2
86,3
*STEP, LINEAR
 SMALL DISPLACEMENT ANALYSIS
*STATIC
*DLOAD
PURLINA , P2, -3.16299
PURLINA , P1,-1.05194
PURLINB , P2, -3.164
PURLINB , P1, -1.04891
*CLOAD
14,4,33
15,4,66
16,4,66
17,4,66
18,4,66
19,4,66
20,4,66
21,4,66
22,4,66
```

Figure B.4 Input Data File for Test R2/2-R-1, Continued

```
23,4,66
24,4,66
25,4,66
26,4,33
42,4,33
43,4,66
44,4,66
45,4,66
46,4,66
47,4,66
48,4,66
49,4,66
50,4,66
51,4,66
52,4,66
53,4,66
54,4,33
*PLOT
 ROOF SYSTEM MODEL FOR TEST NO. R2/2-R-1, J=IX
*DISPLACED
1,
*EL PRINT
*NODE PRINT
2,1,1,1,2,2,2
*END STEP
```

Figure B.4 Input Data File for Test R2/2-R-1

APPENDIX C

STRESS CORRELATION SAMPLE CALCULATIONS

Calculate the predicted failure load in plf for test No. R2/2-R-1 (see Table 1.1) using the stress correlation approach.

Span: 20 ft

Restraint Configuration: Supports

Purlin Data: See Figure C.1 for cross section dimensions and properties

Yield Stress: 56.6 ksi

The predicted failure load for a standing seam system using this approach can be calculated using the following equation:

$$W_{SS} = \frac{f_{AISI}}{f_{max}} \times W \qquad (C.1)$$

Like the previous method, it is necessary to calculate the allowable flexural capacity for the purlins cross-sections using the local buckling provisions of the 1986 AISI specification and analyze the system using the mathematical model to calculate the maximum positive moment of the cross-section.

a. Calculate f_{AISI}

1. Using the dimensions in Figure C.1, an allowable flexural capacity for both cross-sections was calculated (see Figures C.2 and C.3). The minimum of both capacities will be used in the calculations. From Figure C.2:

M_{AISI} = 71.46 k-in

The corresponding stress at point A of the cross-section (see Figure 2.14) due to this allowable flexural capacity can be calculated using the following equation:

$$f_{AISI} = \frac{M_{AISI}\, C}{I_{eff}} \qquad (C.2)$$

where

M_{AISI} = allowable flexural capacity using local buckling provisions of the 1988 AISI Specification

C = distance from centroid to extreme compression fiber of the cross-section

I_{eff} = effective moment of inertia of the cross-section (see Figure C.2)

Therefore

$$f_{AISI} = \frac{71.46(8.06-4.03)}{8.87} = 32.47 \text{ ksi}$$

b. Calculate f_{max}

1. Since this system was already analyzed in Appendix B using the mathematical model, the maximum moment in the cross-section due to the nominal load of 40 plf are known:

M_z = 22.54 k-in

M_y = 5.968 k-in

These moments are about the principal axis of the cross-section, refer to Figure C.1 for the geometry. Now that the applied moments, dimensions and section properties of the cross-secction are known (Fig. C.1), the stress at point A of the cross-section can be calculated using the following equation:

$$f_{xx} = \frac{M_y I_z - M_z I_{zy}}{I_z I_y - I_{zy}^2} z + \frac{M_z I_y - M_y I_{zy}}{I_z I_y - I_{zy}^2} y \qquad (C.3)$$

Therefore, σ_{max} at point A:

$$f_{xx} = \frac{(-4.123)1.27}{0.7645} + \frac{(-23.53)3.82}{11.3487} = 14.8 \text{ ksi}$$

c. Calculate W_{ss}

The predicted failure load for the R2/2-R-1 system using Equation C.1 is:

$$W_{ss} = \frac{32.47}{14.8} \times 40 = 86.1 \text{ plf}$$

(The actual failure load was 85.8 plf.)

Purlin #1

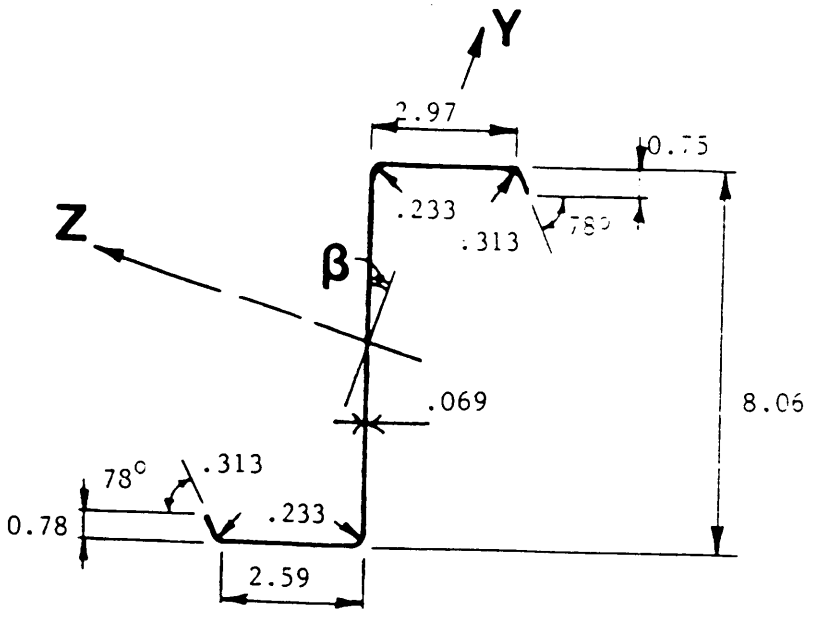

Properties: Span (ft) = 20.0
Area (in^2) = 1.0225
β(deg) = 18.3960

I_x (in^4) = 0.0016
I_y (in^4) = 0.7645
I_z (in^4) = 11.3487

Purlin #2

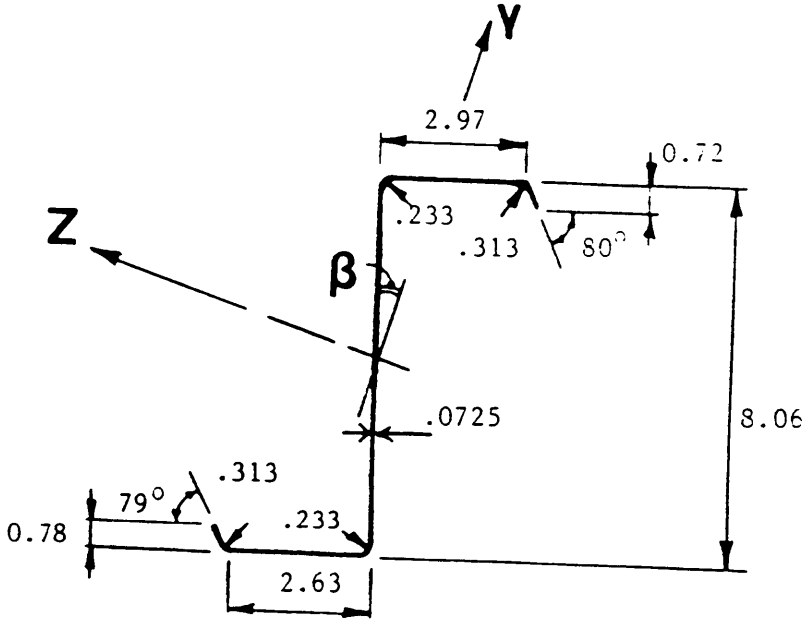

Properties: Span (ft) = 20.0
Area (in^2) = 1.0730
β(deg) = 18.3410

I_x (in^4) = .0019
I_y (in^4) = 0.7964
I_z (in^4) = 11.3071

Figure C.1 Measured Purlin Dimensions and Calculated Properties, Test R2/2-R-1

(a) Purlin #1

GEOMETRY OF CROSS-SECTION

		Top	Bottom
Vertical lip dimensions		0.7500 in.	0.7813 in.
Lip angles		78.0000 deg.	78.0000 deg.
Flange widths		2.9688 in.	2.5938 in.
Radii			
Lip to flange		0.3125 in.	0.3125 in.
Flange to web		0.2330 in.	0.2330 in.
Total purlin depth	8.0625 in.		
Purlin thickness	0.0690 in.		

Material Properties

Material yield stress	56.6 ksi
Modulus of elasticity	29500.0 ksi

General

Flat width of compression flange	2.3579 in.
Gross moment of inertia	9.91 $in.^4$

1986 AISI Procedure

Flange is not fully effective	
Effective flange width	1.7528 in.
Effective moment of inertia	8.87 $in.^4$
Allowable flexural capacity	71.46 kip-in

Figure C.2 Strength Calculations, Test R2/2-R-1, Continued

(b) Purlin #2

GEOMETRY OF CROSS-SECTION

		Top	Bottom
Vertical lip dimensions		0.7188 in.	0.7813 in.
Lip angles		80.0000 deg.	79.0000 deg.
Flange widths		2.9688 in.	2.6250 in.
Radii			
Lip to flange		0.3125 in.	0.3125 in.
Flange to web		0.2330 in.	0.2330 in.
Total purlin depth	8.0625 in.		
Purlin thickness	0.0725 in.		

Material Properties

Material yield stress	56.6 ksi
Modulus of elasticity	29500.0 ksi

General

Flat width of compression flange	2.3402 in.
Gross moment of inertia	10.37 $in.^4$

1986 AISI Procedure

Flange is not fully effective	
Effective flange width	1.7499 in.
Effective moment of inertia	9.31 $in.^4$
Allowable flexural capacity	74.78 kip-in

Figure C.3 Strength Calculations, Test R2/2-R-1

APPENDIX D

BASE TEST SAMPLE CALCULATIONS

Calculate the predicted failure load in plf for test No. P/2-R-2 (see Table 3.7) using the base test method.

Two Spans: 25 ft

Restraint Configuration: Supports

Purlin Data: See Figures D.1, D.2, D.3 and D.4 for cross section properties and dimensions

Yield Stress: 55 ksi

The predicted failure load for a multiple span system using this approach can be calculated using the following equation (see Section 2.4):

$$W_{um} = \text{min. of} \begin{cases} \dfrac{M_{us}}{M_{max(+)}} \times W \\ \dfrac{M_{AISI}}{M_{neg}} \times W \end{cases} \qquad \text{(D.1)}$$

a. Base Test

Span: 25 ft (same as multiple span system)

Restraint Configuration: Supports (same as multiple span system)

Purlin Data: See Figures D.1 and D.2 for cross-section properties and dimensions

Panel Type: pan (same as multiple span system)

The experimental failure load of the base test was:

W_{us} = 99 plf

b. Stiffness Analysis

Using the section properties in Figures D.3, D.4 and a nominal load of 100 plf, a stiffness analysis was done on the multiple span system to determine the maximum positive moment and the negative moment at the beginning of the lap at the middle support. From this analysis, the following values were obtained:

$M_{max(+)} = 50.5$ k-in

$M_{neg} = 78.5$ k-in (at beginning of lap)

a. Calculate W_{um}

The predicted failure load for a multiple span standing seam system using Equation D.1 is the minimum of the following two equations:

$$W_{um} = \frac{M_{us}}{M_{max(+)}} \times W \qquad \text{(D.1a)}$$

$$W_{um} = \frac{M_{AISI}}{M_{neg}} \times W \qquad \text{(D.1b)}$$

where

$$M_u = \frac{W_u l^2}{8} = \frac{99(25)^2}{8} \times 12 = 92.81 \text{ k-in}$$

M_{AISI} = allowable flexural capacity of the cross-section using the local buckling provisions of the 1986 AISI Specification (see Figure D.2) = 119.7 k-in

$M_{max(+)}$ = 50.5 k-in

M_{neg} = 78.5 k-in

W = 100 plf

Evaluating Equation D.1a:

$$W_{um} = \frac{92.81}{50.5} \times 100 = 183.8 \text{ plf}$$

Evaluating Equation D.1b:

$$W_{um} = \frac{119.7}{78.5} \times 100 = 152.5 \text{ plf (controls)}$$

Therefore,

The predicted failure load for Test No. P/2-R-2 is:

$$W_{um} = 152.5 \text{ plf}$$

(The actual failure load was 143.5 plf.)

(a) Purlin #1

GEOMETRY OF CROSS-SECTION

		Top	Bottom
Vertical lip dimensions		1.0900 in.	1.2100 in.
Lip angles		62.0000 deg.	61.0000 deg.
Flange widths		2.6100 in.	3.0000 in.
Radii			
Lip to flange		0.3125 in.	0.3440 in.
Flange to web		0.3750 in.	0.3750 in.
Total purlin depth	9.9500 in.		
Purlin thickness	0.0770 in.		

Material Properties

Material yield stress	55.0 ksi
Modulus of elasticity	29500.0 ksi

General

Flat width of compression flange	1.8113 in.
Gross moment of inertia	19.26 $in.^4$

1986 AISI Procedure

Flange is not fully effective	
Effective flange width	1.6578 in.
Effective moment of inertia	18.88 $in.^4$
Allowable flexural capacity	120.02 kip-in

Figure D.1 Strength Calculations, Test P/2-R-1, Continued

(b) Purlin #2

GEOMETRY OF CROSS-SECTION

		Top	Bottom
Vertical lip dimensions		1.0400 in.	1.1700 in.
Lip angles		61.0000 deg.	62.0000 deg.
Flange widths		2.6700 in.	2.9400 in.
Radii			
Lip to flange		0.3125 in.	0.3125 in.
Flange to web		0.3750 in.	0.3750 in.
Total purlin depth	9.9400 in.		
Purlin thickness	0.0770 in.		

Material Properties

Material yield stress	55.0	ksi
Modulus of elasticity	29500.0	ksi

General

Flat width of compression flange	1.8781	in.
Gross moment of inertia	19.11	$in.^4$

1986 AISI Procedure

Flange is not fully effective		
Effective flange width	1.7457	in.
Effective moment of inertia	18.80	$in.^4$
Allowable flexural capacity	119.7	kip-in

Figure D.2 Strength Calculations, Test P/2-R-1

Purlin #1

North Span

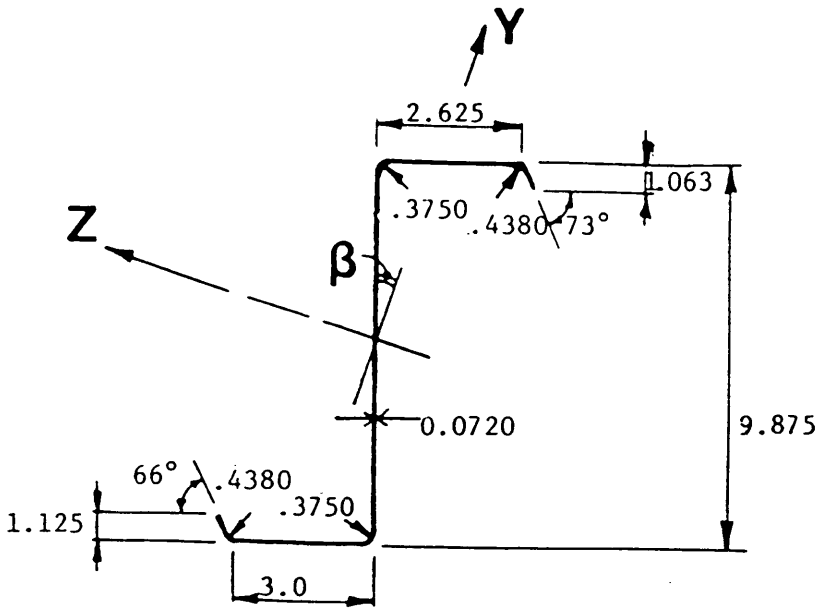

Properties:				
	Span (ft) =	25.0	$I_x(in^4)$ =	0.0019
	Area (in^2) =	1.0735	$I_y(in^4)$ =	0.8061
	$\bar{x}$(deg) =	18.3015	$I_z(in^4)$ =	11.9984

Purlin #2

North Span

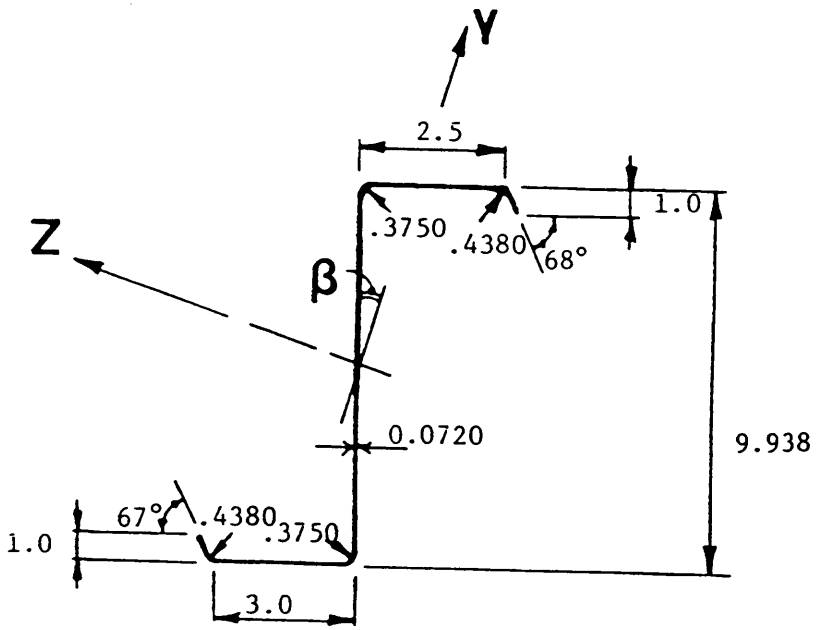

Properties:				
	Span (ft) =	25.0	$I_x(in^4)$ =	0.0019
	Area (in^2) =	1.0712	$I_y(in^4)$ =	0.8022
	$\bar{x}$(deg) =	18.2392	$I_z(in^4)$ =	11.9573

Figure D.3 Measured Purlin Dimensions and Calculated Properties, Test P/2-R-2, Continued

Purlin #1

South Span

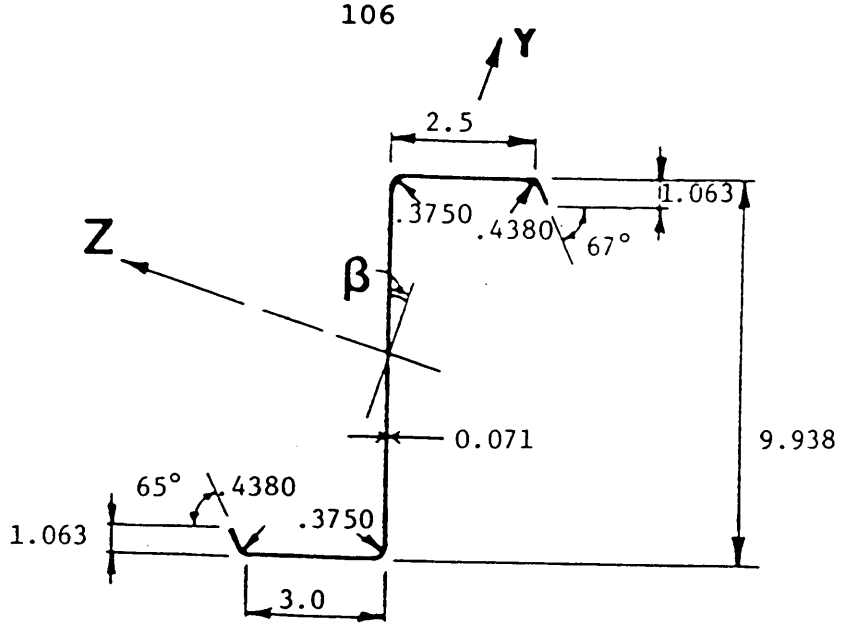

Properties:				
	Span (ft) =	25.0	I_x(in^4) =	0.0021
	Area (in^2) =	1.1033	I_y(in^4) =	0.8190
	β(deg) =	18.2105	I_z(in^4) =	12.2030

Purlin #2

South Span

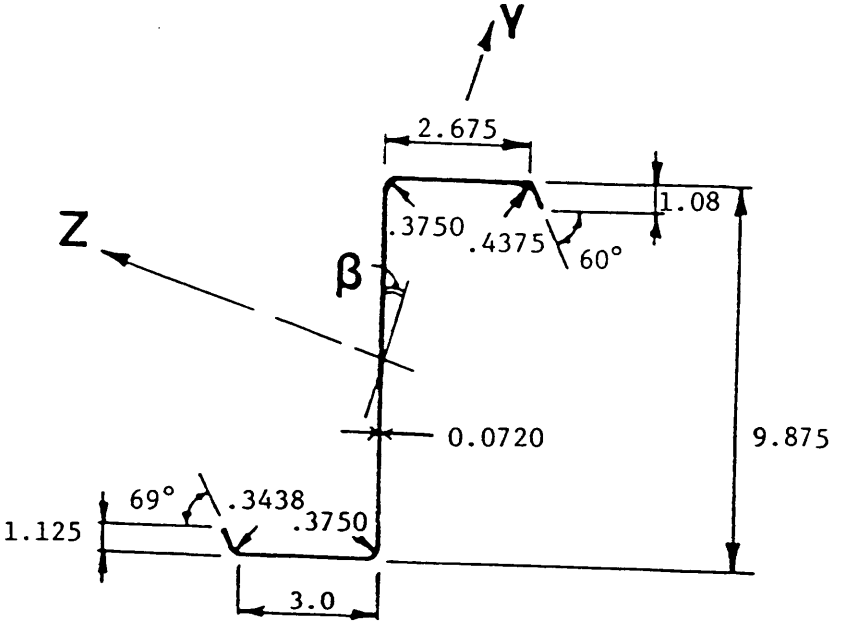

Properties:				
	Span (ft) =	25.0	I_x (in^4) =	0.0021
	Area (in^2) =	1.1143	I_y (in^4) =	0.8279
	β(deg) =	18.1585	I_z (in^4) =	12.4196

Figure D.4 Measured Purlin Dimensions and Calculated Properties, Test P/2-R-2, Continued

APPENDIX E

PROPERTIES OF TESTS IN TABLE 1.1

Purlin #1

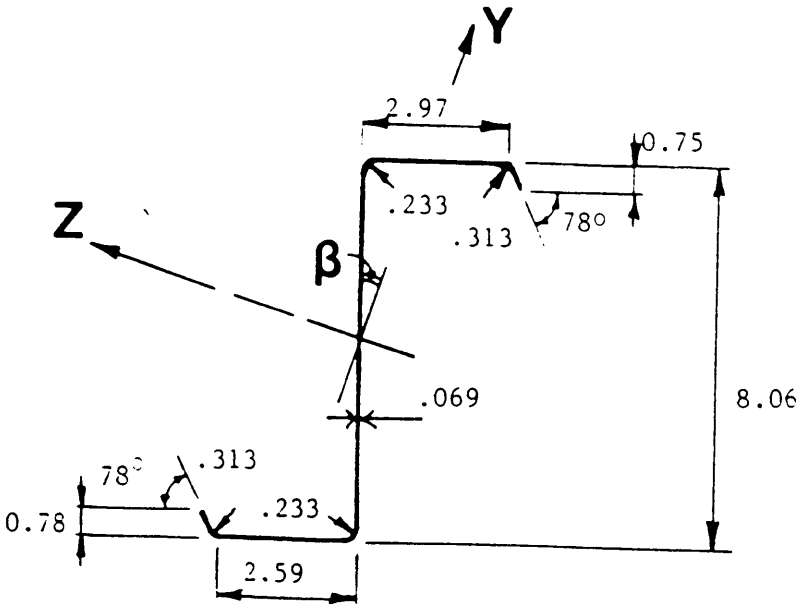

Properties: Span (ft) = 20.0
Area (in^2) = 1.0225
β(deg) = 18.3960
I_x (in^4) = 0.0016
I_y (in^4) = 0.7645
I_z (in^4) = 11.3487

Purlin #2

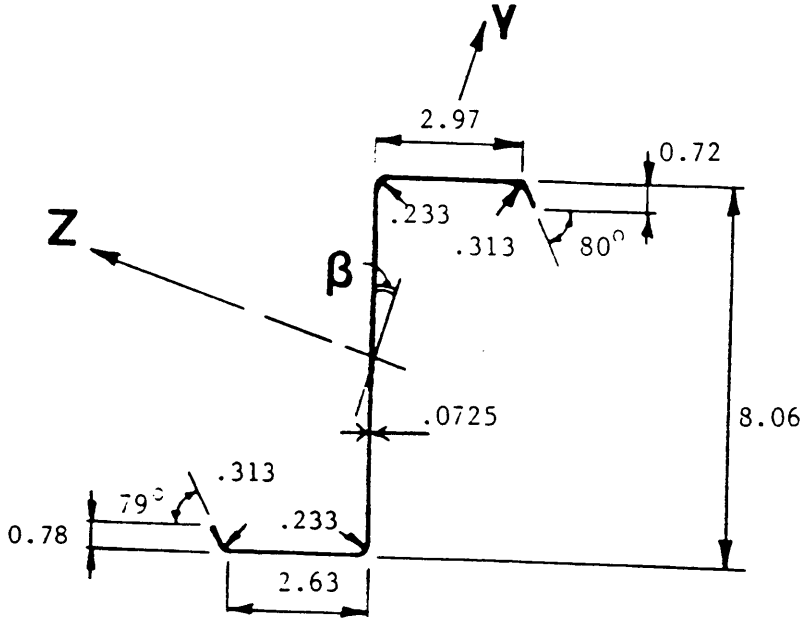

Properties: Span (ft) = 20.0
Area (in^2) = 1.0730
β(deg) = 18.3410
I_x (in^4) = .0019
I_y (in^4) = 0.7954
I_z (in^4) = 11.9071

Figure E.1 Measured Purlin Dimensions and Calculated Properties, Test R2/2-R-1

(a) Purlin #1

GEOMETRY OF CROSS-SECTION

		Top	Bottom
Vertical lip dimensions		0.7500 in.	0.7813 in.
Lip angles		78.0000 deg.	78.0000 deg.
Flange widths		2.9688 in.	2.5938 in.
Radii			
Lip to flange		0.3125 in.	0.3125 in.
Flange to web		0.2330 in.	0.2330 in.
Total purlin depth	8.0625 in.		
Purlin thickness	0.0690 in.		

Material Properties

Material yield stress	56.6 ksi
Modulus of elasticity	29500.0 ksi

General

Flat width of compression flange	2.3579 in.
Gross moment of inertia	9.91 $in.^4$

1986 AISI Procedure

Flange is not fully effective	
Effective flange width	1.7528 in.
Effective moment of inertia	8.87 $in.^4$
Allowable flexural capacity	71.46 kip-in

Figure E.2 Strength Calculations, Test R2/2-R-1, Continued

(b) Purlin #2

GEOMETRY OF CROSS-SECTION

		Top	Bottom
Vertical lip dimensions		0.7188 in.	0.7813 in.
Lip angles		80.0000 deg.	79.0000 deg.
Flange widths		2.9688 in.	2.6250 in.
Radii			
Lip to flange		0.3125 in.	0.3125 in.
Flange to web		0.2330 in.	0.2330 in.
Total purlin depth	8.0625 in.		
Purlin thickness	0.0725 in.		

Material Properties

Material yield stress	56.6	ksi
Modulus of elasticity	29500.0	ksi

General

Flat width of compression flange	2.3402	in.
Gross moment of inertia1	10.37	in.4

1986 AISI Procedure

Flange is not fully effective		
Effective flange width	1.7499	in.
Effective moment of inertia	9.31	$in.^4$
Allowable flexural capacity	74.78	kip-in

Figure E.3 Strength Calculations, Test R2/2-R-1

Purlin #1

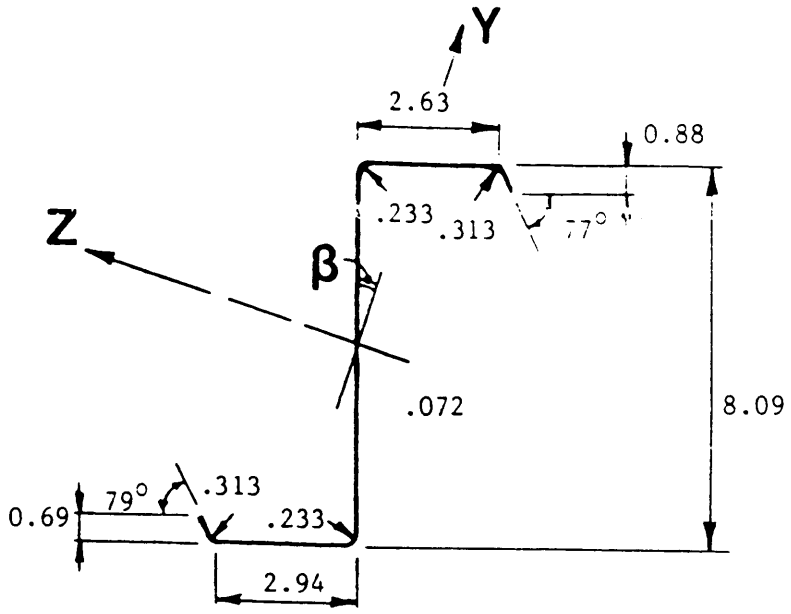

Properties: Span (ft) = 20.0 $I_x(in^4)$ = .0019

Area (in^2) = 1.0735 $I_y(in^4)$ = .8061

β (deg) = 18.3015 $I_z(in^4)$ = 11.9984

Purlin #2

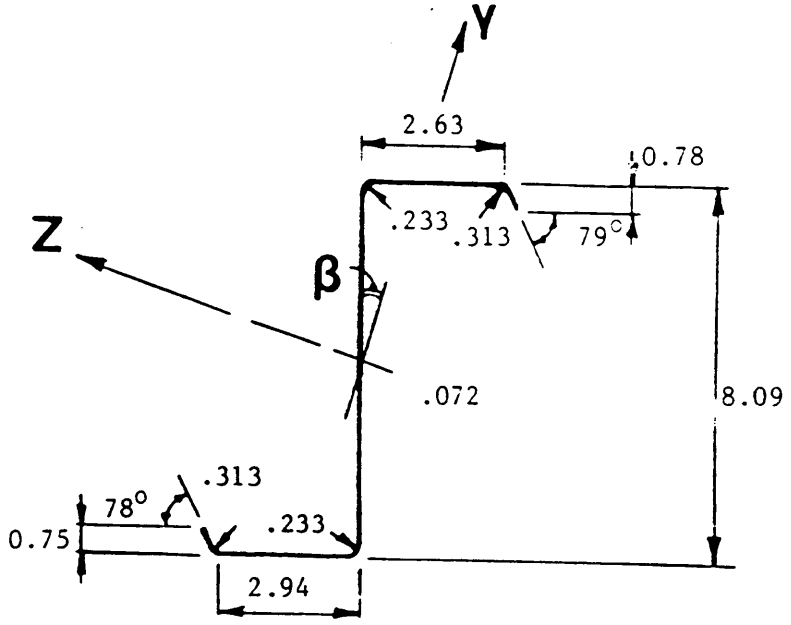

Properties: Span (ft) = 20.0 $I_x(in^4)$ = .0019

Area (in^2) = 1.0712 $I_y(in^4)$ = 0.8022

β(deg) = 18.2392 $I_z(in^4)$ = 11.9573

Figure E.4 Measured Purlin Dimensions and Calculated Properties, Test P1/2-R-1

(a) Purlin #1

GEOMETRY OF CROSS-SECTION

		Top	Bottom
Vertical lip dimensions		0.8750 in.	0.6880 in.
Lip angles		77.0000 deg.	79.0000 deg.
Flange widths		2.6250 in.	2.9380 in.
Radii			
Lip to flange		0.3125 in.	0.3125 in.
Flange to web		0.2330 in.	0.2330 in.
Total purlin depth	8.0940 in.		
Purlin thickness	0.0720 in.		

Material Properties

Material yield stress	56.6 ksi
Modulus of elasticity	29500.0 ksi

General

Flat width of compression flange	2.0142 in.
Gross moment of inertia	10.44 in.4

1986 AISI Procedure

Flange is not fully effective	
Effective flange width	1.7092 in.
Effective moment of inertia	9.75 $in.^4$
Allowable flexural capacity	77.65 kip-in

Figure E.5 Strength Calculations, Test P1/2-R-1, Continued

(b) Purlin #2

GEOMETRY OF CROSS-SECTION

		Top	Bottom
Vertical lip dimensions		0.7810 in.	0.7500 in.
Lip angles		79.0000 deg.	78.0000 deg.
Flange widths		2.6250 in.	2.9380 in.
Radii			
Lip to flange		0.3125 in.	0.3125 in.
Flange to web		0.2330 in.	0.2330 in.
Total purlin depth	8.0940 in.		
Purlin thickness	0.0720 in.		

Material Properties

Material yield stress	56.6	ksi
Modulus of elasticity	29500.0	ksi

General

Flat width of compression flange	2.0030	in.
Gross moment of inertia	10.41	in.4

1986 AISI Procedure

Flange is not fully effective		
Effective flange width	1.6137	in.
Effective moment of inertia	9.54	in.^{4}
Allowable flexural capacity	74.46	kip-in

Figure E.6 Strength Calculations, Test P1/2-R-1

Purlin #1

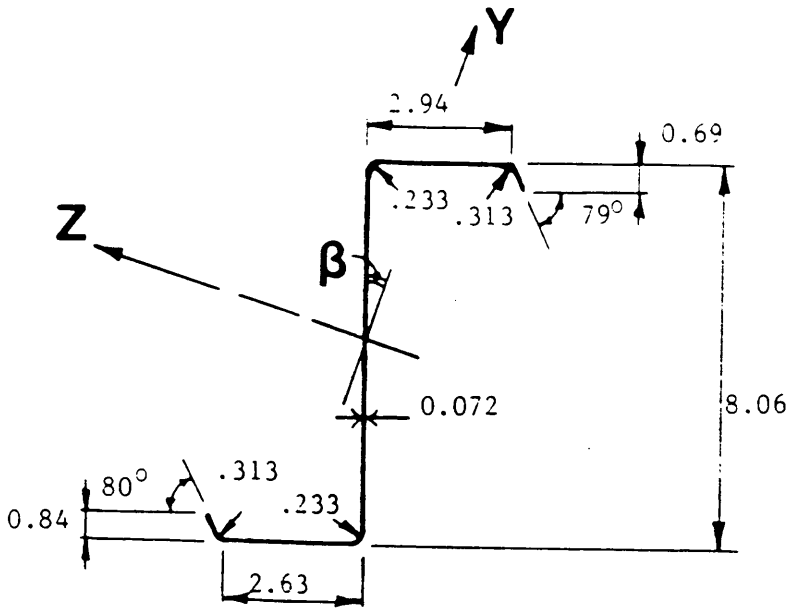

Properties: Span (ft) = 20.0 I_x (in^4) = 0.0019
Area (in^2) = 1.0657 I_y (in^4) = 0.7863
β(deg) = 18.2899 I_z (in^4) = 11.8114

Purlin #2

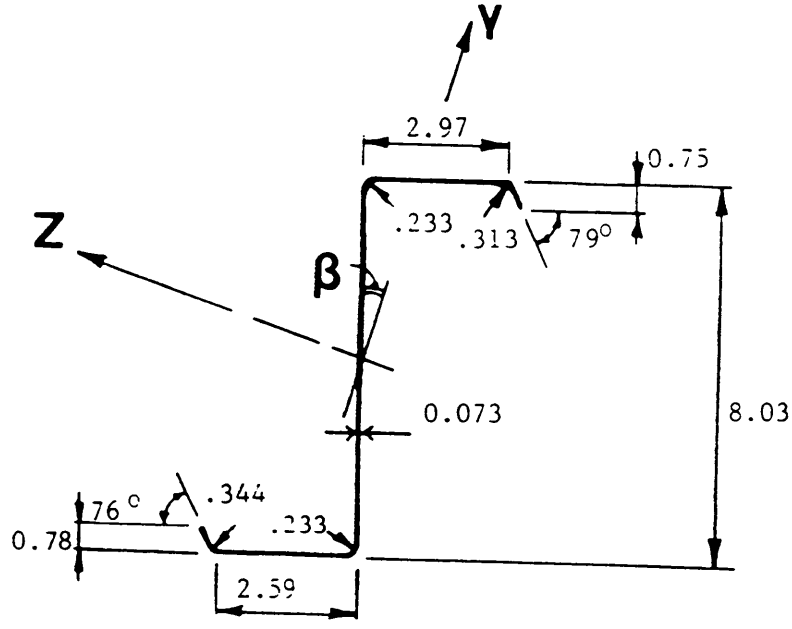

Properties: Span (ft) = 20.0 I_x (in^4) = 0.0019
Area (in^2) = 1.0789 I_y (in^4) = 0.8079
β(deg) = 18.5396 I_z (in^4) = 11.9048

Figure E.7 Measured Purlin Dimensions and Calculated Properties, Test R2/2-T-1

(a) Purlin #1

GEOMETRY OF CROSS-SECTION

		Top	Bottom
Vertical lip dimensions		0.6875 in.	0.8438 in.
Lip angles		79.0000 deg.	80.0000 deg.
Flange widths		2.9375 in.	2.6250 in.
Radii			
Lip to flange		0.3125 in.	0.3125 in.
Flange to web		0.2330 in.	0.2330 in.
Total purlin depth	8.0625 in.		
Purlin thickness	0.0720 in.		

Material Properties

Material yield stress	56.6	ksi
Modulus of elasticity	29500.0	ksi

General

Flat width of compression flange	2.3155	in.
Gross moment of inertia	10.30	in.4

1986 AISI Procedure

Flange is not fully effective		
Effective flange width	1.7168	in.
Effective moment of inertia	9.23	in.4
Allowable flexural capacity	73.63	kip-in

Figure E.8 Strength Calculations, Test R2/2-T-1, Continued

(b) Purlin #2

GEOMETRY OF CROSS-SECTION

		Top	Bottom
Vertical lip dimensions		0.7500 in.	0.7813 in.
Lip angles		79.0000 deg.	76.0000 deg.
Flange widths		2.9688 in.	2.5938 in.
Radii			
Lip to flange		0.3125 in.	0.3438 in.
Flange to web		0.2330 in.	0.2330 in.
Total purlin depth	8.0313 in.		
Purlin thickness	0.0730 in.		

Material Properties

Material yield stress	56.6	ksi
Modulus of elasticity	29500.0	ksi

General

Flat width of compression flange	2.3450	in.
Gross moment of inertia	10.36	$in.^4$

1986 AISI Procedure

Flange is not fully effective		
Effective flange width	1.7921	in.
Effective moment of inertia	9.34	$in.^4$
Allowable flexural capacity	75.67	kip-in

Figure E.9 Strength Calculations, Test R2/2-T-1

Purlin #1

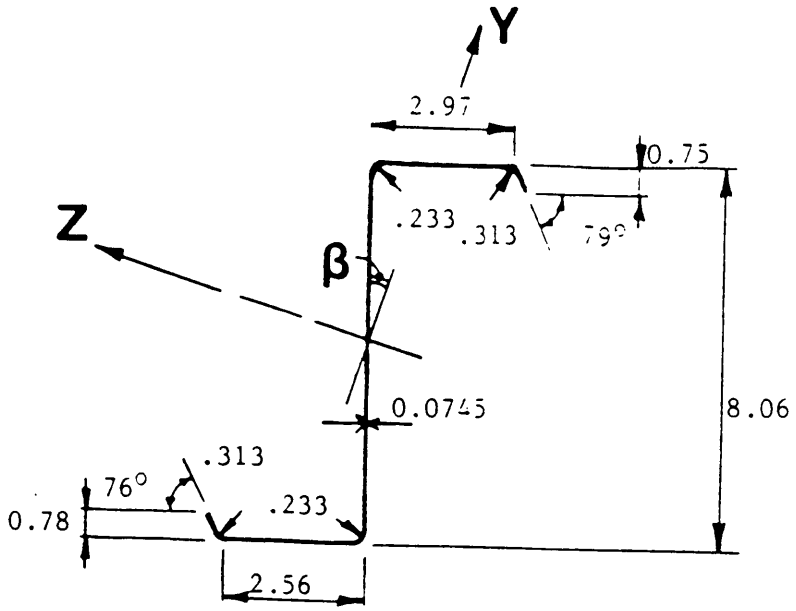

Properties: Span (ft) = 20.0
Area (in^2) = 1.1033
β(deg) = 18.2105
I_x(in^4) = 0.0021
I_y(in^4) = 0.8190
I_z(in^4) = 12.2030

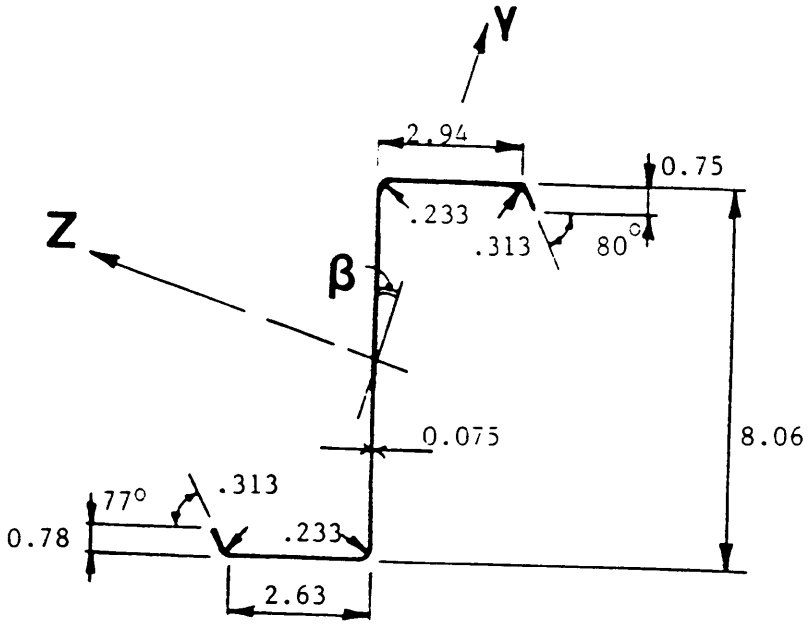

Properties: Span (ft) = 20.0
Area (in^2) = 1.1143
β(deg) = 18.1585
I_x(in^4) = 0.0021
I_y(in^4) = 0.8279
I_z(in^4) = 12.4196

Figure E.10 Measured Purlin Dimensions and Calculated Properties, Test P1/2-T-1

(a) Purlin #1

GEOMETRY OF CROSS-SECTION

		Top	Bottom
Vertical lip dimensions		0.7500 in.	0.7813 in.
Lip angles		79.0000 deg.	76.0000 deg.
Flange widths		2.9690 in.	2.5630 in.
Radii			
Lip to flange		0.3125 in.	0.3125 in.
Flange to web		0.2330 in.	0.2330 in.
Total purlin depth	8.0625 in.		
Purlin thickness	0.0745 in.		

Material Properties

Material yield stress	56.6	ksi
Modulus of elasticity	29500.0	ksi

General

Flat width of compression flange	2.3425	in.
Gross moment of inertia	10.63	in.4

1986 AISI Procedure

Flange is not fully effective		
Effective flange width	1.8095	in.
Effective moment of inertia	9.61	in.^{4}
Allowable flexural capacity	77.76	kip-in

Figure E.11 Strength Calculations, Test P1/2-T-1, Continued

(b) Purlin #2

GEOMETRY OF CROSS-SECTION

		Top	Bottom
Vertical lip dimensions		0.7500 in.	0.7813 in.
Lip angles		80.0000 deg.	77.0000 deg.
Flange widths		2.9375 in.	2.6250 in.
Radii			
Lip to flange		0.3125 in.	0.3125 in.
Flange to web		0.2330 in.	0.2330 in.
Total purlin depth	8.0940 in.		
Purlin thickness	0.0750 in.		

Material Properties

Material yield stress	56.6	ksi
Modulus of elasticity	29500.0	ksi

General

Flat width of compression flange	2.3043	in.4
Gross moment of inertia	10.82	in.4

1986 AISI Procedure

Flange is not fully effective		
Effective flange width	1.7979	in.
Effective moment of inertia	9.81	$in.^4$
Allowable flexural capacity	78.74	kip-in

Figure E.12 Strength Calculations, Test P1/2-T-1

Purlin #1

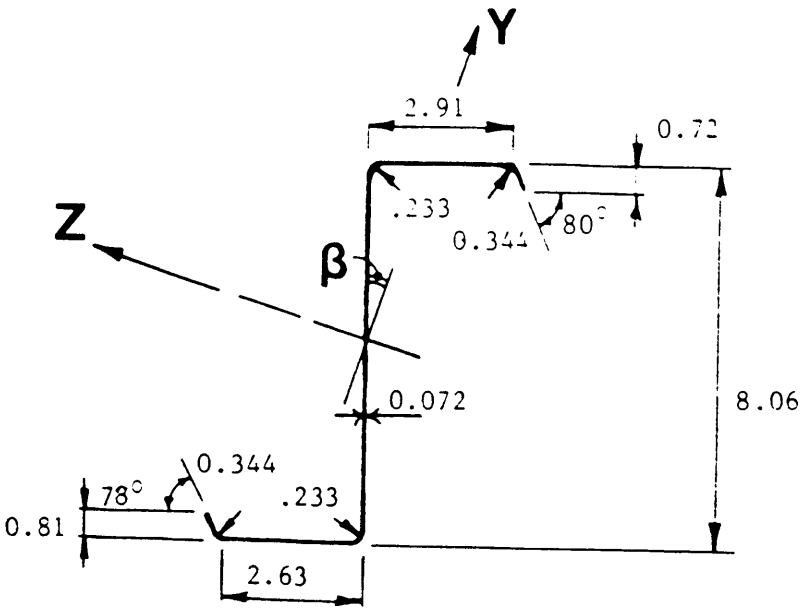

Properties: Span (ft) = 20.0
Area (in^2) = 1.0636
β(deg) = 18.0511
I_x (in^4) = 0.0019
I_y (in^4) = 0.7816
I_z (in^4) = 11.7335

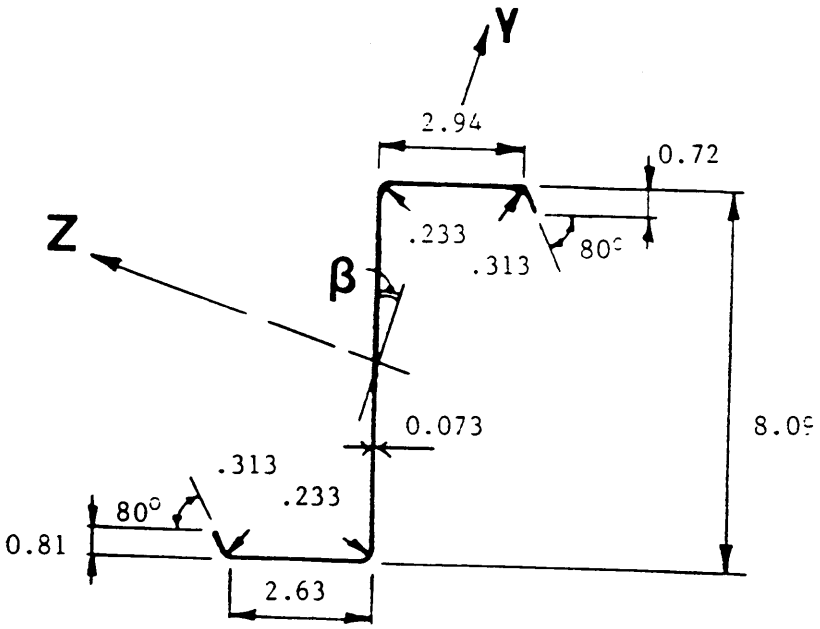

Properties: Span (ft) = 20.0
Area (in^2) = 1.0832
β(deg) = 18.0696
I_x (in^4) = .0020
I_y (in^4) = 0.7990
I_z (in^4) = 12.0541

Figure E.13 Measured Purlin Dimensions and Calculated Properties, Test R2/2-M-1

(a) Purlin #1

GEOMETRY OF CROSS-SECTION

	Top	Bottom
Vertical lip dimensions	0.7188 in.	0.8125 in.
Lip angles	80.0000 deg.	78.0000 deg.
Flange widths	2.9063 in.	2.6250 in.
Radii		
Lip to flange	0.3428 in.	0.3438 in.
Flange to web	0.2330 in.	0.2330 in.

Total purlin depth	8.0625 in.
Purlin thickness	0.0720 in.

Material Properties

Material yield stress	56.6 ksi
Modulus of elasticity	29500.0 ksi

General

Flat width of compression flange	2.2532 in.
Gross moment of inertia	10.25 $in.^4$

1986 AISI Procedure

Flange is not fully effective	
Effective flange width	1.6918 in.
Effective moment of inertia	9.24 $in.^4$
Allowable flexural capacity	73.90 kip-in

Figure E.14 Strength Calculations, Test R2/2-M-1, Continued

(b) Purlin #2

GEOMETRY OF CROSS-SECTION

		Top	Bottom
Vertical lip dimensions		0.7188 in.	0.8125 in.
Lip angles		80.0000 deg.	80.0000 deg.
Flange widths		2.9375 in.	2.6250 in.
Radii			
Lip to flange		0.3125 in.	0.3125 in.
Flange to web		0.2330 in.	0.2330 in.
Total purlin depth	8.0938 in.		
Purlin thickness	0.0730 in.		

Material Properties

Material yield stress	56.6 ksi
Modulus of elasticity	29500.0 ksi

General

Flat width of compression flange	2.3080 in.
Gross moment of inertia	10.52 $in.^4$

1986 AISI Procedure

Flange is not fully effective	
Effective flange width	1.7483 in.
Effective moment of inertia	9.47 $in.^4$
Allowable flexural capacity	75.70 kip-in

Figure E.15 Strength Calculations, Test R2/2-M-1

Purlin #1

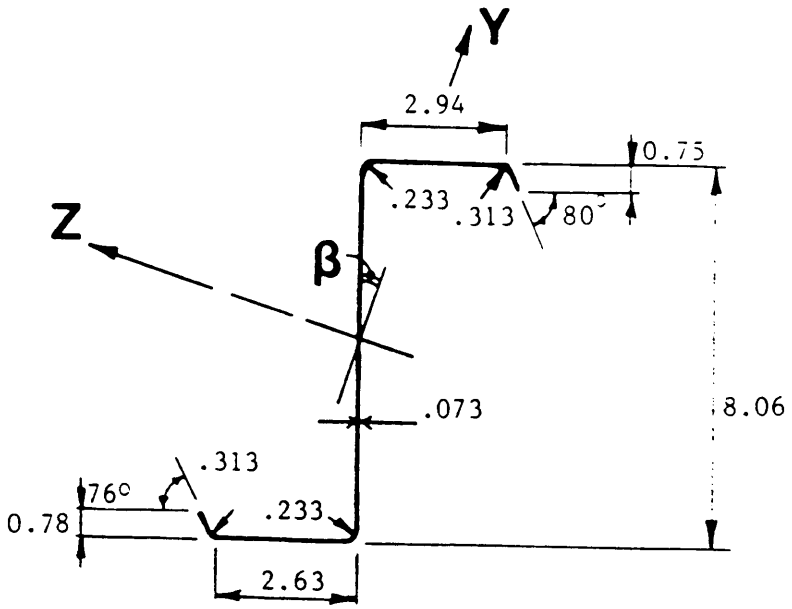

Properties: Span (ft) = 20.0
Area (in^2) = 1.0832
β(deg) = 18.2635
$I_x(in^4)$ = 0.002
$I_y(in^4)$ = 0.8071
$I_z(in^4)$ = 12.0215

Purlin #2

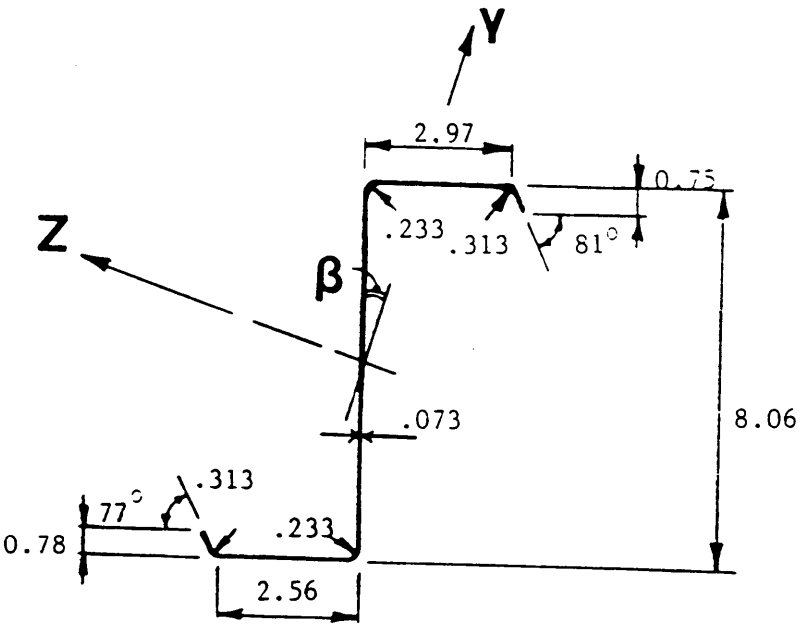

Properties: Span (ft) = 20.0
Area (in^2) = 1.0797
β(deg) = 18.1263
I_x (in^4) = .0019
I_y (in^4) = 0.7964
I_z (in^4) = 11.9255

Figure E.16 Measured Purlin Dimensions and Calculated Properties, Test P1/2-M-1

(a) Purlin #1

GEOMETRY OF CROSS-SECTION

		Top	Bottom
Vertical lip dimensions		0.7500 in.	0.7810 in.
Lip angles		80.0000 deg.	76.0000 deg.
Flange widths		2.9380 in.	2.6250 in.
Radii			
Lip to flange		0.3125 in.	0.3125 in.
Flange to web		0.2330 in.	0.2330 in.
Total purlin depth	8.0680 in.		
Purlin thickness	0.0730 in.		

Material Properties

Material yield stress	56.6 ksi
Modulus of elasticity	29500.0 ksi

General

Flat width of compression flange	2.3085 in.
Gross moment of inertia	10.48 $in.^4$

1986 AISI Procedure

Flange is not fully effective	
Effective flange width	1.7754 in.
Effective moment of inertia	9.46 $in.^4$
Allowable flexural capacity	76.05 kip-in

Figure E.17 Strength Calculations, Test P1/2-M-1, Continued

(b) Purlin #2

GEOMETRY OF CROSS-SECTION

		Top	Bottom
Vertical lip dimensions		0.7500 in.	0.7810 in.
Lip angles		81.0000 deg.	77.0000 deg.
Flange widths		2.9690 in.	2.5630 in.
Radii			
Lip to flange		0.3125 in.	0.3125 in.
Flange to web		0.2330 in.	0.2330 in.
Total purlin depth	8.0630 in.		
Purlin thickness	0.0730 in.		

Material Properties

Material yield stress	56.6 ksi
Modulus of elasticity	29500.0 ksi

General

Flat width of compression flange	2.3338 in.
Gross moment of inertia	10.40 $in.^4$

1986 AISI Procedure

Flange is not fully effective	
Effective flange width	1.7714 in.
Effective moment of inertia	9.37 $in.^4$
Allowable flexural capacity	75.74 kip-in

Figure E.18 Strength Calculations, Test P1/2-M-1

Purlin #1

North Span

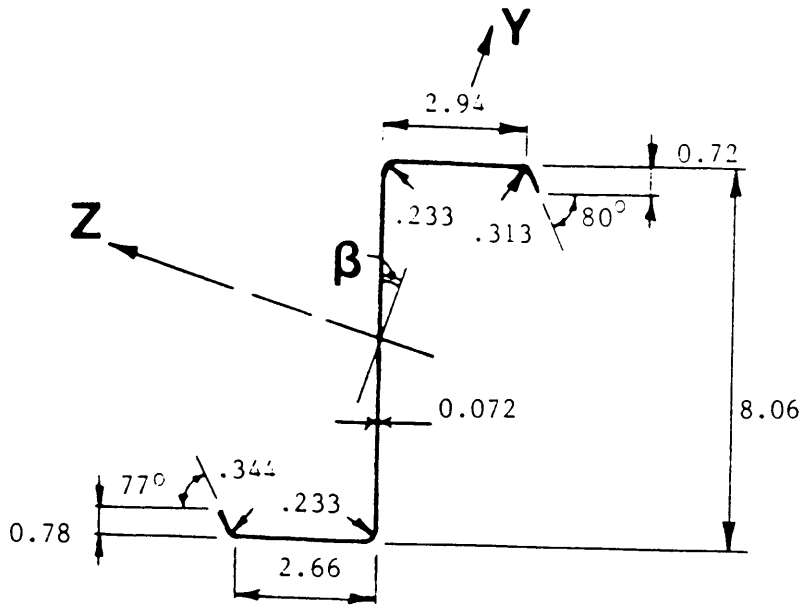

Properties: Span (ft) = 23.0 $I_x(in^4)$ = 0.0019

Area (in^2) = 1.0669 $I_y(in^4)$ = 0.7950

β(deg) = 18.2531 $I_z(in^4)$ = 11.8301

Purlin #2

North Span

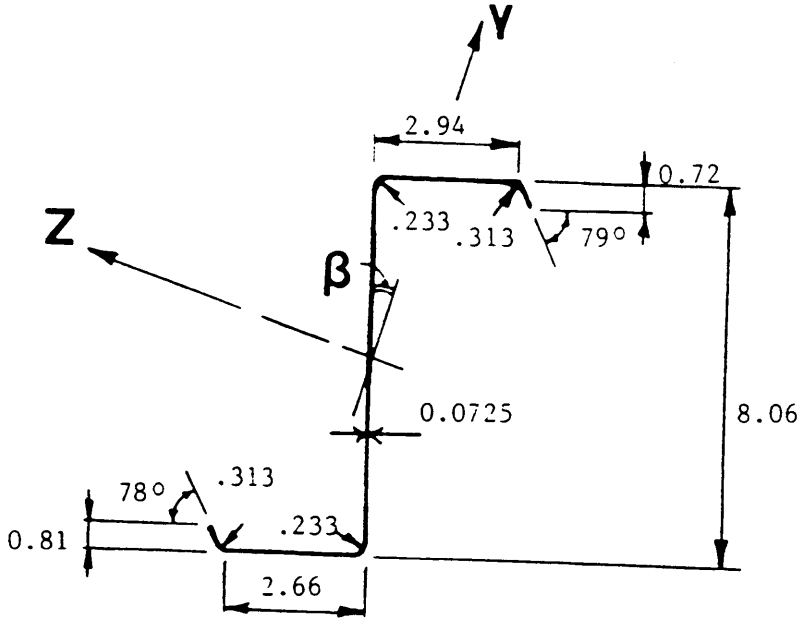

Properties: Span (ft) = 23.0 I_x (in^4) = 0.0019

Area (in^2) = 1.0772 I_y (in^4) = 0.8065

β(deg) = 18.3530 I_z (in^4) = 11.9653

Figure E.19 Measured Purlin Dimensions and Calculated Properties, Test R3/2-R-3, Continued

Purlin #1

Center Span

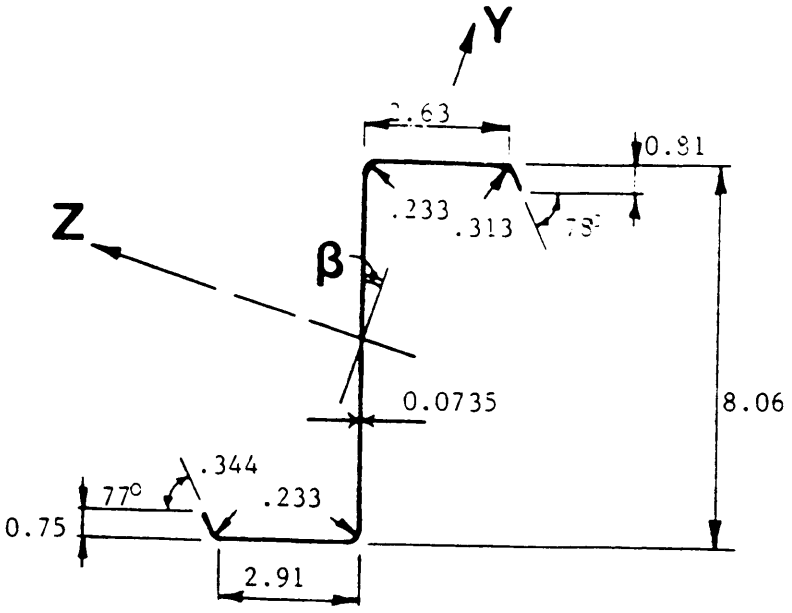

Properties: Span (ft) = 23.0 I_x(in^4) = 0.0020

Area (in^2) = 1.0901 I_y(in^4) = 0.8146

β(deg) = 18.2603 I_z(in^4) = 12.0635

Purlin #2

Center Span

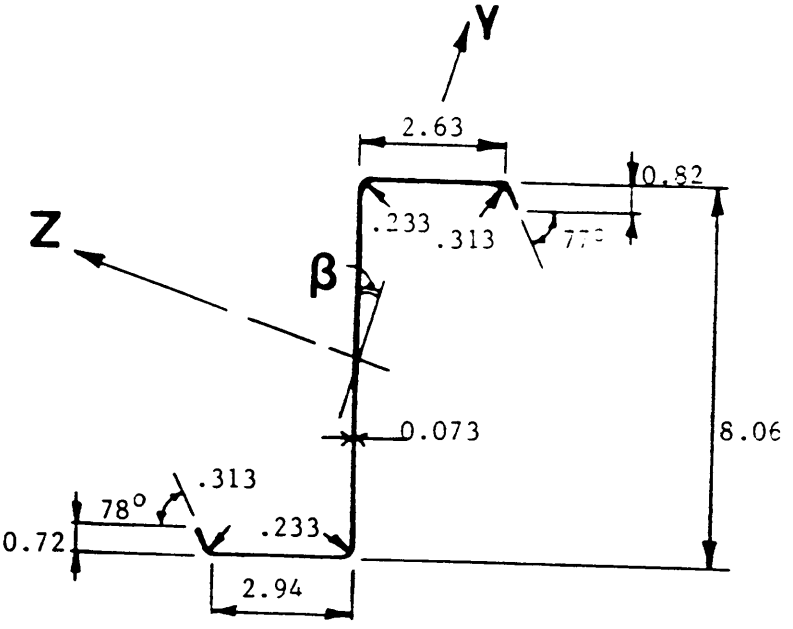

Properties: Span (ft) = 23.0 I_x(in^4) = 0.0020

Area (in^2) = 1.0833 I_y(in^4) = 0.8076

β(deg) = 18.2974 I_z(in^4) = 12.0150

Figure E.20 Measured Ourlin Dimensions and Calculated Properties, Test R3/2-R-3, Continued

Purlin #1

South Span

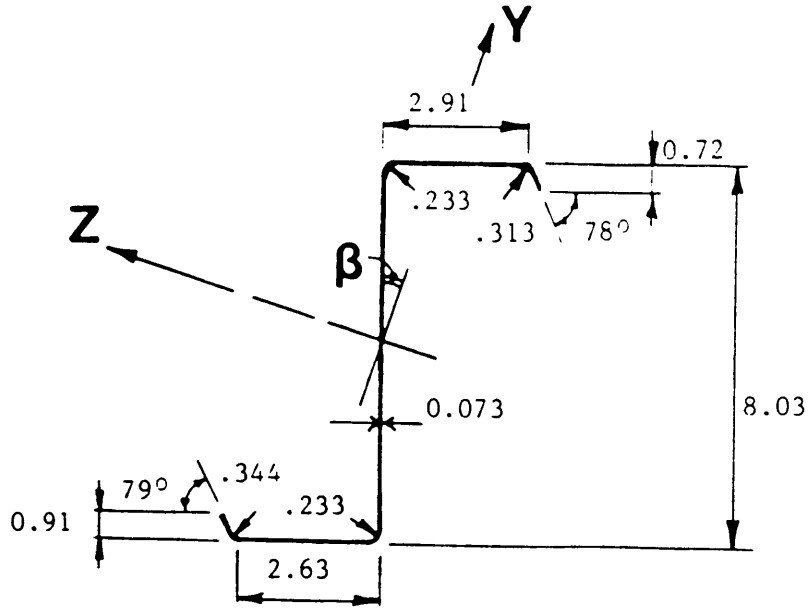

Properties: Span (ft) = 23.0 $I_x(in^4)$ = 0.0020

Area (in^2) = 1.0841 $I_y(in^4)$ = 0.8125

β(deg) = 18.4315 $I_z(in^4)$ = 11.9414

Purlin #2

South Span

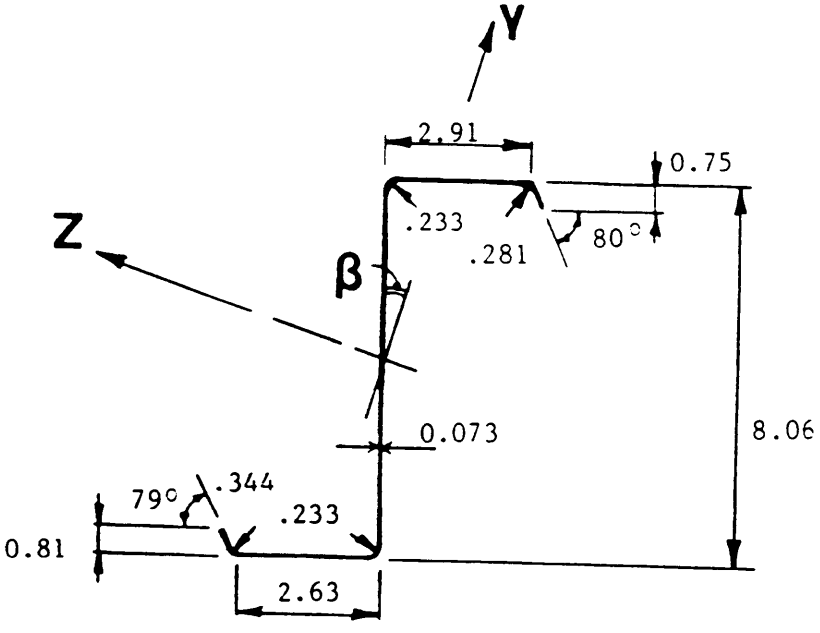

Properties: Span (ft) = 23.0 $I_x(in^4)$ = 0.0020

Area (in^2) = 1.0808 $I_y(in^4)$ = 0.7978

β(deg) = 18.1372 $I_z(in^4)$ = 11.9384

Figure E.21 Measured Purlin Dimensions and Calculated Properties, Test R3/2-R-3

(a) Purlin #1, North Span

GEOMETRY OF CROSS-SECTION

	Top	Bottom
Vertical lip dimensions	0.7188 in.	0.7813 in.
Lip angles	80.0000 deg.	77.0000 deg.
Flange widths	2.9380 in.	2.6560 in.
Radii		
Lip to flange	0.3125 in.	0.3438 in.
Flange to web	0.2330 in.	0.2330 in.

Total purlin depth	8.0625 in.
Purlin thickness	0.0720 in.

Material Properties

Material yield stress	56.6 ksi
Modulus of elasticity	29500.0 ksi

General

Flat width of compression flange	2.3104 in.
Gross moment of inertia	10.32 $in.^4$

1986 AISI Procedure

Flange is not fully effective	
Effective flange width	1.7369 in.
Effective moment of inertia	9.27 $in.^4$
Allowable flexural capacity	74.21 kip-in

Figure E.22 Strength Calculations, Test R3/2-R-3, Continued

(b) Purlin #2, North Span

GEOMETRY OF CROSS-SECTION

		Top	Bottom
Vertical lip dimensions		0.7188 in.	0.8125 in.
Lip angles		79.0000 deg.	78.0000 deg.
Flange widths		2.9375 in.	2.6563 in.
Radii			
Lip to flange		0.3125 in.	0.3125 in.
Flange to web		0.2330 in.	0.2330 in.
Total purlin depth	8.0625 in.		
Purlin thickness	0.0725 in.		

Material Properties

Material yield stress	56.6 ksi
Modulus of elasticity	29500.0 ksi

General

Flat width of compression flange	2.3146 in.
Gross moment of inertia	10.42 $in.^4$

1986 AISI Procedure

Flange is not fully effective	
Effective flange width	1.7519 in.
Effective moment of inertia	9.38 $in.^4$
Allowable flexural capacity	74.96 kip-in

Figure E.23 Strength Calculations, Test R3/2-R-3, Continued

(c) Purlin #1, Center Span

GEOMETRY OF CROSS-SECTION

		Top	Bottom
Vertical lip dimensions		0.8125 in.	0.7500 in.
Lip angles		78.0000 deg.	77.0000 deg.
Flange widths		2.6250 in.	2.9063 in.
Radii			
Lip to flange		0.3125 in.	0.3125 in.
Flange to web		0.2330 in.	0.2330 in.
Total purlin depth	7.9700 in.		
Purlin thickness	0.0640 in.		

Material Properties

Material yield stress	56.6 ksi
Modulus of elasticity	29500.0 ksi

General

Flat width of compression flange	2.0059 in.
Gross moment of inertia	10.52 $in.^4$

1986 AISI Procedure

Flange is not fully effective	
Effective flange width	1.6806 in.
Effective moment of inertia	9.75 $in.^4$
Allowable flexural capacity	77.12 kip-in

Figure E.24 Strength Calculations, Test R3/2-R-3, Continued

(d) Purlin #2, Center Span

GEOMETRY OF CROSS-SECTION

	Top	Bottom
Vertical lip dimensions	0.8125 in.	0.7188 in.
Lip angles	77.0000 deg.	78.0000 deg.
Flange widths	2.6250 in.	2.9375 in.
Radii		
Lip to flange	0.3125 in.	0.3125 in.
Flange to web	0.2330 in.	0.2330 in.

Total purlin depth	8.0625 in.
Purlin thickness	0.0730 in.

Material Properties

Material yield stress	56.6 ksi
Modulus of elasticity	29500.0 ksi

General

Flat width of compression flange	2.0124 in.
Gross moment of inertia	10.47 $in.^4$

1986 AISI Procedure

Flange is not fully effective	
Effective flange width	1.6785 in.
Effective moment of inertia	9.69 $in.^4$
Allowable flexural capacity	76.61 kip-in

Figure E.25 Strength Calculations, Test R3/2-R-3, Continued

(e) Purlin #1, South Span

GEOMETRY OF CROSS-SECTION

		Top	Bottom
Vertical lip dimensions		0.7500 in.	0.8125 in.
Lip angles		82.0000 deg.	79.0000 deg.
Flange widths		2.9063 in.	2.6250 in.
Radii			
Lip to flange		0.3125 in.	0.3438 in.
Flange to web		0.2330 in.	0.2330 in.
Total purlin depth	8.0625 in.		
Purlin thickness	0.0730 in.		

Material Properties

Material yield stress	56.6	ksi
Modulus of elasticity	29500.0	ksi

General

Flat width of compression flange	2.2768	in.
Gross moment of inertia	10.41	$in.^4$

1986 AISI Procedure

Flange is not fully effective		
Effective flange width	1.7671	in.
Effective moment of inertia	9.43	$in.^4$
Allowable flexural capacity	75.82	kip-in

Figure E.26 Strength Calculations, Test R3/2-R-3, Continued

(f) Purlin #2, South Span

GEOMETRY OF CROSS-SECTION

		Top	Bottom
Vertical lip dimensions		0.7188 in.	0.9063 in.
Lip angles		78.0000 deg.	79.0000 deg.
Flange widths		2.9063 in.	2.6250 in.
Radii			
Lip to flange		0.3125 in.	0.3438 in.
Flange to web		0.2330 in.	0.2330 in.
Total purlin depth	8.0313 in.		
Purlin thickness	0.0730 in.		

Material Properties

Material yield stress	56.6 ksi
Modulus of elasticity	29500.0 ksi

General

Flat width of compression flange	2.2881 in.
Gross moment of inertia	10.39 $in.^4$

1986 AISI Procedure

Flange is not fully effective	
Effective flange width	1.7591 in.
Effective moment of inertia	9.38 $in.^4$
Allowable flexural capacity	75.14 kip-in

Figure E.27 Strength Calculations, Test R3/2-R-3

Purlin #1

North Span

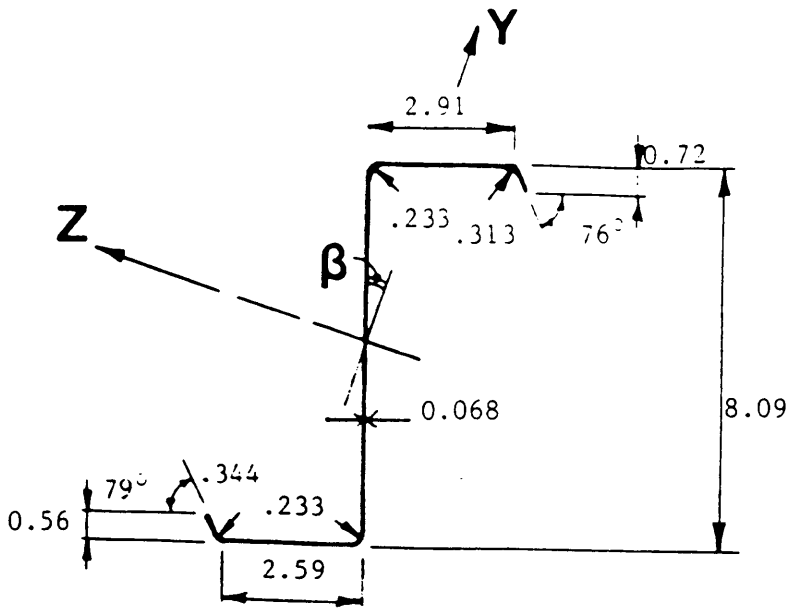

Properties: Span (ft) = 23.0 $I_x(in^4)$ = 0.0015

Area (in^2) = 0.9890 $I_y(in^4)$ = 0.6924

β(deg) = 17.3001 $I_z(in^4)$ = 10.8555

Purlin #2

North Span

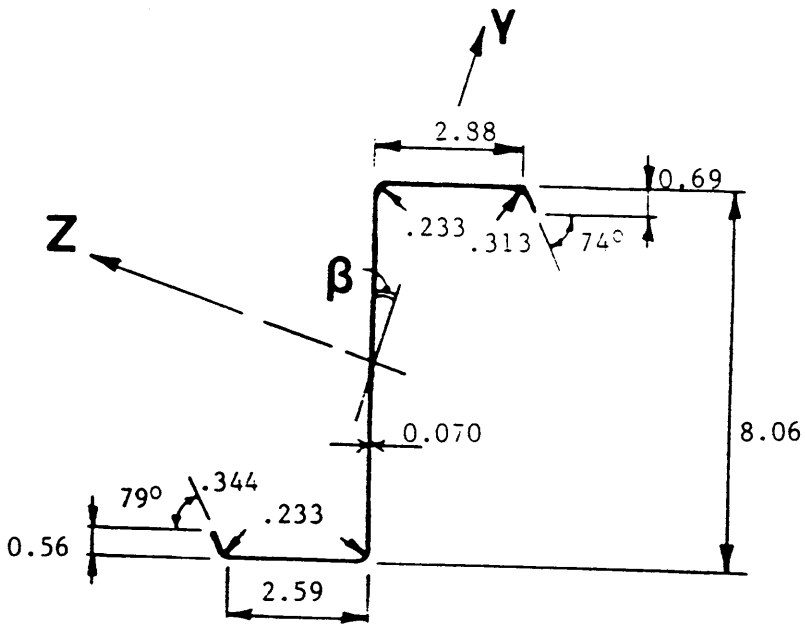

Properties: Span (ft) = 23.0 $I_x(in^4)$ = 0.0016

Area (in^2) = 1.0051 $I_y(in^4)$ = 0.6927

β(deg) = 17.2361 $I_z(in^4)$ = 10.9396

Figure E.28 Measured Purlin Dimensions and Calculated Properties, Test P2/2-R-3, Continued

Purlin #1

Center Span

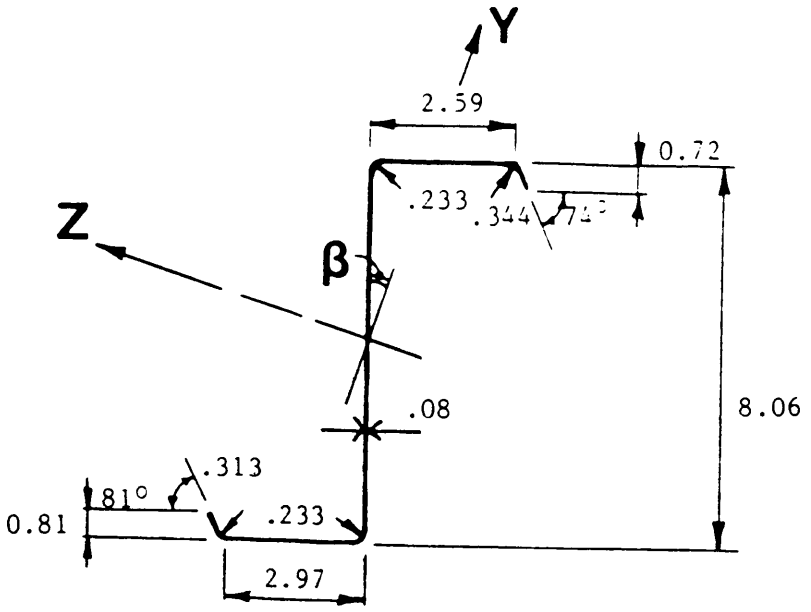

Properties: Span (ft) = 23.0 $I_x(in^4)$ = 0.0026

Area (in^2) = 1.1866 $I_y(in^4)$ = 0.8901

β(deg) = 18.3066 $I_z(in^4)$ = 13.1412

Purlin #2

Center Span

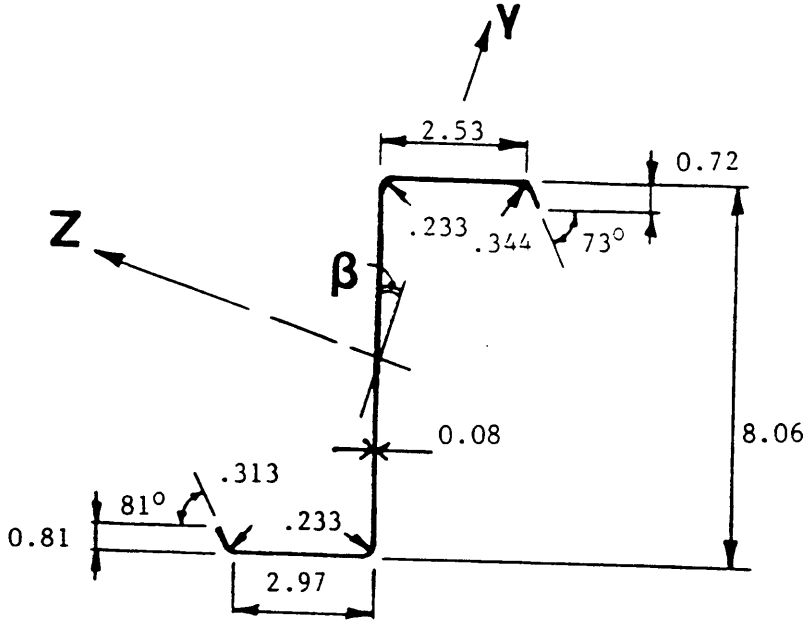

Properties: Span (ft) = 23.0 $I_x(in^4)$ = 0.0026

Area (in^2) = 1.1822 $I_y(in^4)$ = 0.8751

β(deg) = 18.1213 $I_z(in^4)$ = 13.0318

Figure E.29 Measured Purlin Dimensions and Calculated Properties, Test P2/2-R-3, Continued

Purlin #1

South Span

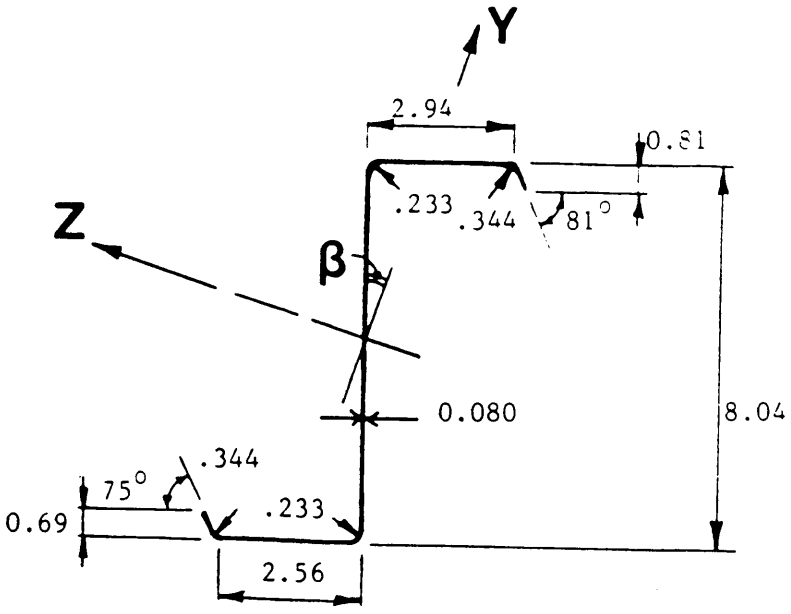

Properties: Span (ft) = 23.0 $I_x(in^4)$ = 0.0025

Area (in^2) = 1.1759 $I_y(in^4)$ = 0.8597

β(deg) = 18.0085 $I_z(in^4)$ = 12.8681

Purlin #2

South Span

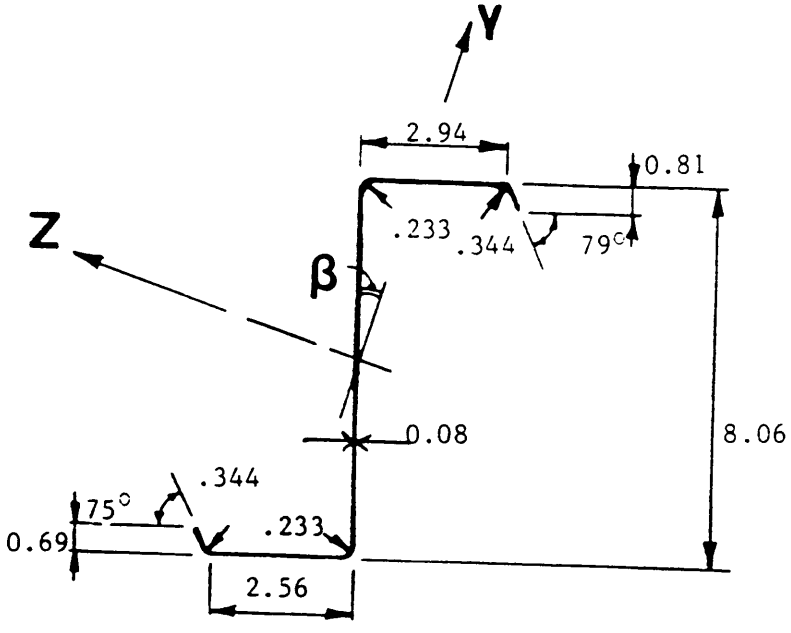

Properties: Span (ft) = 23.0 $I_x(in^4)$ = 0.0025

Area (in^2) = 1.1786 $I_y(in^4)$ = 0.8662

β(deg) = 18.0086 $I_z(in^4)$ = 12.9600

Figure E.30 Measured Purlin Dimensions and Calculated Properties, Test P2/2-R-3

(a) Purlin #1, North Span

GEOMETRY OF CROSS-SECTION

	Top	Bottom
Vertical lip dimensions	0.7190 in.	0.5630 in.
Lip angles	76.0000 deg.	79.0000 deg.
Flange widths	2.9060 in.	2.5940 in.
Radii		
Lip to flange	0.3130 in.	0.3440 in.
Flange to web	0.2330 in.	0.2330 in.

Total purlin depth	8.0900 in.
Purlin thickness	0.0680 in.

Material Properties

Material yield stress	56.6 ksi
Modulus of elasticity	29500.0 ksi

General

Flat width of compression flange	2.3073 in.
Gross moment of inertia	9.49 $in.^4$

1986 AISI Procedure

Flange is not fully effective	
Effective flange width	1.7214 in.
Effective moment of inertia	8.54 $in.^4$
Allowable flexural capacity	69.37 kip-in

Figure E.31 Strength Calculations, Test P2/2-R-3, Continued

(b) Purlin #2, North Span

GEOMETRY OF CROSS-SECTION

	Top	Bottom
Vertical lip dimensions	0.6880 in.	0.5630 in.
Lip angles	74.0000 deg.	79.0000 deg.
Flange widths	2.8750 in.	2.5940 in.
Radii		
Lip to flange	0.3130 in.	0.3440 in.
Flange to web	0.2330 in.	0.2330 in.

Total purlin depth	8.0600 in.
Purlin thickness	0.0700 in.

Material Properties

Material yield stress	56.6 ksi
Modulus of elasticity	29500.0 ksi

General

Flat width of compression flange	2.2834 in.
Gross moment of inertia	9.63 in.4

1986 AISI Procedure

Flange is not fully effective	
Effective flange width	1.7292 in.
Effective moment of inertia	8.69 in.4
Allowable flexural capacity	70.79 kip-in

Figure E.32 Strength Calculations, Test P2/2-R-3, Continued

(c) Purlin #1, Center Span

GEOMETRY OF CROSS-SECTION

		Top	Bottom
Vertical lip dimensions		0.7190 in.	0.8130 in.
Lip angles		74.0000 deg.	81.0000 deg.
Flange widths		2.5940 in.	2.9690 in.
Radii			
Lip to flange		0.3440 in.	0.3130 in.
Flange to web		0.2330 in.	0.2330 in.
Total purlin depth	8.0600 in.		
Purlin thickness	0.0800 in.		

Material Properties

Material yield stress	56.6	ksi
Modulus of elasticity	29500.0	ksi

General

Flat width of compression flange	1.9615	in.
Gross moment of inertia	11.29	in.4

1986 AISI Procedure

Flange is not fully effective		
Effective flange width	1.7242	in.
Effective moment of inertia	10.62	in.4
Allowable flexural capacity	83.77	kip-in

Figure E.33 Strength Calculations, Test P2/2-R-3, Continued

(d) Purlin #2, Center Span

GEOMETRY OF CROSS-SECTION

	Top	Bottom
Vertical lip dimensions	0.7190 in.	0.8130 in.
Lip angles	73.0000 deg.	81.0000 deg.
Flange widths	2.5310 in.	2.9690 in.
Radii		
Lip to flange	0.3440 in.	0.3130 in.
Flange to web	0.2330 in.	0.2330 in.

Total purlin depth	8.0600 in.
Purlin thickness	0.0800 in.

Material Properties

Material yield stress	56.6 ksi
Modulus of elasticity	29500.0 ksi

General

Flat width of compression flange	1.9043 in.
Gross moment of inertia	11.22 in.4

1986 AISI Procedure

Flange is not fully effective	
Effective flange width	1.7383 in.
Effective moment of inertia	10.66 in.4
Allowable flexural capacity	84.28 kip-in

Figure E.34 Strength Calculations, Test P2/2-R-3, Continued

(e) Purlin #1, South Span

GEOMETRY OF CROSS-SECTION

		Top	Bottom
Vertical lip dimensions		0.8100 in.	0.6900 in.
Lip angles		81.0000 deg.	75.0000 deg.
Flange widths		2.9400 in.	2.5600 in.
Radii			
Lip to flange		0.3440 in.	0.3440 in.
Flange to web		0.2330 in.	0.2330 in.
Total purlin depth	8.0400 in.		
Purlin thickness	0.0800 in.		

Material Properties

Material yield stress	56.6 ksi
Modulus of elasticity	29500.0 ksi

General

Flat width of compression flange	2.2649 in.
Gross moment of inertia	11.09 in.4

1986 AISI Procedure

Flange is not fully effective	
Effective flange width	1.7206 in.
Effective moment of inertia	10.05 $in.^4$
Allowable flexural capacity	82.06 kip-in

Figure E.35 Strength Calculations, Test P2/2-R-3, Continued

(f) Purlin #2, South Span

GEOMETRY OF CROSS-SECTION

		Top	Bottom
Vertical lip dimensions		0.8100 in.	0.6900 in.
Lip angles		79.0000 deg.	75.0000 deg.
Flange widths		2.9400 in.	2.5600 in.
Radii			
Lip to flange		0.3440 in.	0.3440 in.
Flange to web		0.2330 in.	0.2330 in.
Total purlin depth	8.0600 in.		
Purlin thickness	0.0800 in.		

Material Properties

Material yield stress	56.6 ksi
Modulus of elasticity	29500.0 ksi

General

Flat width of compression flange	2.2775 in.
Gross moment of inertia	11.18 in.4

1986 AISI Procedure

Flange is not fully effective	
Effective flange width	1.7406 in.
Effective moment of inertia	10.13 in.^{4}
Allowable flexural capacity	82.61 kip-in

Figure E.36 Strength Calculations, Test P2/2-R-3

Purlin #1

North Span

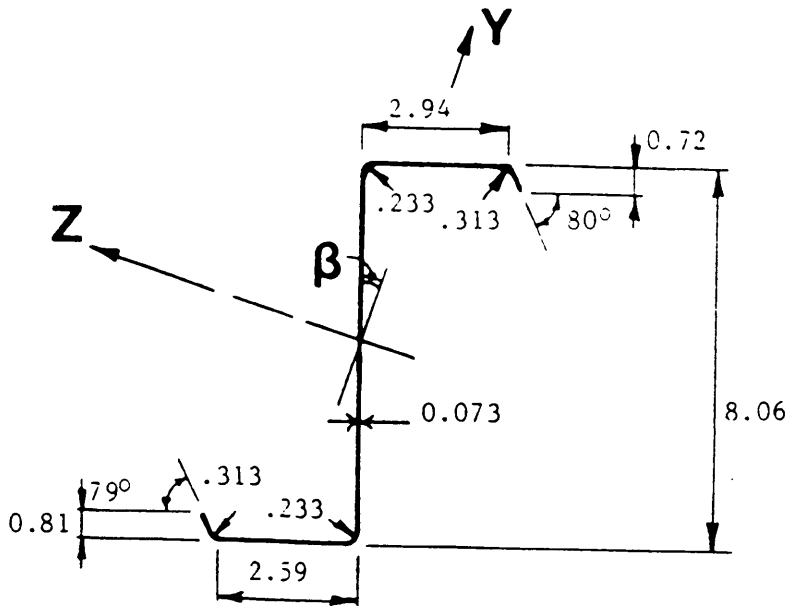

Properties: Span (ft) = 23.0 I_x (in^4) = 0.0019

Area (in^2) = 1.0791 I_y (in^4) = 0.7909

β(deg) = 18.0803 I_z (in^4) = 11.9140

Purlin #2

North Span

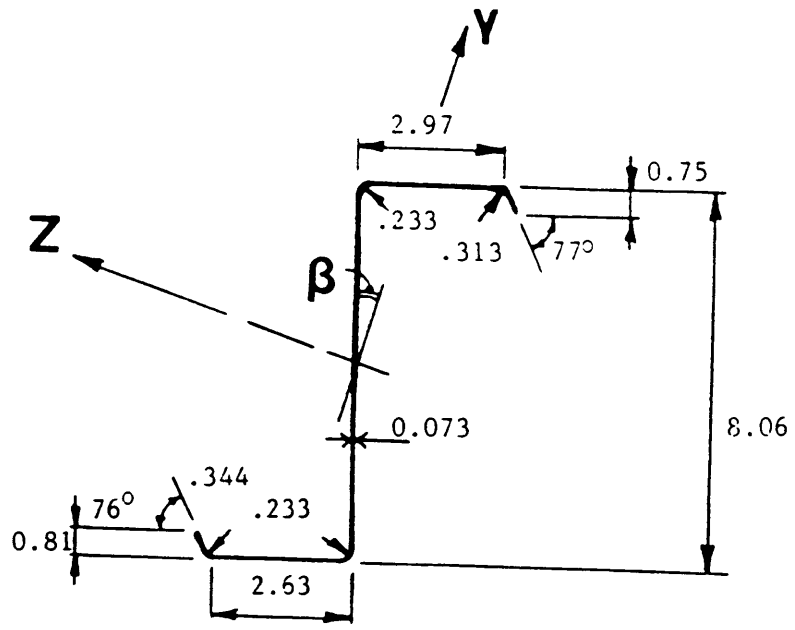

Properties: Span (ft) = 23.0 I_x (in^4) = 0.0020

Area (in^2) = 1.0888 I_y (in^4) = 0.8303

β(deg) = 18.5602 I_z (in^4) = 12.1325

Figure E.37 Measured Purlin Dimensions and Calculated Properties, Test R3/2-T-3, Continued

Purlin #1

Center Span

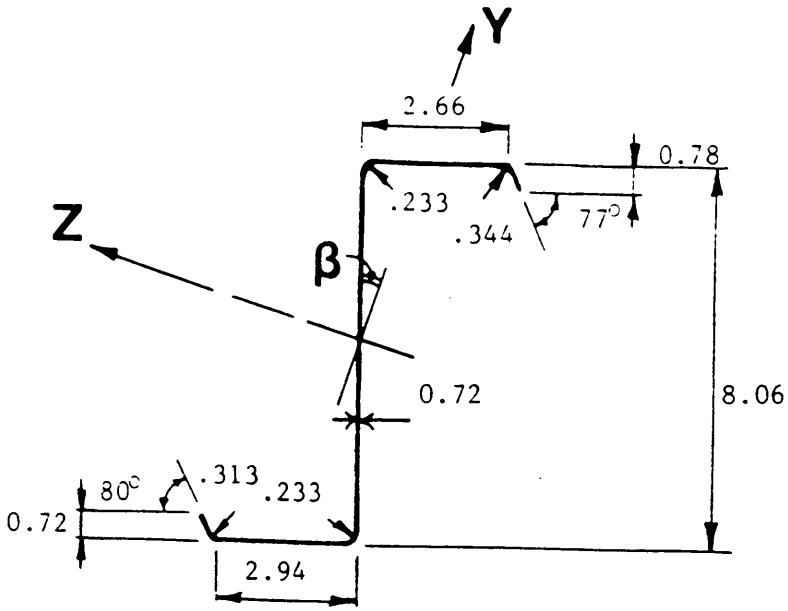

Properties: Span (ft) = 23.0
Area (in^2) = 1.0669
β(deg) = 18.2522
I_x (in^4) = 0.0019
I_y (in^4) = 0.7949
I_z (in^4) = 11.8297

Purlin #2

Center Span

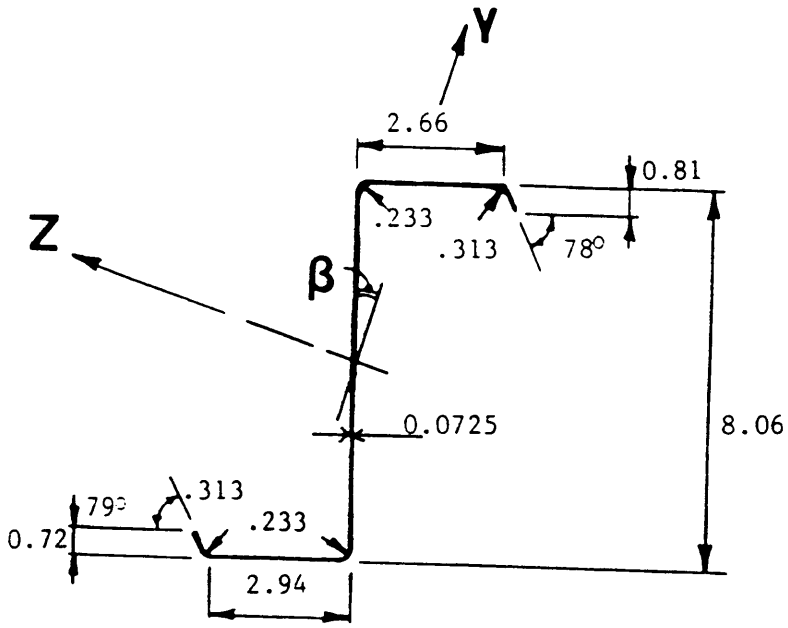

Properties: Span (ft) = 23.0
Area (in^2) = 1.0772
β(deg) = 18.3530
I_x (in^4) = 0.0019
I_y (in^4) = 0.8065
I_z (in^4) = 11.9653

Figure E.38 Measured Purlin Dimensions and Calculated Properties, Test R3/2-T-3, Continued

Purlin #1
South Span

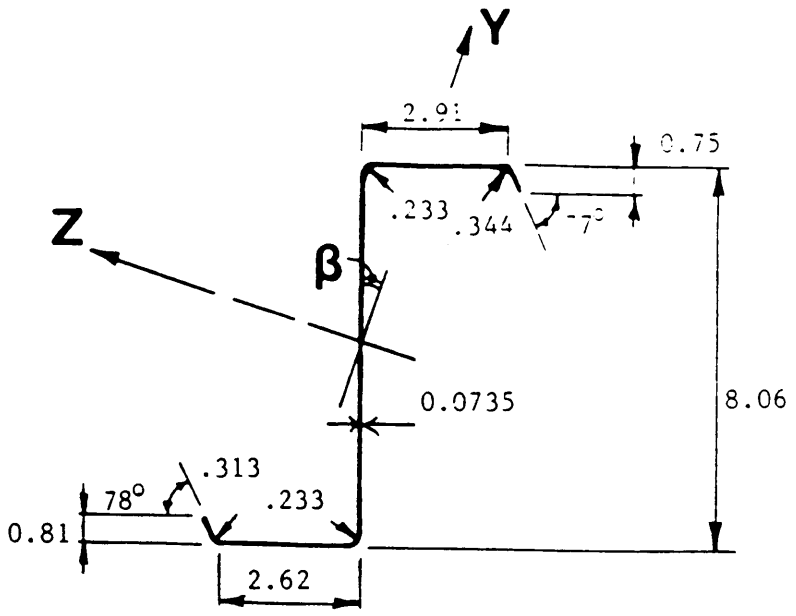

Properties: Span (ft) = 23.0
Area (in^2) = 1.0901
β(deg) = 18.2457
I_x (in^4) = 0.0020
I_y (in^4) = 0.8116
I_z (in^4) = 12.0673

Purlin #2
South Span

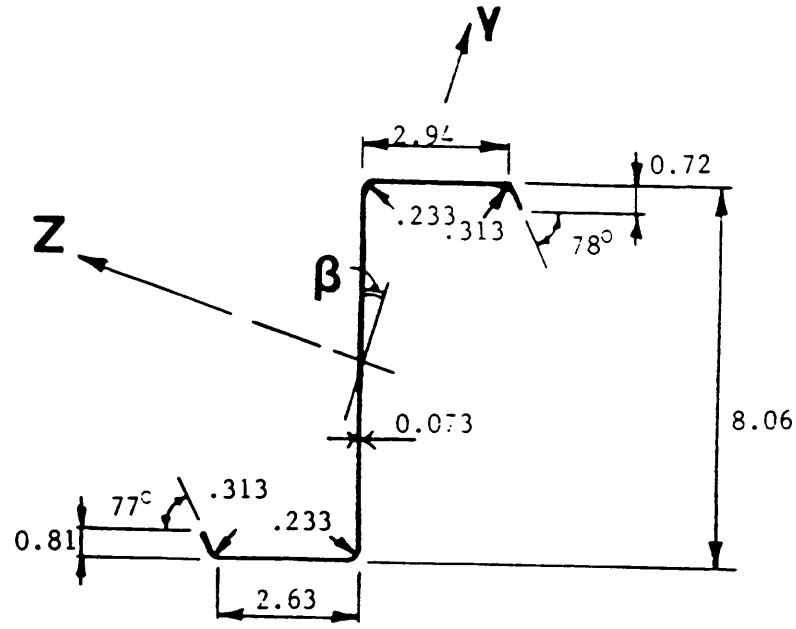

Properties: Span (ft) = 23.0
Area (in^2) = 1.0969
β(deg) = 18.9657
I_x (in^4) = 0.0020
I_y (in^4) = 0.8614
I_z (in^4) = 12.3503

Figure E.39 Measured Purlin Dimensions and Calculated Properties, Test R3/2-T-3

(a) Purlin #1, North Span

GEOMETRY OF CROSS-SECTION

		Top	Bottom
Vertical lip dimensions		0.7500 in.	0.8125 in.
Lip angles		77.0000 deg.	78.0000 deg.
Flange widths		2.9063 in.	2.6250 in.
Radii			
Lip to flange		0.3438 in.	0.3125 in.
Flange to web		0.2330 in.	0.2330 in.
Total purlin depth	8.0625 in.		
Purlin thickness	0.0735 in.		

Material Properties

Material yield stress	56.6	ksi
Modulus of elasticity	29500.0	ksi

General

Flat width of compression flange	2.2679	in.
Gross moment of inertia	10.52	in.4

1986 AISI Procedure

Flange is not fully effective		
Effective flange width	1.7643	in.
Effective moment of inertia	9.53	in.4
Allowable flexural capacity	76.67	kip-in

Figure E.40 Strength Calculations, Test R3/2-T-3, Continued

(b) Purlin #2, North Span

GEOMETRY OF CROSS-SECTION

		Top	Bottom
Vertical lip dimensions		0.7188 in.	0.8125 in.
Lip angles		78.0000 deg.	77.0000 deg.
Flange widths		2.9375 in.	2.8125 in.
Radii			
Lip to flange		0.3125 in.	0.3125 in.
Flange to web		0.2330 in.	0.2330 in.
Total purlin depth	8.0625 in.		
Purlin thickness	0.0730 in.		

Material Properties

Material yield stress	56.6	ksi
Modulus of elasticity	29500.0	ksi

General

Flat width of compression flange	2.3193	in.
Gross moment of inertia	10.69	in.4

1986 AISI Procedure

Flange is not fully effective		
Effective flange width	1.7668	in.
Effective moment of inertia	9.62	in.4
Allowable flexural capacity	76.21	kip-in

Figure E.41 Strength Calculations, Test R3/2-T-3, Continued

(c) Purlin #1, Center Span

GEOMETRY OF CROSS-SECTION

	Top	Bottom
Vertical lip dimensions	0.7813 in.	0.7188 in.
Lip angles	77.0000 deg.	80.0000 deg.
Flange widths	2.6563 in.	2.9375 in.
Radii		
Lip to flange	0.3438 in.	0.3125 in.
Flange to web	0.2330 in.	0.2330 in.

Total purlin depth	8.0625 in.
Purlin thickness	0.0720 in.

Material Properties

Material yield stress	56.6 ksi
Modulus of elasticity	29500.0 ksi

General

Flat width of compression flange	2.0206 in.4
Gross moment of inertia	10.32 in.4

1986 AISI Procedure

Flange is not fully effective	
Effective flange width	1.5961 in.
Effective moment of inertia	9.41 $in.^4$
Allowable flexural capacity	73.93 kip-in

Figure E.42 Strength Calculations, Test R3/2-T-3, Continued

(d) Purlin #2, Center Span

GEOMETRY OF CROSS-SECTION

		Top	Bottom
Vertical lip dimensions		0.8125 in.	0.7188 in.
Lip angles		78.0000 deg.	79.0000 deg.
Flange widths		2.6563 in.	2.9375 in.
Radii			
Lip to flange		0.3125 in.	0.3125 in.
Flange to web		0.2330 in.	0.2330 in.
Total purlin depth	8.0625 in.		
Purlin thickness	0.0725 in.		

Material Properties

Material yield stress	56.6	ksi
Modulus of elasticity	29500.0	ksi

General

Flat width of compression flange	2.0390	in.
Gross moment of inertia	10.41	$in.^4$

1986 AISI Procedure

Flange is not fully effective		
Effective flange width	1.6584	in.
Effective moment of inertia	9.57	$in.^4$
Allowable flexural capacity	75.56	kip-in

Figure E.43 Strength Calculations, Test R3/2-T-3, Continued

(e) Purlin #1, South Span

GEOMETRY OF CROSS-SECTION

		Top	Bottom
Vertical lip dimensions		0.7188 in.	0.8125 in.
Lip angles		80.0000 deg.	79.0000 deg.
Flange widths		2.9375 in.	2.5938 in.
Radii			
Lip to flange		0.3125 in.	0.3125 in.
Flange to web		0.2330 in.	0.2330 in.
Total purlin depth	8.0625 in.		
Purlin thickness	0.0730 in.		

Material Properties

Material yield stress	56.6	ksi
Modulus of elasticity	29500.0	ksi

General

Flat width of compression flange	2.3080	in.
Gross moment of inertia	10.40	$in.^4$

1986 AISI Procedure

Flange is not fully effective		
Effective flange width	1.7483	in.
Effective moment of inertia	9.36	$in.^4$
Allowable flexural capacity	75.21	kip-in

Figure E.44 Strength Calculations, Test R3/2-T-3

(f) Purlin #2, South Span

GEOMETRY OF CROSS-SECTION

		Top	Bottom
Vertical lip dimensions		0.7500 in.	0.8125 in.
Lip angles		77.0000 deg.	76.0000 deg.
Flange widths		2.9688 in.	2.6250 in.
Radii			
Lip to flange		0.3125 in.	0.3125 in.
Flange to web		0.2330 in.	0.2330 in.
Total purlin depth	8.0680 in.		
Purlin thickness	0.0730 in.		

Material Properties

Material yield stress	56.6	ksi
Modulus of elasticity	29500.0	ksi

General

Flat width of compression flange	2.3562	in.
Gross moment of inertia	10.54	$in.^4$

1986 AISI Procedure

Flange is not fully effective		
Effective flange width	1.8096	in.
Effective moment of inertia	9.50	$in.^4$
Allowable flexural capacity	76.47	kip-in

Figure E.45 Strength Calculations, Test R3/2-T-3

Purlin #1

North Span

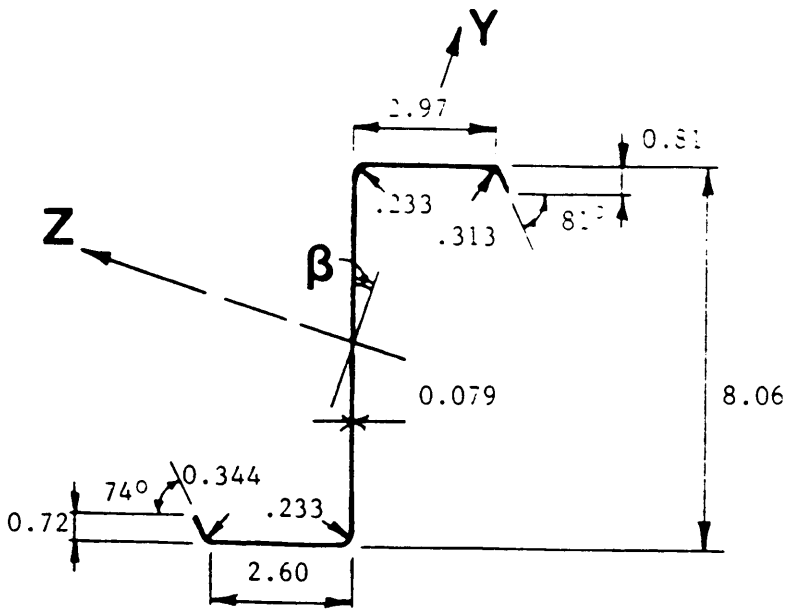

Properties: Span (ft) = 23.0
Area (in^2) = 1.1719
β(deg) = 18.3078
I_x (in^4) = 0.0025
I_y (in^4) = 0.8795
I_z (in^4) = 12.9806

Purlin #2

North Span

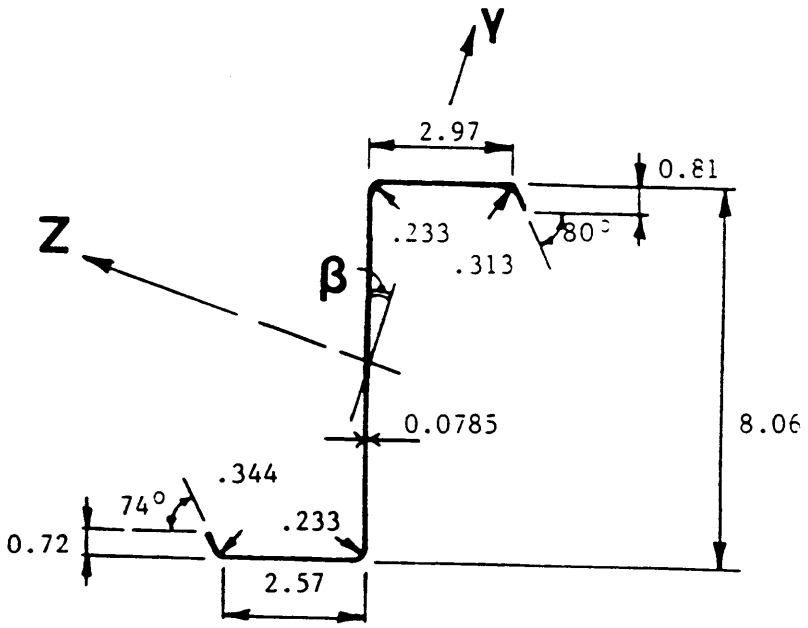

Properties: Span (ft) = 23.0
Area (in^2) = 1.1626
β(deg) = 18.2302
I_x (in^4) = 0.0024
I_y (in^4) = 0.8653
I_z (in^4) = 12.9503

Figure E.46 Measured Purlin Dimensions and Calculated Properties, Test P2/2-T-3, Continued

Purlin #1

Center Span

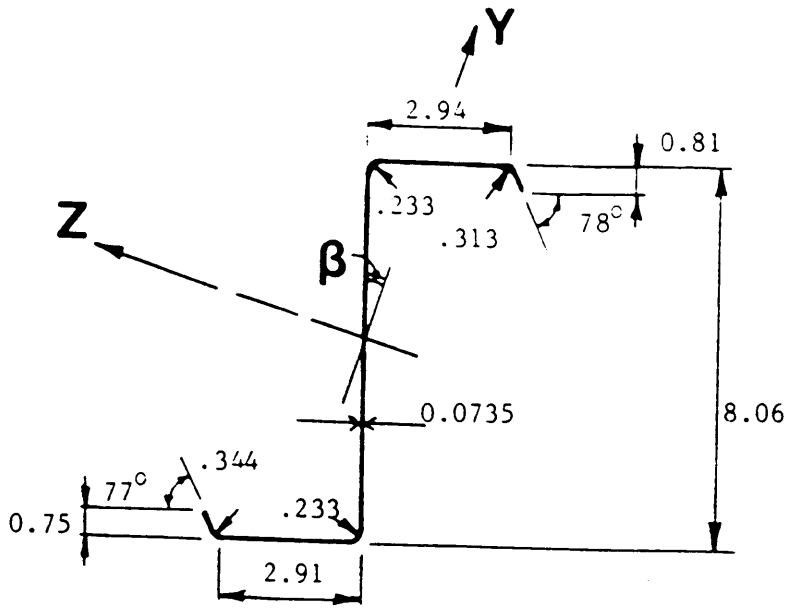

Properties: Span (ft) = 23.0 I_x (in^4) = 0.0020

Area (in^2) = 1.0901 I_y (in^4) = 0.8146

$\bar{x}$(deg) = 18.2603 I_z (in^4) = 12.0635

Purlin #2

Center Span

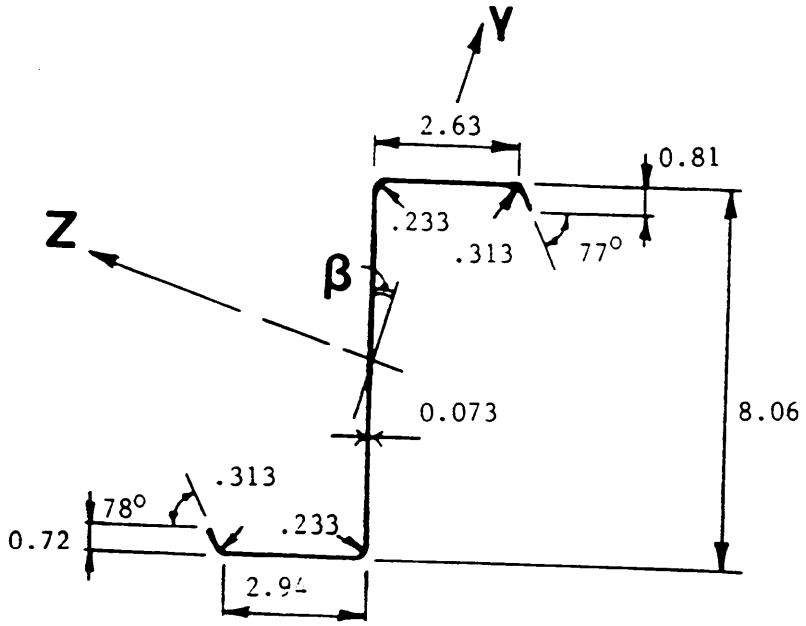

Properties: Span (ft) = 23.0 I_x (in^4) = 0.0020

Area (in^2) = 1.0833 I_y (in^4) = 0.8076

$\bar{x}$(deg) = 18.2974 I_z (in^4) = 12.0150

Figure E.47 Measured Purlin Dimensions and Calculated Properties, Test P2/2-T-3, Continued

Purlin #1

South Span

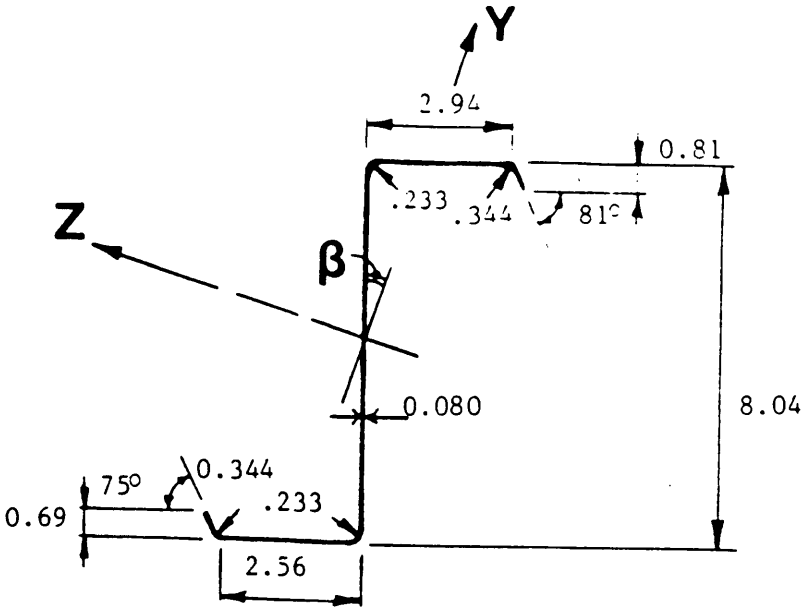

Properties: Span (ft) = 23.0
Area (in^2) = 1.1762
β(deg) = 17.9974
I_x (in^4) = 0.0025
I_y (in^4) = 0.8597
I_z (in^4) = 12.8797

Purlin #2

South Span

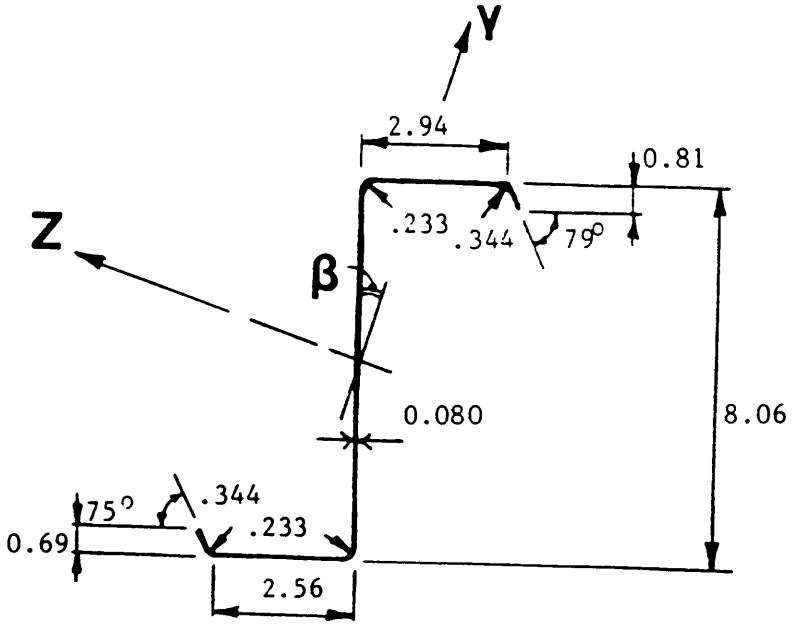

Properties: Span (ft) = 23.0
Area (in^2) = 1.1788
β(deg) = 18.0006
I_x (in^4) = 0.0026
I_y (in^4) = 0.8662
I_z (in^4) = 12.9683

Figure E.48 Measured Purlin Dimensions and Calculated Properties, Test P2/2-T-3

(a) Purlin #1, North Span

GEOMETRY OF CROSS-SECTION

		Top	Bottom
Vertical lip dimensions		0.8130 in.	0.7190 in.
Lip angles		81.0000 deg.	74.0000 deg.
Flange widths		2.9690 in.	2.5940 in.
Radii			
Lip to flange		0.3125 in.	0.3440 in.
Flange to web		0.2330 in.	0.2330 in.
Total purlin depth	8.0630 in.		
Purlin thickness	0.0790 in.		

Material Properties

Material yield stress	56.6	ksi
Modulus of elasticity	29500.0	ksi

General

Flat width of compression flange	2.3220	in.
Gross moment of inertia	11.27	$in.^4$

1986 AISI Procedure

Flange is not fully effective		
Effective flange width	1.8897	in.
Effective moment of inertia	10.31	$in.^4$
Allowable flexural capacity	84.26	kip-in

Figure E.49 Strength Calculations, Test P2/2-T-3, Continued

(b) Purlin #2, North Span

GEOMETRY OF CROSS-SECTION

		Top	Bottom
Vertical lip dimensions		0.8130 in.	0.7190 in.
Lip angles		80.0000 deg.	74.0000 deg.
Flange widths		2.9690 in.	2.5630 in.
Radii			
Lip to flange		0.3125 in.	0.3440 in.
Flange to web		0.2330 in.	0.2330 in.
Total purlin depth	8.0630 in.		
Purlin thickness	0.0785 in.		

Material Properties

Material yield stress	56.6 ksi
Modulus of elasticity	29500.0 ksi

General

Flat width of compression flange	2.3294 in.
Gross moment of inertia	11.17 $in.^4$

1986 AISI Procedure

Flange is not fully effective	
Effective flange width	1.8930 in.
Effective moment of inertia	10.21 $in.^4$
Allowable flexural capacity	83.67 kip-in

Figure E.50 Strength Calculations, Test P2/2-T-3, Continued

(c) Purlin #1, Center Span

GEOMETRY OF CROSS-SECTION

		Top	Bottom
Vertical lip dimensions		0.8125 in.	0.7500 in.
Lip angles		78.0000 deg.	77.0000 deg.
Flange widths		2.6250 in.	2.9063 in.
Radii			
Lip to flange		0.3125 in.	0.3125 in.
Flange to web		0.2330 in.	0.2330 in.
Total purlin depth	8.0625 in.		
Purlin thickness	0.0735 in.		

Material Properties

Material yield stress	56.6 ksi
Modulus of elasticity	29500.0 ksi

General

Flat width of compression flange	2.0059 in.
Gross moment of inertia	10.52 $in.^4$

1986 AISI Procedure

Flange is not fully effective	
Effective flange width	1.6806 in.
Effective moment of inertia	9.75 $in.^4$
Allowable flexural capacity	77.12 kip-in

Figure E.51 Strength Calculations, Test P2/2-T-3, Continued

(d) Purlin #2, Center Span

GEOMETRY OF CROSS-SECTION

	Top	Bottom
Vertical lip dimensions	0.8125 in.	0.7188 in.
Lip angles	77.0000 deg.	78.0000 deg.
Flange widths	2.6250 in.	2.9375 in.
Radii		
Lip to flange	0.3125 in.	0.3125 in.
Flange to web	0.2330 in.	0.2330 in.

Total purlin depth	8.0625 in.
Purlin thickness	0.0730 in.

Material Properties

Material yield stress	56.6 ksi
Modulus of elasticity	29500.0 ksi

General

Flat width of compression flange	2.0124 in.
Gross moment of inertia	10.47 $in.^4$

1986 AISI Procedure

Flange is not fully effective	
Effective flange width	1.6785 in.
Effective moment of inertia	9.69 $in.^4$
Allowable flexural capacity	76.61 kip-in

Figure E.52 Strength Calculations, Test P2/2-T-3, Continued

(e) Purlin #1, South Span

GEOMETRY OF CROSS-SECTION

		Top	Bottom
Vertical lip dimensions		0.8125 in.	0.6875 in.
Lip angles		81.0000 deg.	75.0000 deg.
Flange widths		2.9375 in.	2.5625 in.
Radii			
Lip to flange		0.3438 in.	0.3438 in.
Flange to web		0.2330 in.	0.2330 in.
Total purlin depth	8.0435 in.		
Purlin thickness	0.0800 in.		

Material Properties

Material yield stress	56.6 ksi
Modulus of elasticity	29500.0 ksi

General

Flat width of compression flange	2.2625 in.
Gross moment of inertia	11.21 $in.^4$

1986 AISI Procedure

Flange is not fully effective	
Effective flange width	1.7129 in.
Effective moment of inertia	10.10 $in.^4$
Allowable flexural capacity	82.29 kip-in

Figure E.53 Strength Calculations, Test P2/2-T-3, Continued

(f) Purlin #2, South Span

GEOMETRY OF CROSS-SECTION

		Top	Bottom
Vertical lip dimensions		0.8125 in.	0.6875 in.
Lip angles		79.0000 deg.	75.0000 deg.
Flange widths		2.9375 in.	2.5625 in.
Radii			
Lip to flange		0.3438 in.	0.3438 in.
Flange to web		0.2330 in.	0.2330 in.
Total purlin depth	8.0625 in.		
Purlin thickness	0.0800 in.		

Material Properties

Material yield stress	56.6 ksi
Modulus of elasticity	29500.0 ksi

General

Flat width of compression flange	2.2751 in.
Gross moment of inertia	11.29 $in.^4$

1986 AISI Procedure

Flange is not fully effective	
Effective flange width	1.7327 in.
Effective moment of inertia	10.18 $in.^4$
Allowable flexural capacity	82.82 kip-in

Figure E.54 Strength Calculations, Test P2/2-T-3

Purlin #1

North Span

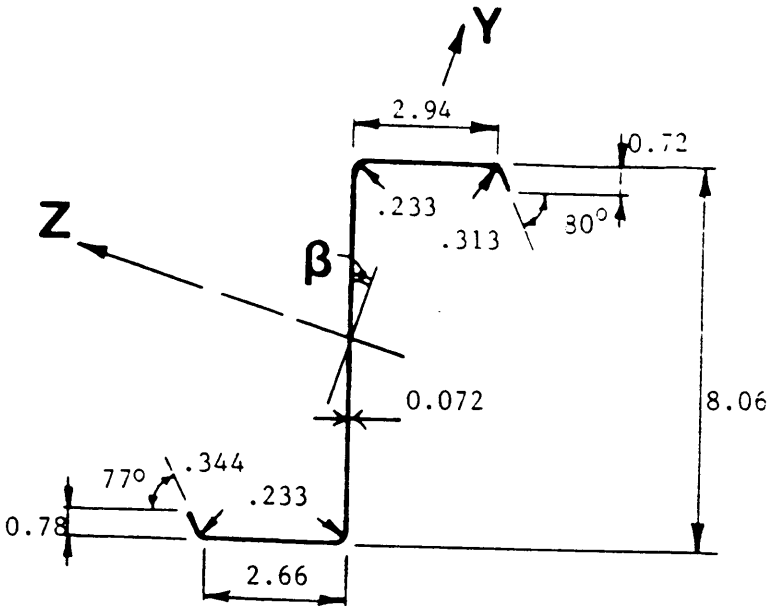

Properties: Span (ft) = 23.0
Area (in^2) = 1.0669
β(deg) = 18.2531
I_x (in^4) = 0.0019
I_y (in^4) = 0.7950
I_z (in^4) = 11.8301

Purlin #2

North Span

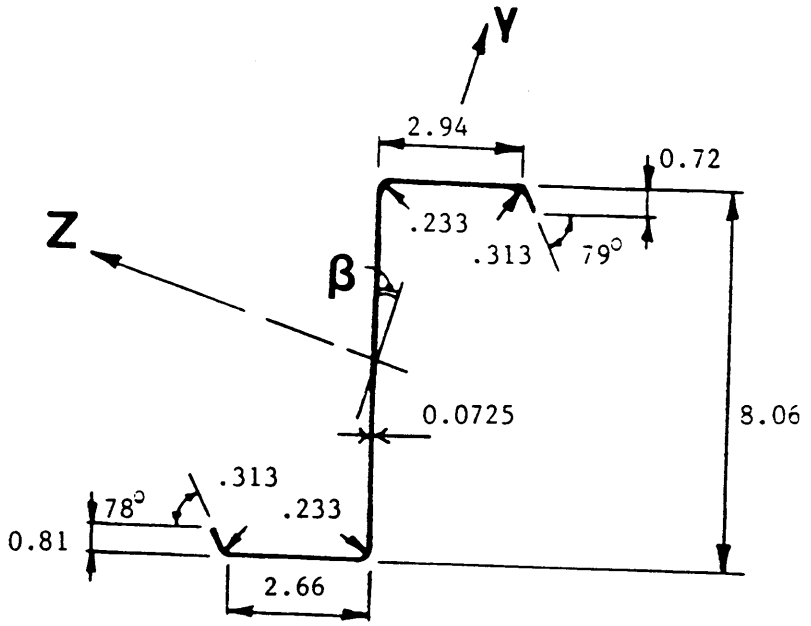

Properties: Span (ft) = 23.0
Area (in^2) = 1.0772
β(deg) = 18.3530
I_x (in^4) = 0.0019
I_y (in^4) = 0.8065
I_z (in^4) = 11.9653

Figure E.55 Measured Purlin Dimensions and Calculated Properties, Test R3/2-M-3, Continued

Purlin #1

Center Span

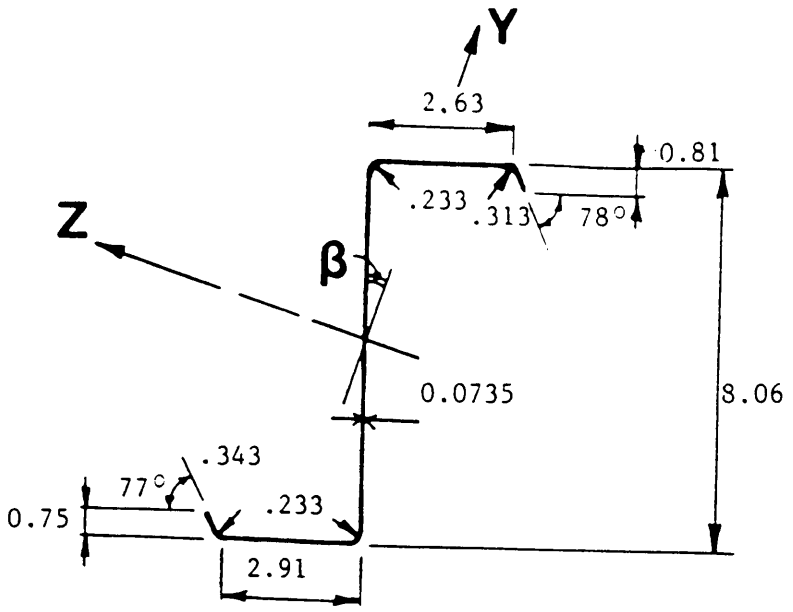

Properties: Span (ft) = 23.0

Area (in^2) = 1.0901

β(deg) = 18.2603

I_x (in^4) = 0.0020

I_y (in^4) = 0.8146

I_z (in^4) = 12.0635

Purlin #2

Center Span

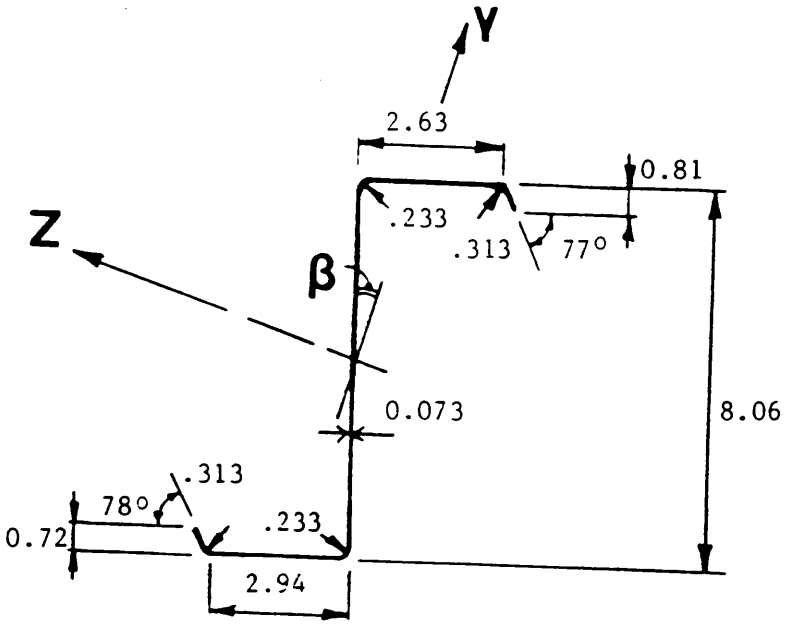

Properties: Span (ft) = 23.0

Area (in^2) = 1.0833

β(deg) = 18.2974

I_x (in^4) = 0.0020

I_y (in^4) = 0.8076

I_z (in^4) = 12.0150

Figure E.56 Measured Purlin Dimensions and Calculated Properties, Test R3/2-M-3, Continued

Purlin #1

South Span

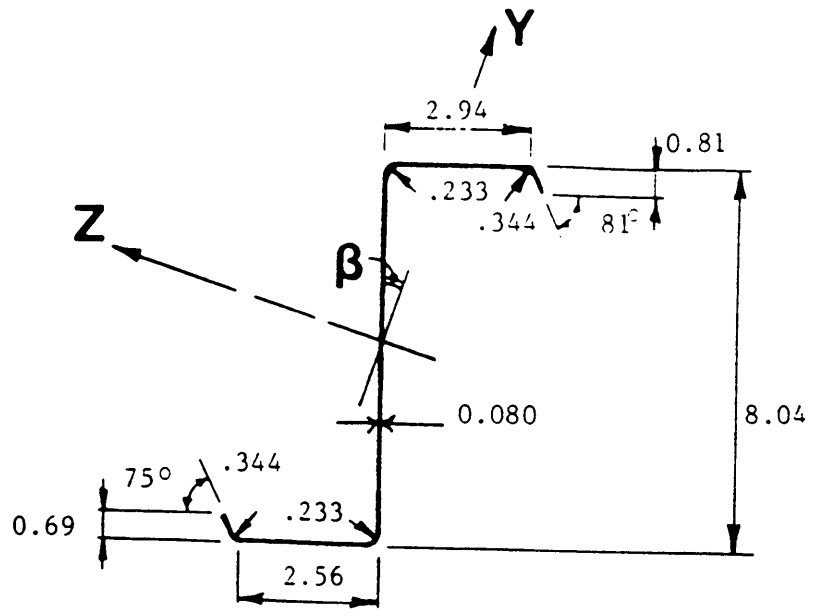

Properties: Span (ft) = 23.0 $I_x(in^4)$ = 0.0025

Area (in^2) = 1.1762 $I_y(in^4)$ = 0.8597

β(deg) = 17.9974 $I_z(in^4)$ = 12.8797

Purlin #2

South Span

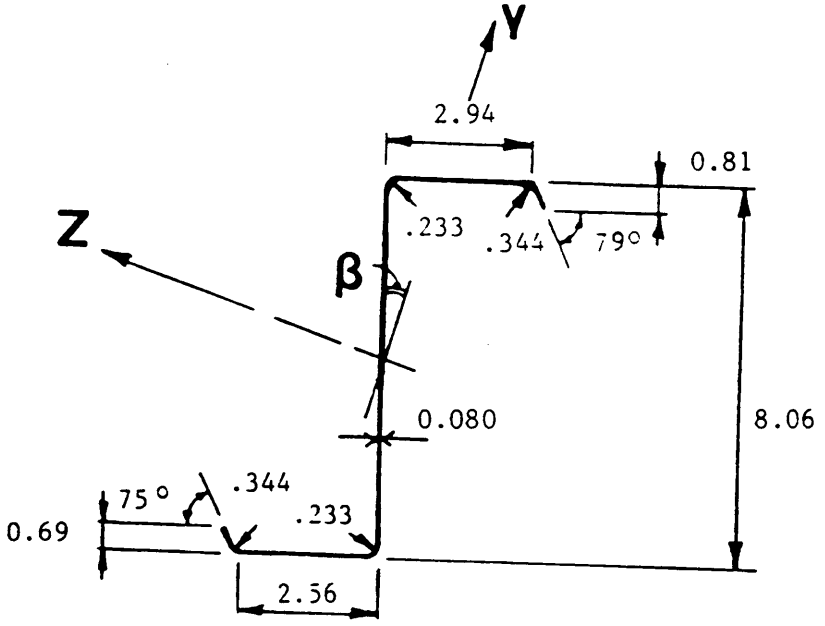

Properties: Span (ft) = 23.0 I (in^4) = 0.0026

Area (in^2) = 1.1788 I (in^4) = 0.8662

β(deg) = 18.0006 I (in^4) = 12.9683

Figure E.57 Measured Purlin Dimensions and Calculated Properties, Test R3/2-M-3

(a) Purlin #1, North Span

GEOMETRY OF CROSS-SECTION

		Top	Bottom
Vertical lip dimensions		0.7188 in.	0.7813 in.
Lip angles		80.0000 deg.	77.0000 deg.
Flange widths		2.9380 in.	2.6560 in.
Radii			
Lip to flange		0.3125 in.	0.3438 in.
Flange to web		0.2330 in.	0.2330 in.
Total purlin depth	8.0625 in.		
Purlin thickness	0.0720 in.		

Material Properties

Material yield stress	56.6 ksi
Modulus of elasticity	29500.0 ksi

General

Flat width of compression flange	2.3104 in.
Gross moment of inertia	10.32 $in.^4$

1986 AISI Procedure

Flange is not fully effective	
Effective flange width	1.7369 in.
Effective moment of inertia	9.27 $in.^4$
Allowable flexural capacity	74.21 kip-in

Figure E.58 Strength Calculations, Test R3/2-M-3, Continued

(b) Purlin #2, North Span

GEOMETRY OF CROSS-SECTION

		Top	Bottom
Vertical lip dimensions		0.7188 in.	0.8125 in.
Lip angles		79.0000 deg.	78.0000 deg.
Flange widths		2.9375 in.	2.6563 in.
Radii			
Lip to flange		0.3125 in.	0.3125 in.
Flange to web		0.2330 in.	0.2330 in.
Total purlin depth	8.0625 in.		
Purlin thickness	0.0725 in.		

Material Properties

Material yield stress	56.6 ksi
Modulus of elasticity	29500.0 ksi

General

Flat width of compression flange	2.3146 in.
Gross moment of inertia	10.42 $in.^4$

1986 AISI Procedure

Flange is not fully effective	
Effective flange width	1.7519 in.
Effective moment of inertia	9.38 $in.^4$
Allowable flexural capacity	74.96 kip-in

Figure E.59 Strength Calculations, Test R3/2-M-3, Continued

(c) Purlin #1, Center Span

GEOMETRY OF CROSS-SECTION

		Top	Bottom
Vertical lip dimensions		0.8125 in.	0.7500 in.
Lip angles		78.0000 deg.	77.0000 deg.
Flange widths		2.6250 in.	2.9063 in.
Radii			
Lip to flange		0.3125 in.	0.3438 in.
Flange to web		0.2330 in.	0.2330 in.
Total purlin depth	8.0625 in.		
Purlin thickness	0.0735 in.		

Material Properties

Material yield stress	56.6 ksi
Modulus of elasticity	29500.0 ksi

General

Flat width of compression flange	2.0059 in.
Gross moment of inertia	10.52 $in.^4$

1986 AISI Procedure

Flange is not fully effective	
Effective flange width	1.6806 in.
Effective moment of inertia	9.75 $in.^4$
Allowable flexural capacity	77.12 kip-in

Figure E.60 Strength Calculations, Test R3/2-M-3, Continued

(d) Purlin #2, Center Span

GEOMETRY OF CROSS-SECTION

		Top	Bottom
Vertical lip dimensions		0.8125 in.	0.7188 in.
Lip angles		77.0000 deg.	78.0000 deg.
Flange widths		2.6250 in.	2.9375 in.
Radii			
Lip to flange		0.3125 in.	0.3125 in.
Flange to web		0.2330 in.	0.2330 in.
Total purlin depth	8.0625 in.		
Purlin thickness	0.0730 in.		

Material Properties

Material yield stress	56.6	ksi
Modulus of elasticity	29500.0	ksi

General

Flat width of compression flange	2.0124	in.
Gross moment of inertia	10.47	$in.^4$

1986 AISI Procedure

Flange is not fully effective		
Effective flange width	1.6785	in.
Effective moment of inertia	9.69	$in.^4$
Allowable flexural capacity	76.61	kip-in

Figure E.61 Strength Calculations, Test R3/2-M-3, Continued

(e) Purlin #1, South Span

GEOMETRY OF CROSS-SECTION

		Top	Bottom
Vertical lip dimensions		0.8125 in.	0.6875 in.
Lip angles		81.0000 deg.	75.0000 deg.
Flange widths		2.9375 in.	2.5625 in.
Radii			
Lip to flange		0.3438 in.	0.3438 in.
Flange to web		0.2330 in.	0.2330 in.
Total purlin depth	8.0435 in.		
Purlin thickness	0.0800 in.		

Material Properties

Material yield stress	56.6 ksi
Modulus of elasticity	29500.0 ksi

General

Flat width of compression flange	2.2625 in.
Gross moment of inertia	11.21 in.4

1986 AISI Procedure

Flange is not fully effective	
Effective flange width	1.7129 in.
Effective moment of inertia	10.10 $in.^4$
Allowable flexural capacity	82.29 kip-in

Figure E.62 Strength Calculations, Test R3/2-M-3, Continued

(f) Purlin #2, South Span

GEOMETRY OF CROSS-SECTION

		Top	Bottom
Vertical lip dimensions		0.8125 in.	0.6875 in.
Lip angles		79.0000 deg.	75.0000 deg.
Flange widths		2.9375 in.	2.5625 in.
Radii			
Lip to flange		0.3438 in.	0.3438 in.
Flange to web		0.2330 in.	0.2330 in.
Total purlin depth	8.0625 in.		
Purlin thickness	0.0800 in.		

Material Properties

Material yield stress	56.6 ksi
Modulus of elasticity	29500.0 ksi

General

Flat width of compression flange	2.2751 in.
Gross moment of inertia	11.29 in.4

1986 AISI Procedure

Flange is not fully effective	
Effective flange width	1.7327 in.
Effective moment of inertia	10.18 in.4
Allowable flexural capacity	82.82 kip-in

Figure E.63 Strength Calculations, Test R3/2-M-3

Purlin #1

North Span

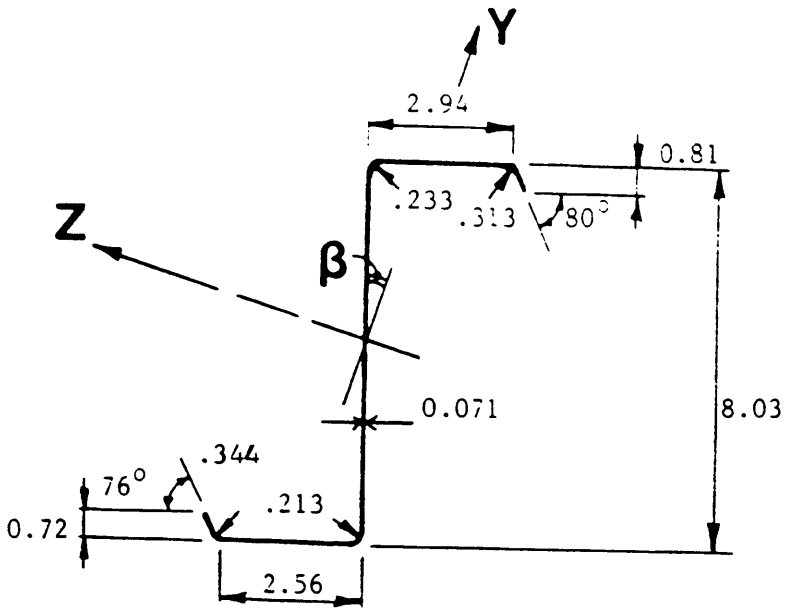

Properties: Span (ft) = 23.0 $I_x(in^4)$ = 0.0018

Area (in^2) = 1.0459 $I_y(in^4)$ = 0.7713

β(deg) = 18.1421 $I_z(in^4)$ = 11.4534

Purlin #2

North Span

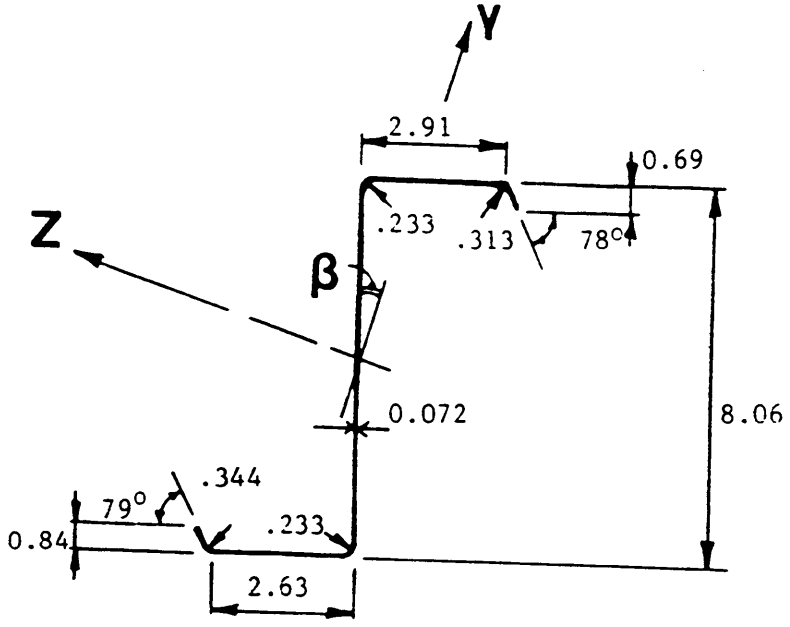

Properties: Span (ft) = 23.0 $I_x(in^4)$ = 0.0019

Area (in^2) = 1.0646 $I_y(in^4)$ = 0.7822

β(deg) = 18.0915 $I_z(in^4)$ = 11.7572

Figure E.64 Measured Purlin Dimensions and Calculated Properties, Test P2/2-M-3, Continued

Purlin #1
Center Span

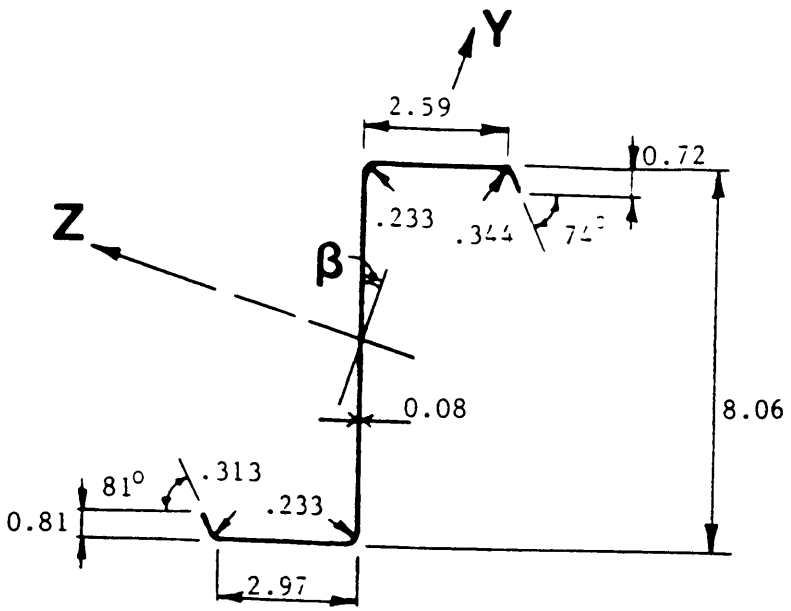

Properties: Span (ft) = 23.0
Area (in^2) = 1.1866
β (deg) = 18.3066
I_x (in^4) = 0.0026
I_y (in^4) = 0.8901
I_z (in^4) = 13.1412

Purlin #2
Center Span

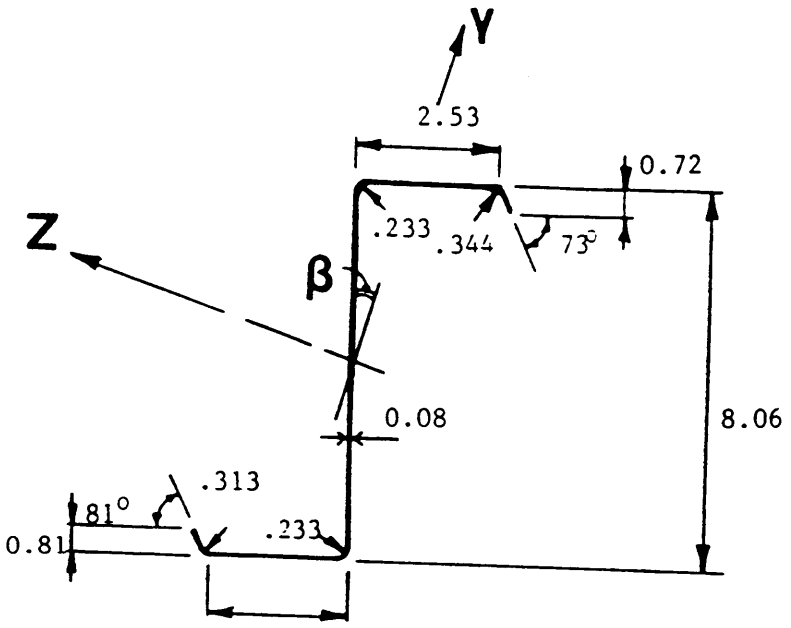

Properties: Span (ft) = 23.0
Area (in^2) = 1.1822
β (deg) = 18.1213
I_x (in^4) = 0.0026
I_y (in^4) = 0.8751
I_z (in^4) = 13.0318

Figure E.65 Measured Purlin Dimensions and Calculated Properties, Test P2/2-M-3, Continued

Purlin #1

South Span

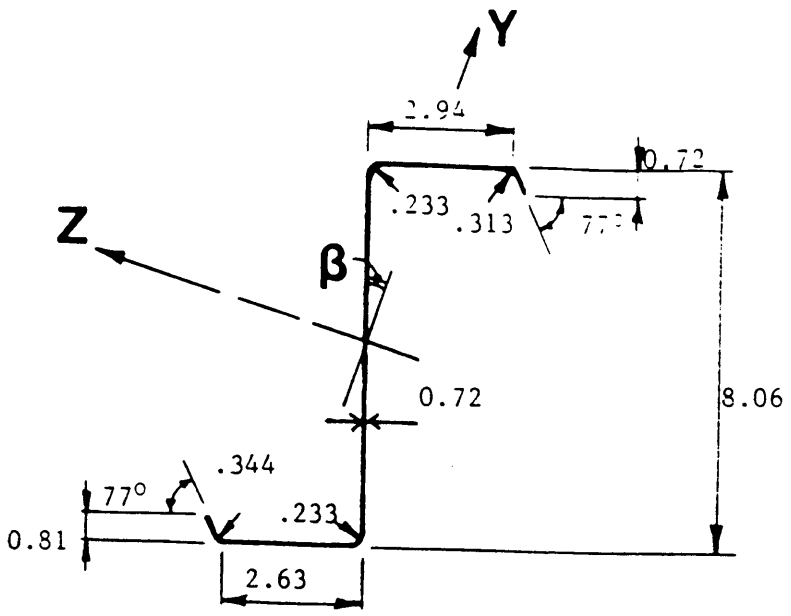

Properties: Span (ft) = 23.0 $I_x(in^4)$ = 0.0019

Area (in^2) = 1.0683 $I_y(in^4)$ = 0.7995

β(deg) = 18.3028 $I_z(in^4)$ = 11.8466

Purlin #2

South Span

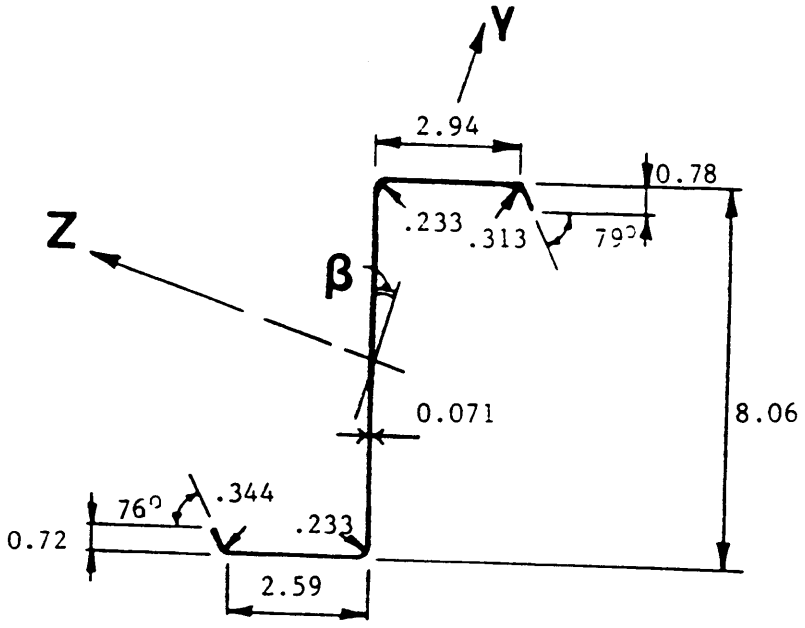

Properties: Span (ft) = 23.0 $I_x(in^4)$ = 0.0018

Area (in^2) = 1.0485 $I_y(in^4)$ = 0.7729

β(deg) = 18.0981 $I_z(in^4)$ = 11.5748

Figure E.66 Measured Purlin Dimensions and Calculated Properties, Test P2/2-M-3

(a) Purlin #1, North Span

GEOMETRY OF CROSS-SECTION

		Top	Bottom
Vertical lip dimensions		0.8125 in.	0.7188 in.
Lip angles		80.0000 deg.	76.0000 deg.
Flange widths		2.9375 in.	2.5625 in.
Radii			
Lip to flange		0.3130 in.	0.3440 in.
Flange to web		0.2330 in.	0.2330 in.
Total purlin depth	8.0313 in.		
Purlin thickness	0.0710 in.		

Material Properties

Material yield stress	56.6	ksi
Modulus of elasticity	29500.0	ksi

General

Flat width of compression flange	2.3113	in.
Gross moment of inertia	9.92	in.4

1986 AISI Procedure

Flange is not fully effective		
Effective flange width	1.8028	in.
Effective moment of inertia	9.03	in.4
Allowable flexural capacity	73.98	kip-in

Figure E.67 Strength Calculations, Test P2/2-M-3, Continued

(b) Purlin #2, North Span

GEOMETRY OF CROSS-SECTION

		Top	Bottom
Vertical lip dimensions		0.6875 in.	0.8438 in.
Lip angles		78.0000 deg.	79.0000 deg.
Flange widths		2.9063 in.	2.8438 in.
Radii			
Lip to flange		0.3130 in.	0.3440 in.
Flange to web		0.2330 in.	0.2330 in.
Total purlin depth	8.0625 in.		
Purlin thickness	0.0720 in.		

Material Properties

Material yield stress	56.6	ksi
Modulus of elasticity	29500.0	ksi

General

Flat width of compression flange	2.2895	in.
Gross moment of inertia	10.43	in.4

1986 AISI Procedure

Flange is not fully effective		
Effective flange width	1.7230	in.
Effective moment of inertia	9.40	in.^{4}
Allowable flexural capacity	74.13	kip-in

Figure E.68 Strength Calculations, Test P2/2-M-3, Continued

(c) Purlin #1, Center Span

GEOMETRY OF CROSS-SECTION

	Top	Bottom
Vertical lip dimensions	0.7190 in.	0.8130 in.
Lip angles	74.0000 deg.	81.0000 deg.
Flange widths	2.5940 in.	2.9690 in.
Radii		
Lip to flange	0.3130 in.	0.3440 in.
Flange to web	0.2330 in.	0.2330 in.

Total purlin depth	8.0630 in.
Purlin thickness	0.0800 in.

Material Properties

Material yield stress	56.6 ksi
Modulus of elasticity	29500.0 ksi

General

Flat width of compression flange	1.9849 in.
Gross moment of inertia	11.30 in.4

1986 AISI Procedure

Flange is not fully effective	
Effective flange width	1.7565 in.
Effective moment of inertia	10.63 in.4
Allowable flexural capacity	83.95 kip-in

Figure E.69 Strength Calculations, Test P2/2-M-3, Continued

(d) Purlin #2, Center Span

GEOMETRY OF CROSS-SECTION

		Top	Bottom
Vertical lip dimensions		0.7190 in.	0.8130 in.
Lip angles		73.0000 deg.	81.0000 deg.
Flange widths		2.5310 in.	2.9690 in.
Radii			
Lip to flange		0.3440 in.	0.3130 in.
Flange to web		0.2330 in.	0.2330 in.
Total purlin depth	8.0630 in.		
Purlin thickness	0.0800 in.		

Material Properties

Material yield stress	56.6	ksi
Modulus of elasticity	29500.0	ksi

General

Flat width of compression flange	1.9043	in.
Gross moment of inertia	11.23	in.4

1986 AISI Procedure

Flange is not fully effective		
Effective flange width	1.7383	in.
Effective moment of inertia	10.67	in.4
Allowable flexural capacity	84.33	kip-in

Figure E.70 Strength Calculations, Test P2/2-M-3, Continued

(e) Purlin #1, South Span

GEOMETRY OF CROSS-SECTION

		Top	Bottom
Vertical lip dimensions		0.7188 in.	0.8125 in.
Lip angles		77.0000 deg.	77.0000 deg.
Flange widths		2.9375 in.	2.6255 in.
Radii			
Lip to flange		0.3130 in.	0.3440 in.
Flange to web		0.2330 in.	0.2330 in.
Total purlin depth	8.0625 in.		
Purlin thickness	0.0720 in.		

Material Properties

Material yield stress	56.6	ksi
Modulus of elasticity	29500.0	ksi

General

Flat width of compression flange	2.3263	in.
Gross moment of inertia	10.24	in.4

1986 AISI Procedure

Flange is not fully effective		
Effective flange width	1.7681	in.
Effective moment of inertia	9.24	in.^{4}
Allowable flexural capacity	74.27	kip-in

Figure E.71 Strength Calculations, Test P2/2-M-3, Continued

(f) Purlin #2, South Span

GEOMETRY OF CROSS-SECTION

		Top	Bottom
Vertical lip dimensions		0.7813 in.	0.7188 in.
Lip angles		79.0000 deg.	76.0000 deg.
Flange widths		2.9375 in.	2.5938 in.
Radii			
Lip to flange		0.3130 in.	0.3440 in.
Flange to web		0.2330 in.	0.2330 in.
Total purlin depth	8.0625 in.		
Purlin thickness	0.0710 in.		

Material Properties

Material yield stress	56.6	ksi
Modulus of elasticity	29500.0	ksi

General

Flat width of compression flange	2.3170	in.4
Gross moment of inertia	10.03	in.4

1986 AISI Procedure

Flange is not fully effective		
Effective flange width	1.7890	in.
Effective moment of inertia	9.10	$in.^4$
Allowable flexural capacity	73.94	kip-in

Figure E.72 Strength Calculations, Test P2/2-M-3

APPENDIX F

PROPERTIES OF TESTS IN TABLE 3.6

Purlin #1

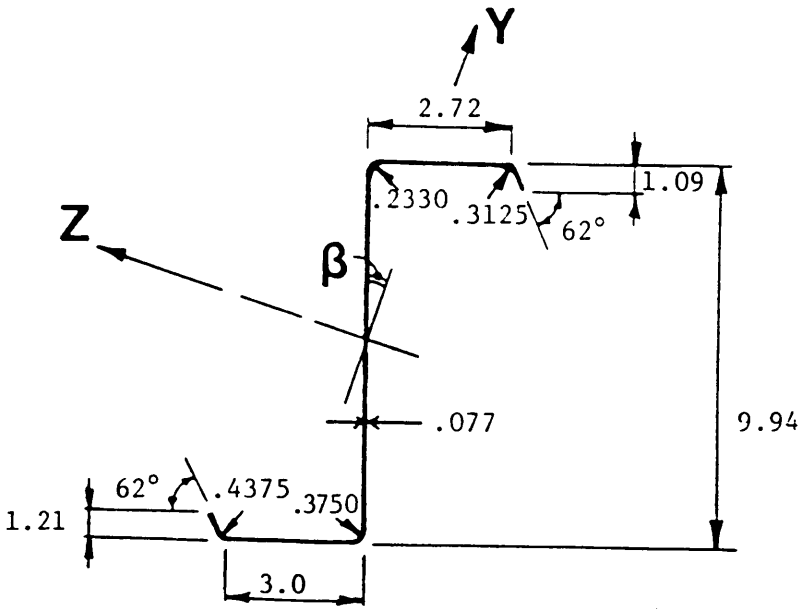

Properties:				
	Span (ft) =	25.0	I_x(in^4) =	0.0015
	Area (in^2) =	0.9890	I_y(in^4) =	0.6924
	β(deg) =	17.3001	I_z(in^4) =	10.8555

Purlin #2

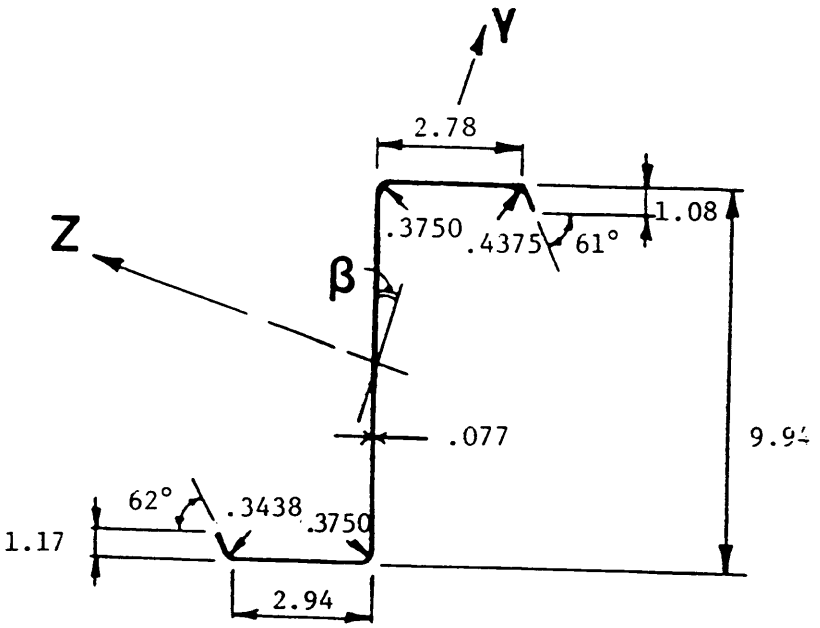

Properties:				
	Span (ft) =	25.0	I_x (in^4) =	0.0016
	Area (in^2) =	1.0051	I_y (in^4) =	0.6927
	β(deg) =	17.2361	I_z (in^4) =	10.9396

Figure F.1 Measured Purlin Dimensions and Calculated Properties, Test R/2-R-1

(a) Purlin #1

GEOMETRY OF CROSS-SECTION

		Top	Bottom
Vertical lip dimensions		1.0900 in.	1.2100 in.
Lip angles		62.0000 deg.	62.0000 deg.
Flange widths		2.7200 in.	3.0000 in.
Radii			
Lip to flange		0.3125 in.	0.4375 in.
Flange to web		0.2330 in.	0.3750 in.
Total purlin depth	9.9400 in.		
Purlin thickness	0.0770 in.		

Material Properties

Material yield stress	55.0	ksi
Modulus of elasticity	29500.0	ksi

General

Flat width of compression flange	1.8588	in.
Gross moment of inertia	19.35	$in.^4$

1986 AISI Procedure

Flange is not fully effective		
Effective flange width	1.6984	in.
Effective moment of inertia	18.96	$in.^4$
Allowable flexural capacity	121.28	kip-in

Figure F.2 Strength Calculations, Test R/2-R-1, Continued

(b) Purlin #2

GEOMETRY OF CROSS-SECTION

		Top	Bottom
Vertical lip dimensions		1.0800 in.	1.1700 in.
Lip angles		61.0000 deg.	62.0000 deg.
Flange widths		2.7800 in.	2.9400 in.
Radii			
Lip to flange		0.4375 in.	0.3438 in.
Flange to web		0.3750 in.	0.3750 in.
Total purlin depth	9.9400 in.		
Purlin thickness	0.0770 in.		

Material Properties

Material yield stress	55.0	ksi
Modulus of elasticity	29500.0	ksi

General

Flat width of compression flange	1.9881	in.
Gross moment of inertia	19.33	$in.^4$

1986 AISI Procedure

Flange is not fully effective		
Effective flange width	1.8005	in.
Effective moment of inertia	18.88	$in.^4$
Allowable flexural capacity	122.05	kip-in

Figure F.3 Strength Calculations, Test R/2-R-1

Purlin #1

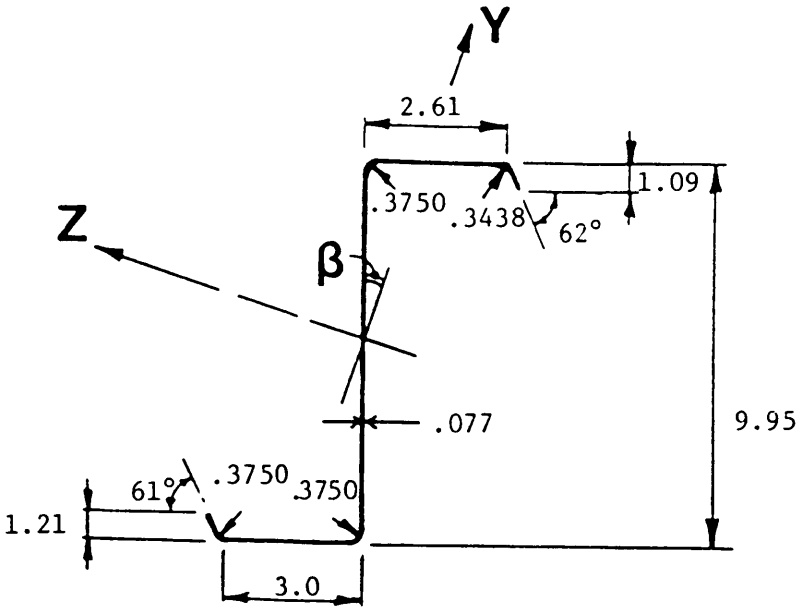

Properties:				
	Span (ft) =	25.0	I_x(in^4) =	0.0020
	Area (in^2) =	1.0841	I_y(in^4) =	0.8125
	β(deg) =	18.4315	I_z(in^4) =	11.9414

Purlin #2

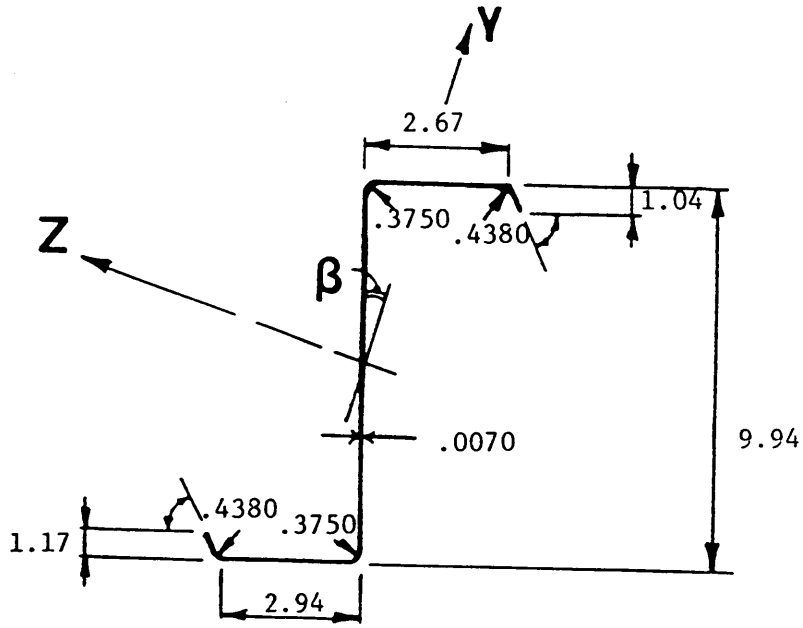

Properties:				
	Span (ft) =	25.0	I_x (in^4) =	0.0020
	Area (in^2) =	1.0808	I_y (in^4) =	0.7978
	β(deg) =	18.1375	I_z (in^4) =	11.9384

Figure F.4 Measured Purlin Dimensions and Calculated Properties, Test P/2-R-1

(a) Purlin #1

GEOMETRY OF CROSS-SECTION

		Top	Bottom
Vertical lip dimensions		1.0900 in.	1.2100 in.
Lip angles		62.0000 deg.	61.0000 deg.
Flange widths		2.6100 in.	3.0000 in.
Radii			
Lip to flange		0.3438 in.	0.3750 in.
Flange to web		0.3750 in.	0.3750 in.
Total purlin depth	9.9500 in.		
Purlin thickness	0.0770 in.		

Material Properties

Material yield stress	55.0 ksi
Modulus of elasticity	29500.0 ksi

General

Flat width of compression flange	1.8113 in.
Gross moment of inertia	19.26 $in.^4$

1986 AISI Procedure

Flange is not fully effective	
Effective flange width	1.6578 in.
Effective moment of inertia	18.88 $in.^4$
Allowable flexural capacity	120.02 kip-in

Figure F.5 Strength Calculations, Test P/2-R-1, Continued

(b) Purlin #2

GEOMETRY OF CROSS-SECTION

		Top	Bottom
Vertical lip dimensions		1.0400 in.	1.1700 in.
Lip angles		61.0000 deg.	62.0000 deg.
Flange widths		2.6700 in.	2.9400 in.
Radii			
Lip to flange		0.4380 in.	0.4380 in.
Flange to web		0.3750 in.	0.3750 in.
Total purlin depth	9.9400 in.		
Purlin thickness	0.0770 in.		

Material Properties

Material yield stress	55.0	ksi
Modulus of elasticity	29500.0	ksi

General

Flat width of compression flange	1.8781	in.
Gross moment of inertia	19.11	$in.^4$

1986 AISI Procedure

Flange is not fully effective		
Effective flange width	1.7457	in.
Effective moment of inertia	18.80	$in.^4$
Allowable flexural capacity	120.87	kip-in

Figure F.6 Strength Calculations, Test P/2-R-1

Purlin #1

North Span

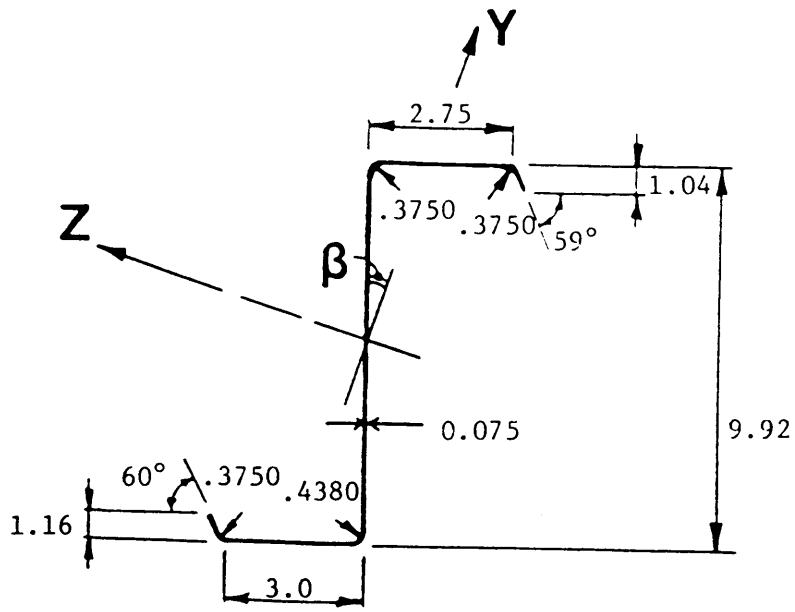

Properties:	Span (ft) =	25.0		I_x(in^4) =	0.0019
	Area (in^2) =	1.0657		I_y(in^4) =	0.7863
	β(deg) =	18.2899		I_z(in^4) =	11.8114

Purlin #2

North Span

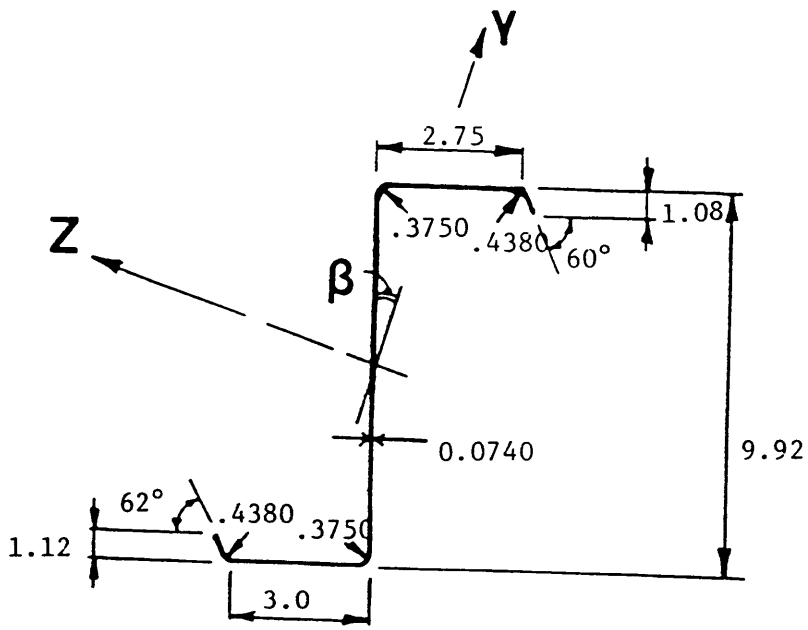

Properties:	Span (ft) =	25.0		I_x (in^4) =	0.0019
	Area (in^2) =	1.0789		I_y (in^4) =	0.8079
	β(deg) =	18.5396		I_z (in^4) =	11.9043

Figure F.7 Measured Purlin Dimensions and Calculated Properties, Test R/2-R-2, Continued

Purlin #1

South Span

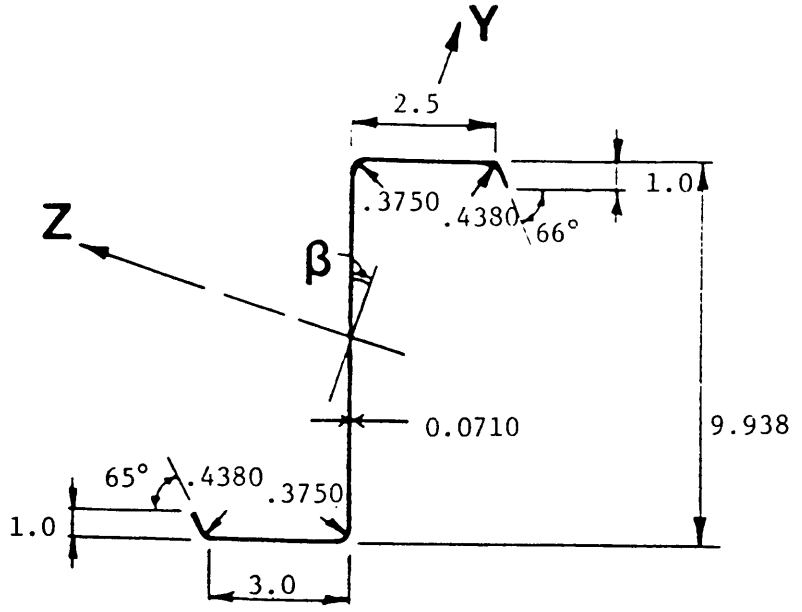

Properties: Span (ft) = 25.0 $I_x(in^4)$ = 0.0016

Area (in^2) = 1.0225 $I_y(in^4)$ = 0.7645

β(deg) = 18.3960 $I_z(in^4)$ = 11.3487

Purlin #2

South Span

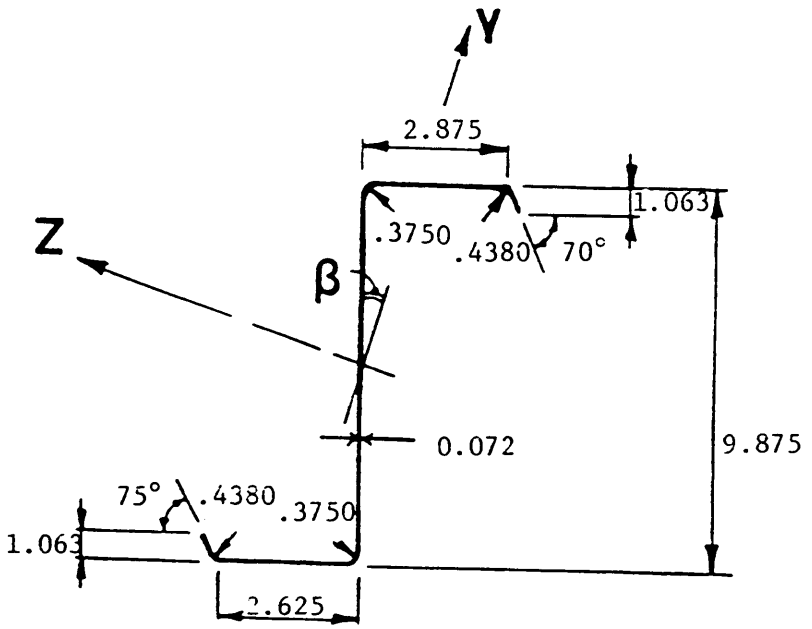

Properties: Span (ft) = 25.0 I_x (in^4) = 0.0019

Area (in^2) = 1.0730 I_y (in^4) = 0.7964

β(deg) = 18.3410 I_z (in^4) = 11.9071

Figure F.8 Measured Purlin Dimensions and Calculated Properties, Test R/2-R-2

(a) Purlin #1, North Span

GEOMETRY OF CROSS-SECTION

		Top	Bottom
Vertical lip dimensions		1.0400 in.	1.1600 in.
Lip angles		59.0000 deg.	60.0000 deg.
Flange widths		2.7500 in.	3.0000 in.
Radii			
Lip to flange		0.3750 in.	0.3750 in.
Flange to web		0.4380 in.	0.4380 in.
Total purlin depth	9.9200 in.		
Purlin thickness	0.0750 in.		

Material Properties

Material yield stress	55.0 ksi
Modulus of elasticity	29500.0 ksi

General

Flat width of compression flange	1.9117 in.
Gross moment of inertia	18.83 $in.^4$

1986 AISI Procedure

Flange is not fully effective	
Effective flange width	1.7278 in.
Effective moment of inertia	18.39 $in.^4$
Allowable flexural capacity	117.91 kip-in

Figure F.9 Strength Calculations, Test R/2-R-2, Continued

(b) Purlin #2, North Span

GEOMETRY OF CROSS-SECTION

		Top	Bottom
Vertical lip dimensions		1.0800 in.	1.1200 in.
Lip angles		60.0000 deg.	62.0000 deg.
Flange widths		2.7500 in.	3.0000 in.
Radii			
Lip to flange		0.4380 in.	0.4380 in.
Flange to web		0.3750 in.	0.3750 in.
Total purlin depth	9.9200 in.		
Purlin thickness	0.0740 in.		

Material Properties

Material yield stress	55.0 ksi
Modulus of elasticity	29500.0 ksi

General

Flat width of compression flange	1.9066 in.
Gross moment of inertia	18.54 $in.^4$

1986 AISI Procedure

Flange is not fully effective	
Effective flange width	1.6859 in.
Effective moment of inertia	18.00 $in.^4$
Allowable flexural capacity	115.55 kip-in

Figure F.10 Strength Calculations, Test R/2-R-2, Continued

(c) Purlin #1, South Span

GEOMETRY OF CROSS-SECTION

		Top	Bottom
Vertical lip dimensions		1.0000 in.	1.0000 in.
Lip angles		66.0000 deg.	65.0000 deg.
Flange widths		2.5000 in.	3.0000 in.
Radii			
Lip to flange		0.4380 in.	0.4380 in.
Flange to web		0.3750 in.	0.3750 in.
Total purlin depth	9.9380 in.		
Purlin thickness	0.0710 in.		

Material Properties

Material yield stress	55.0 ksi
Modulus of elasticity	29500.0 ksi

General

Flat width of compression flange	1.7235 in.
Gross moment of inertia	17.08 $in.^4$

1986 AISI Procedure

Flange is not fully effective	
Effective flange width	1.6043 in.
Effective moment of inertia	16.82 $in.^4$
Allowable flexural capacity	107.33 kip-in

Figure F.11 Strength Calculations, Test R/2-R-2, Continued

(d) Purlin #2, South Span

GEOMETRY OF CROSS-SECTION

		Top	Bottom
Vertical lip dimensions		1.0630 in.	1.0630 in.
Lip angles		70.0000 deg.	75.0000 deg.
Flange widths		2.8750 in.	2.6250 in.
Radii			
Lip to flange		0.4380 in.	0.4380 in.
Flange to web		0.3750 in.	0.3750 in.
Total purlin depth	9.8750 in.		
Purlin thickness	0.0720 in.		

Material Properties

Material yield stress	55.0 ksi
Modulus of elasticity	29500.0 ksi

General

Flat width of compression flange	2.0709 in.
Gross moment of inertia	16.97 $in.^4$

1986 AISI Procedure

Flange is not fully effective	
Effective flange width	1.8106 in.
Effective moment of inertia	16.39 $in.^4$
Allowable flexural capacity	108.97 kip-in

Figure F.12 Strength Calculations, Test R/2-R-2

Purlin #1

North Span

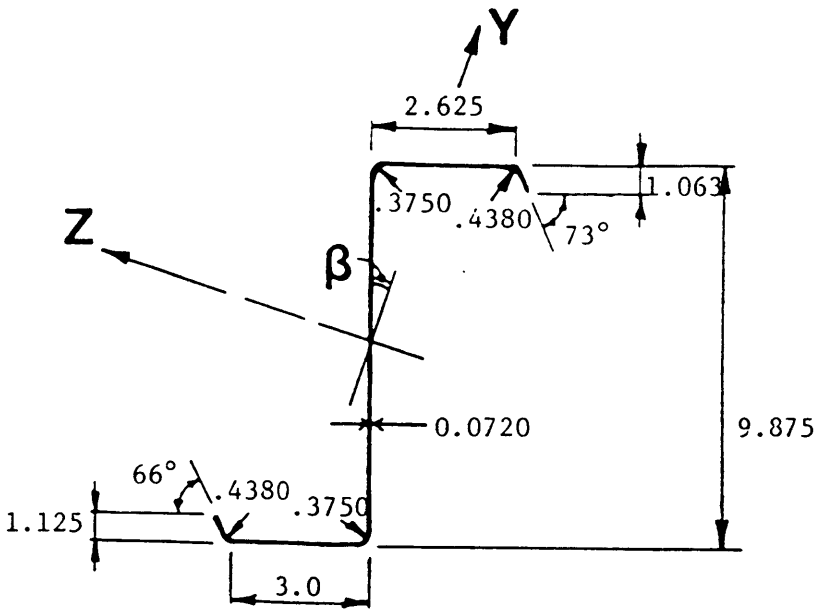

Properties: Span (ft) = 25.0 $I_x(in^4)$ = .0019

Area (in^2) = 1.0735 $I_y(in^4)$ = .8061

β(deg) = 18.3015 $I_z(in^4)$ = 11.9984

Purlin #2

North Span

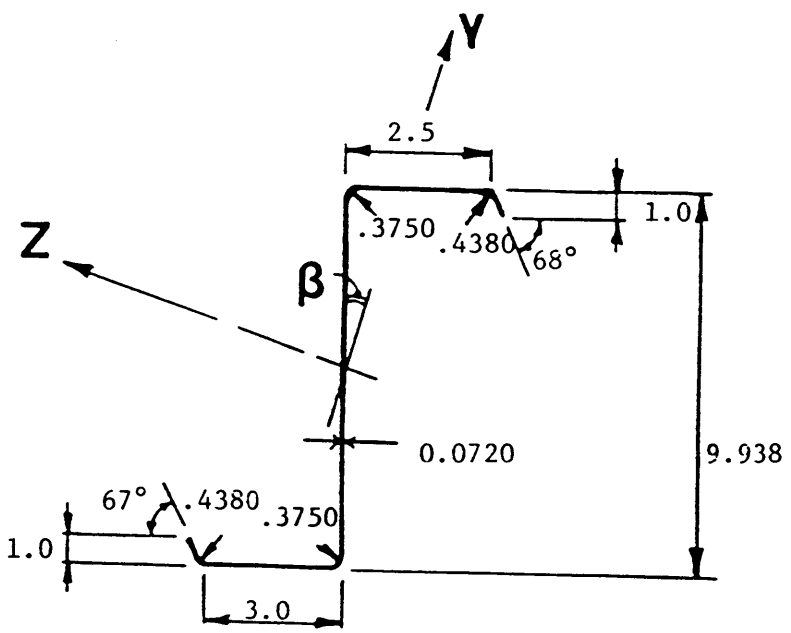

Properties: Span (ft) = 25.0 I_x (in^4) = .0019

Area (in^2) = 1.0712 I_y (in^4) = 0.8022

β(deg) = 18.2392 I_z (in^4) = 11.9573

Figure F.12 Measured Purlin Dimensions and Calculated Properties, Test P/2-R-2, Continued

Purlin #1

South Span

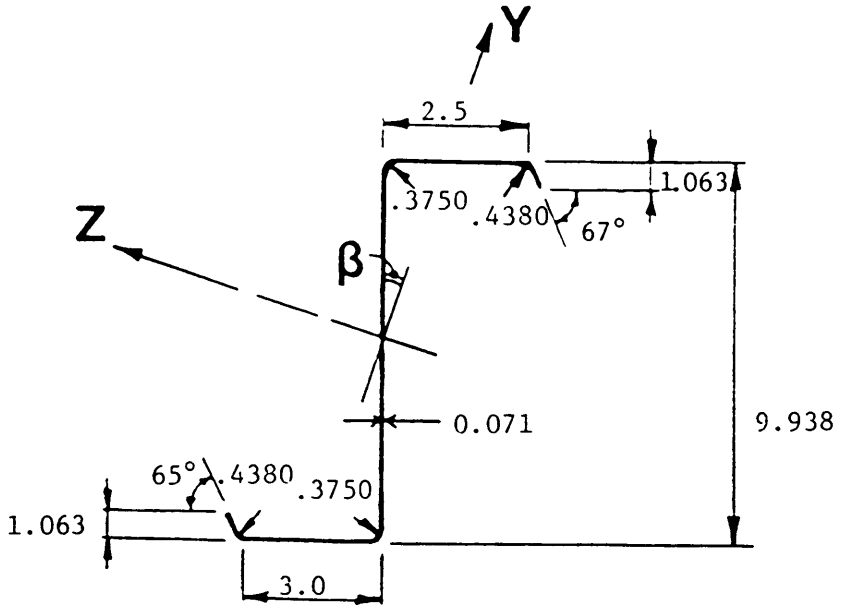

Properties: Span (ft) = 25.0 $I_x(in^4)$ = 0.0021

Area (in^2) = 1.1033 $I_y(in^4)$ = 0.8190

β(deg) = 18.2105 $I_z(in^4)$ = 12.2030

Purlin #2

South Span

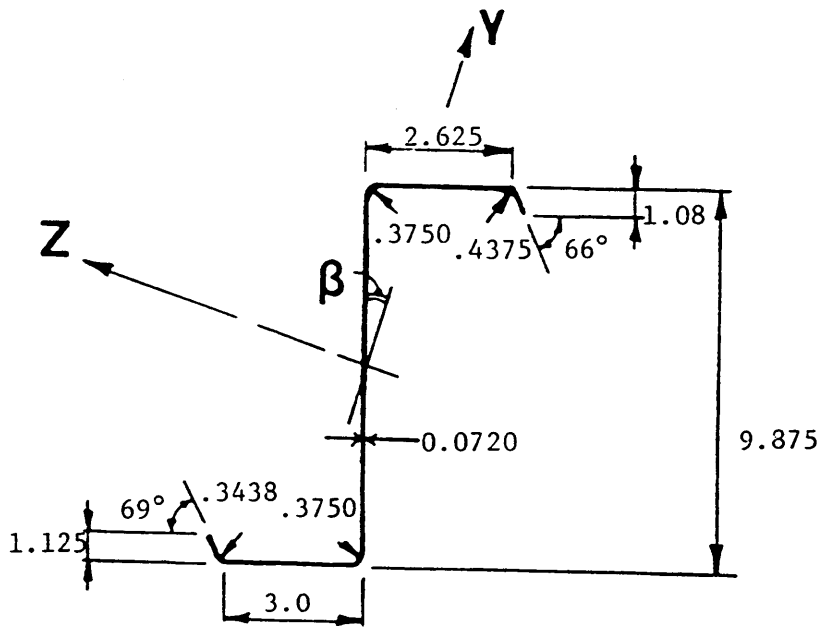

Properties: Span (ft) = 25.0 $I_x(in^4)$ = 0.0021

Area (in^2) = 1.1143 $I_y(in^4)$ = 0.8279

β(deg) = 18.1585 $I_z(in^4)$ = 12.4196

Figure F.13 Measured Purlin Dimensions and Calculated Properties, Test P/2-R-2

(a) Purlin #1, North Span

GEOMETRY OF CROSS-SECTION

	Top	Bottom
Vertical lip dimensions	1.0630 in.	1.1250 in.
Lip angles	73.0000 deg.	66.0000 deg.
Flange widths	2.6250 in.	3.0000 in.
Radii		
Lip to flange	0.4380 in.	0.4380 in.
Flange to web	0.3750 in.	0.3750 in.

Total purlin depth	9.8750 in.
Purlin thickness	0.0720 in.

Material Properties

Material yield stress	55.0 ksi
Modulus of elasticity	29500.0 ksi

General

Flat width of compression flange	1.8006 in.
Gross moment of inertia	17.35 $in.^4$

1986 AISI Procedure

Flange is not fully effective	
Effective flange width	1.6673 in.
Effective moment of inertia	17.09 $in.^4$
Allowable flexural capacity	109.85 kip-in

Figure F.14 Strength Calculations, Test P/2-R-2, Continued

(b) Purlin #2, North Span

GEOMETRY OF CROSS-SECTION

		Top	Bottom
Vertical lip dimensions		1.0000 in.	1.0000 in.
Lip angles		68.0000 deg.	67.0000 deg.
Flange widths		2.5000 in.	3.0000 in.
Radii			
Lip to flange		0.4380 in.	0.4380 in.
Flange to web		0.3750 in.	0.3750 in.
Total purlin depth	9.9380 in.		
Purlin thickness	0.0720 in.		

Material Properties

Material yield stress	55.0 ksi
Modulus of elasticity	29500.0 ksi

General

Flat width of compression flange	2.2090 in.
Gross moment of inertia	17.24 $in.^4$

1986 AISI Procedure

Flange is not fully effective	
Effective flange width	1.8683 in.
Effective moment of inertia	16.33 $in.^4$
Allowable flexural capacity	107.65 kip-in

Figure F.15 Strength Calculations, Test P/2-R-2, Continued

(c) Purlin #1, South Span

GEOMETRY OF CROSS-SECTION

	Top	Bottom
Vertical lip dimensions	1.0630 in.	1.0630 in.
Lip angles	67.0000 deg.	65.0000 deg.
Flange widths	2.5000 in.	3.0000 in.
Radii		
Lip to flange	0.4380 in.	0.4380 in.
Flange to web	0.3750 in.	0.3750 in.

Total purlin depth	9.9380 in.
Purlin thickness	0.0710 in.

Material Properties

Material yield stress	55.0 ksi
Modulus of elasticity	29500.0 ksi

General

Flat width of compression flange	1.7171 in.
Gross moment of inertia	17.21 $in.^4$

1986 AISI Procedure

Flange is not fully effective	
Effective flange width	1.5566 in.
Effective moment of inertia	16.80 $in.^4$
Allowable flexural capacity	106.50 kip-in

Figure F.16 Strength Calculations, Test P/2-R-2, Continued

(d) Purlin #2, South Span

GEOMETRY OF CROSS-SECTION

	Top	Bottom
Vertical lip dimensions	1.0800 in.	1.1250 in.
Lip angles	66.0000 deg.	69.0000 deg.
Flange widths	2.6250 in.	3.0000 in.
Radii		
Lip to flange	0.4375 in.	0.3438 in.
Flange to web	0.3750 in.	0.3750 in.

Total purlin depth	9.8750	in.
Purlin thickness	0.0720	in.

Material Properties

Material yield stress	55.0	ksi
Modulus of elasticity	29500.0	ksi

General

Flat width of compression flange	2.0127	in.
Gross moment of inertia	17.58	$in.^4$

1986 AISI Procedure

Flange is not fully effective		
Effective flange width	1.8266	in.
Effective moment of inertia	17.10	$in.^4$
Allowable flexural capacity	109.35	kip-in

Figure F.17 Strength Calculations, Test P/2-R-2

The vita has been removed from the scanned document

STRENGTH OF Z-PURLIN SUPPORTED STANDING SEAM ROOF SYSTEMS UNDER GRAVITY LOADING

by

Manuel F. Carballo

(ABSTRACT)

The objective of the Standing Seam Roof Systems Research Project at the Virginia Polytechnic Institute and State University is to develop a design procedure for the strength of Z-purlin supported standing seam roof systems under gravity loading. Various approaches were taken to calculate the strength of systems with either torsional restraint, third point span restraint, or midspan restraint. Since few test results are available for single and three span continuous, two purlin line systems, the primary focus of this research is analytical. Even though the test setup used for these tests does not represent actual field conditions, the data obtained will be extremely useful in the development of analytical models to predict system strength. However, at least four multiple purlin line tests will be required to verify the accuracy of the design procedure. The analytical formulation will include the effects of sliding friction in the clips and "drape" restraint effects of the standing seam deck.